THE EFFECTS OF RETINOIC ACID, NICOTINAMIDE RIBOSIDE AND CHRONIC CONTRACTILE ACTIVITY ON MITOCHONDRIAL BIOGENESIS IN SKELETAL MUSCLE CELLS

NEMANJA DOVIJARSKI

A THESIS SUBMITTED TO THE FACULTY OF GRADUATE STUDIES IN PARTIAL FULFILLMENT OF THE REQUIREMENTS FOR THE DEGREE OF

MASTER OF SCIENCE

GRADUATE PROGRAM IN KINESIOLOGY AND HEALTH SCIENCE

YORK UNIVERSITY

TORONTO, ONTARIO

APRIL 2019

Abstract

Mitochondrial biogenesis is a process by which the cell increases its mitochondrial content, involving nuclear-derived and mitochondrial -derived protein synthesis and assembly. Previous literature has identified retinoic acid as a viable agonist of mitochondrial biogenesis in liver and fat tissue, but whether retinoic acid has this effect on muscle is currently unknown. We decided to investigate the effects of retinoic acid on muscle mitochondrial biogenesis by testing it on muscle cells. We also combined RA isomers with known activators of mitochondrial biogenesis, including the drug Nicotinamide Riboside (NR), as well as a model of contracting muscle cells, in order to observe whether there are any interactions. Our results indicate that RA isomer treatment can induce mitochondrial biogenesis, and when combined with chronic contractile activity, has the potential to be additive or synergistic. This suggests that RA may be a useful supplement to accompany exercise training.

ACKNOWLEDGEMENTS

Thank you to my parents Aleksandar and Nada Dovijarski, as well as my brother Aleksa, for their continued support throughout my Masters and my whole life. I could not have done this without your support. I would also like to thank Dr. David Hood for bringing me into his lab and being a great supervisor, mentor and councilor throughout my journey. I could not be more thankful for all your help and guidance.

TABLE OF CONTENTS

List of Figures

Chapter 1: Review of Literature

Chapter 2: Manuscript

Appendix B: Additional Data

List of Tables

Chapter 2: Manuscript

Table 6- PGC-1α- associated kinase protein expression during 30min RA treatment

List of Abbreviations

9cisRA	9-cis retinoic acid
ADP	Adenosine diphosphate
ALP	Autophagosome-lysosome pathway
AMP	Adenosine monophosphate
AMPK	AMP-activated protein kinase
ANOVA	Analysis of Variance
ATP	Adenosine triphosphate
ATRA	All-trans retinoic acid
Ca^{2+}	Calcium Ion
CaMK	Ca^{2+} /calmodulin- dependent protein kinase
cAMP	Cyclic AMP
CCA	Chronic Contractile Activity
COX	Cytochrome Oxidase
CRBP	Cellular Retinoid Binding Protein
CREB	cAMP response element-binding protein
DNA	Deoxyribonucleic Acid
GLUT	Glucose Transporter
ERK	Extracellular signal-regulated kinases
ETC	Electron transport chain
FABP-5	Fatty acid binding protein 5
FAD	Flavin Adenine Nucleotide
IMF	Intermyofibrillar
IMM	Inner mitochondrial membrane
IMS	Intermembrane Space
LC3	Microtubule-associated protein 1A/1B-light chain 3
MAPK	Mitogen-activated protein kinase

MEFC2	Myocyte-specific enhancer factor 2C
mRNA	Messenger RNA
mtDNA	Mitochondrial DNA
NAD	Nicotinamide adenine dinucleotide
NIX	NIP3-like protein X
NR	Nicotinamide Riboside
NRF	Nuclear Respiratory Factor
NUGEMP	Nuclear genes encoding mitochondrial proteins
OMM	Outer mitochondrial membrane
OXPHOS	Oxidative phosphorylation
PARL	Presenilins-associated rhomboid-like protein
PPAR	Peroxisome proliferator-activated receptor
PGC-1α	Peroxisome proliferator- activated receptor gamma coactivator alpha
PI3K	Phosphoinositide 3-kinases
PINK1	PTEN-induced kinase 1
RAR	Retinoic acid receptor
RARE	Retinoic acid response elements
RNA	Ribonucleic Acid
ROS	Reactive oxygen species
RXR	Retinoic X Receptor
SDHA	Succinate dehydrogenase complex, subunit A
SDS-PAGE	Sodium dodecyl sulfate polyacrylamide gel electrophoresis
Tfam	Mitochondrial Transcription Factor A
TIM	Translocase of the Inner Mitochondrial Membrane
TOM	Translocase of the Outer Mitochondrial Membrane
ULK	Unc-51 like autophagy activating kinase
VDAC	Voltage-dependent Anion Channel

CHAPTER 1- REVIEW OF LITERATURE

1.0 Mitochondria

The presence of energy-producing organelles known as mitochondria was known as early as 1890 due to the histology research of Richard Altmann. Mitochondria have been postulated to originate in eukaryotic cells as engulfed endosymbiotic descendants of α-proteobacteria (4, 5, 41). Mitochondria produce energy in the form of adenosine triphosphate (ATP) and play a part in maintaining metabolic homeostasis in the cell. These dynamic organelles are able to grow, divide and fuse into granular or reticular structures (65, 68, 87, 156) and localize to areas of the tissue that require more energy. The distribution and organization of mitochondria changes across different tissue types, with cardiac muscle having a high mitochondrial content, while skeletal muscle has a relatively low content per gram of tissue (46, 52, 65)The mitochondrion is divided into four compartments: 1) the outer mitochondrial membrane (OMM), 2) the intermembrane space (IMS), 3) the inner mitochondrial membrane (IMM), and 4) the matrix.

Mitochondria are unique organelles that contain their own set of genomes (4, 51, 65, 72, 107, 120, 124). The genome encodes 13 of the ≈1200 proteins responsible for oxidative phosphorylation (OXPHOS (5) which is the process responsible for generating most of the ATP in the cell. The remaining proteins that are found in the mitochondria are nuclear-encoded precursors, which are synthesized outside of the mitochondria in the cytosol (72, 134). These precursor proteins are imported by chaperones into mitochondria through the protein import machinery(12, 53, 58, 67, 104, 139). The precursors typically enter through the Tom (translocase of the outer mitochondrial membrane) and Tim (translocase of the inner mitochondrial membrane) complexes (11, 34), and are incorporated into the electron transport chain (ETC). The ETC is responsible for OXPHOS and energy generation. The OMM is implicated in apoptosis, due to an increase in membrane permeability, leading to a disruption in mitochondrial

function, and a release in pro-apoptotic proteins(30, 55, 116). The IMS serves as the region where protons from the matrix by the ETC are expelled to in order to create a electrochemical gradient that allows ATP synthase to produce ATP (42, 69, 70). The IMM is characterized by membrane folds that maximize surface area, and are termed cristae. The IMM separates the IMS and the matrix, and contains the ETC and its components (58). The matrix, the final component, contains about 2/3 of the total protein in a mitochondrion, and contains hundreds of enzymes, special mitochondrial ribosomes, tRNAs, and multiple copies of the mitochondrial DNA genome (34). The major functions include the oxidation of pyruvate and fatty acids, and the citric acid cycle.

1.1 Mitochondrial Structure and Function in Muscle

Skeletal muscle has a low basal level of mitochondrial content (46). However, muscle tissue is incredibly plastic in terms of mitochondrial turnover. In skeletal muscle, there are two distinct populations of mitochondria; one positioned close to the sarcolemma (SS mitochondria), other embedded among the myofibrils (IMF mitochondria) (1, 53) .With physiological stimuli such as exercise, muscle tissue expands the reticular mitochondrial network (32, 65, 74, 89) and contains more mitochondria to meet the new metabolic demands. The concentration of mitochondria and formation of this reticular network is governed by mitochondrial turnover and mitochondrial fission and fusion. Mitochondria are also involved in cellular handling of Ca^{2+}, via their uptake and release ability through their mitochondrial permeability transition pore, and can also play a role in apoptosis and programmed cell death (39, 97).

1.2 Electron Transport Chain

The ETC is a complex of proteins responsible for the production of ATP from the products of lipid oxidation, citric acid cycle products and amino acid oxidation. The ETC contains a series of redox reactions, in which electrons are transferred from donor molecule to an acceptor molecule. Five complexes are found in the ETC (Complexes I-V), which functions to carry electrons to the terminal electron acceptor, oxygen. The reduced equivalents of NAD and FAD deliver the electrons to the complexes, NADH to complex 1 and FADH to complex 2. The electron flow, combined with the translocation of protons from the matrix to the intermembrane space (via complexes I, III and IV) generate an electrochemical proton gradient or membrane potential ($\Delta\Psi_m$) across the inner mitochondrial membrane. This gradient is utilized by ATP synthase to generate ATP from ADP and inorganic phosphate (Pi). Over the course of this process, some of the electrons can leak out of this pathway, and reduce O_2 to superoxide radical ($O_2^{\bullet-}$), leading to the production of reactive oxygen species (ROS). ROS can be detoxified by the action of antioxidant enzymes such as superoxide dismutase, catalase, and glutathione peroxidase (5, 85, 134). In cases where the ROS production outpaces the ability of antioxidants to scavenge, a buildup of ROS can occur and cause mitochondrial dysfunction and oxidative stress, which is highly damaging to cellular components. ROS buildup has been linked to multiple pathologies including neurodegenerative diseases, diabetes, cancer and premature aging (2, 16, 20, 30, 68, 143). Higher energy-demanding tissues like muscle are more susceptible to such oxidative stress.

2.0 Mitochondrial Turnover

Mitochondrial Turnover is a process by which optimal functioning of the mitochondrial pool is achieved, and energy homeostasis is maintained. The mitochondrial network consists of many

mitochondria, which can be added or removed from the network via fusion or fission (7, 23, 39, 65, 147). The turnover of these organelles is comprised of two processes: the creation of new and healthy mitochondria via biogenesis, and the removal of old and dysfunctional mitochondria via autophagy (mitophagy). This balance can be tilted toward either biogenesis or autophagy, depending on the stimulus. Exercise and pharmacological treatment are able to activate signaling events leading to elevations in the activity of downstream proteins like transcription factors responsible for impacting the expression of nuclear genes encoding mitochondrial proteins (NUGEMPS) (33, 65, 72, 87, 124, 134). This leads to the mRNA expression of NUGEMPS, which are translated into precursor proteins attached to a chaperone and transported to the site of mitochondrial protein import machinery (58, 111, 139). Precursor proteins are then guided to the appropriate compartments, such as the matrix, or inner or outer mitochondrial membrane, and integrated into the mitochondrion. Conversely, an elevation in the mitophagy to mitochondrial biogenesis ratio will lead to the activation of mitochondrial degradation via the autophagosome-lysosome pathway (ALP), and this mechanism is regulated in a similar coordinated signaling mechanism. Potential triggers of mitophagy include hypoxia (74, 90, 123), ROS (2, 30, 52, 143) or a decrease in mitochondrial membrane potential (30, 55). Enough damage done to the mitochondrion will result in the dysfunctional portion of the mitochondrial reticulum being sectioned off by fission, and specifically targeted for degradation (21, 29, 55). Dysfunction in the proper maintenance of mitochondrial turnover has the potential to lead to the development of cardiovascular diseases (36, 83, 135), cancer (5, 20, 143), metabolic impairment (5, 19, 36, 57, 96), and earlier aging.

2.1 **Mitochondrial Biogenesis in Muscle**

As previously mentioned, skeletal muscle is a very plastic tissue that can adapt to the metabolic demands placed upon it. These metabolic demands can come from either muscle regeneration, the development of the myoblast into a myotube, or, through exercise-stimulated mitochondrial biogenesis (37, 46, 61, 63, 66, 70, 74, 79, 85, 87 92, 107, 116, 126, 151). As a muscle develops from the immature myoblasts into myotubes, the cells undergo a switch in metabolic profile from one that is glycolytic to a primarily oxidative phosphorylation profile with complex mitochondrial networks built to support the metabolic demands of the new muscle fibre. Along with the increase in mitochondria, there is a reorganization of the mitochondrial networks to areas of greatest metabolic demand (37, 49, 145, 147, 155).

When the metabolic demands placed on the tissue exceed the capacity of the existing mitochondrial networks, there is a cascade of signaling events that activates transcription factors such as cAMP response element-binding protein (CREB). The CREB transcription factors function to modify and activate other transcription factors, which facilitate an increase in mitochondrial content in a process termed mitochondrial biogenesis. The peroxisome proliferator- activated receptor gamma coactivator alpha (PGC-1α) has been identified as the master regulator and transcriptional coactivator that facilitates the activation of these transcription factors in muscle and other tissues (17, 34, 56, 156, 62, 64, 66, 71, 74, 81, 86,93, 95, 98, 112,127, 134–136,140,153). Additional research on PGC-1α had revealed that it interacts with the nuclear respiration factors (NRFs) 1 and 2 (25, 42, 61, 72, 82, 109, 119, 120, 124, 133) in order to facilitate mitochondrial biogenesis by promoting the transcription of NUGEMPS. The result is an increase in NUGEMP mRNAs, which includes components of the mitochondrial ETC, as well as mitochondrial transcription factor A (Tfam), a protein that serves to interact with

the mtDNA to facilitate the transcription and mRNA synthesis of the 13 mitochondrially-derived proteins (27, 51, 67, 82, 87, 106, 107, 120, 147). The increase in mitochondrial content allows for improved metabolic function and exercise capacity. The following chapter will examine the role of exercise in mitochondrial biogenesis in muscle.

2.1.1 Mitochondrial Biogenesis and Exercise Training

The pioneering work of Dr. John Holloszy in the 1960's on rats undergoing strenuous bouts of treadmill running revealed that several ETC components increased approximately 2-fold in hindlimb muscles in response to the training, while the total protein content of the mitochondrial fraction increased approximately 60% (62). This study served as a strong foundational link between exercise and mitochondrial biogenesis. Exercise training, for the most part, can be broken down into endurance training and resistance training. Endurance training has been implicated with mitochondrial biogenesis by increasing the lactate threshold (32, 40), OXPHOS components of the ETC (66, 69) and oxygen utilizing capacity (65, 68, 72, 74, 94). Endurance training can vary by frequency, intensity, time and type (89), and consists of repetitive submaximal contractile activation of large muscle groups in the body. Depending on the intensity of the exercise regimen, between 50-100% increases in mitochondrial content in a 6 week period was observed, resulting in elevated endurance capacity and higher maximal oxygen consumption. Conversely, resistance training does not serve to expand total mitochondrial content; rather, it functions to optimize the quality of currently present mitochondria via functional improvement (38).

Continuous contractile activity triggers four main signalling molecules: 1) a rise in cytosolic calcium (Ca^{2+}) accumulation, sensed by Calcium/calmodulin-dependent protein kinases (CaMKs) (63, 118, 153); 2) phosphorylation of p38 MAPK (6, 10, 85, 153), 3) phosphorylation

of AMP-activated protein kinase (AMPK) in response to decreases in ATP to AMP ratio (18, 72); and 4) production of reactive oxygen species (ROS) (68, 153). These pathways facilitate the activation of the master regulator of mitochondrial biogenesis, PGC-1α.

2.2 Cell Culture Model of Mitochondrial Biogenesis

In order to elucidate the mechanisms of mitochondrial biogenesis in muscle, cell culture models can be used to provide an isolated and well-controlled environment with minimal confounding variables. Typically when investigating biochemical processes, *in-vitro* studies allow scientists to examine the effect of drug treatments or knockouts on a specific cell type, while *in-vivo* treatment involves the whole organism, and may lead to other confound effects leading to adverse reactions or offspring that are not viable past development. Cell culture offers an alternative avenue where drug safety/knockout effects can be tested with great specificity on one cell type. When examining muscle cell biogenesis *in vitro,* it can be separated into two sections: differentiation-based biogenesis and chronic contractile activity (CCA)-based biogenesis (31, 65, 133).

Differentiation-induced mitochondrial biogenesis occurs during the cell developmental process, by which quiescent muscle stem cells are activated by stimuli from their environment. The stem cells are stimulated to undergo division, creating a replicate of the original stem cell and a myogenic progenitor cell called a myoblast (155). The myoblast undergoes differentiation in which several myoblasts fuse into multinucleated contractile units called myotubes (59, 146). The process of myogenesis requires considerable amounts of energy, leading to the activation of regulatory pathways and mitochondrial biogenesis in order to support the elevated metabolic demands (138). The knockout of mtDNA in myoblasts impaired differentiation, while proliferation remained unaffected (60). Additionally, blocking mitochondrial protein synthesis

with the inhibitor chloramphenicol also stunted differentiation (56). Taking these two observations together, it appears that differentiation is a powerful stimulus for mitochondrial biogenesis. The importance of mitochondrial networks and biogenesis is also supplemented by the discovery of the remodeling of previously formed mitochondrial networks in myoblasts preceeds the formation of new mitochondrial networks that are optimized to support myotubes (7, 23, 99). The myoblasts are much more reliant on glycolysis and their mitochondria are not as metabolically potent as those of a myotube (125).

Chronic Contractile Activity (CCA) is the second model for mitochondrial biogenesis, and it involves electrically-induced chronic contractions (31, 78). The electrical activation in motor neurons during *in vivo* training can be mimicked with electrical stimulation. *In vitro* stimulation of myotubes involves the input of parallel platinum wires attached to an external stimulator that sends a current through the myotubes, depolarizing them and initiating contractile activity. Previous studies have indicated that 3 hours of stimulation over the course of 4 days is sufficient to elucidate significant mitochondrial adaptations (31, 94, 133). The muscle cells adapt in a manner similar to that during exercise. Cell culture offers the additional benefit of investigating the effect on muscle tissue alone, removing the systemic whole body effects of exercise. CCA stimulates action potentials, causing calcium release and augmenting the levels of COX proteins, Tfam, NUGEMPS and PGC-1α, thus showing mitochondrial biogenesis (2, 69, 133).

2.3 Mitophagy

Mitophagy is the process by which damaged and dysfunctional mitochondria are removed from the mitochondrial network and broken down into simple amino acids and lipids (23, 29, 66, 122, 125). Mitophagy functions as a quality control mechanism in the cell to preserve optimal

mitochondrial function. The term was adapted from autophagy, where mitophagy refers to the specific autophagy of mitochondria. Dysfunctional mitochondria exert damaging effects on the cell, and to manage this risk, mitochondria display several lines of quality control mechanisms. Some of these mechanisms include mitochondria-specific chaperones and proteases that protect against misfolded proteins at the molecular level, as well as antioxidants to scavenge ROS produced by the mitochondria (104). However, if the damage accrued to the mitochondrion cannot be handled by these mechanisms, dysfunctional mitochondria will be removed from the network by fission proteins (7, 67) and targeted for mitophagy. Mitophagy is typically triggered due to loss of mitochondrial potential, leading to an impairment in the ability of the ETC to produce ATP, an increase in ROS production and subsequent damage to the cell. Once targeted, E3 ubiquitin ligases will bind to mitochondrial proteins on the outer membrane, and stimulate the activation of adaptor proteins like p62 that bind to microtubule associated protein 1 light chain 3 (LC3) proteins. LC3 is lipidated from LC3-1 to LC3-2 by autophagy related protein 3 (Atg3) and this begins to form a vesicle encapsulating the mitochondrion, forming a structure called an autophagosome (48, 54, 55). The autophagosome is transported along microtubules to the lysosome, until it interacts with the lysosome associated membrane proteins-1 (LAMP-1) and LAMP-2, and is engulfed into the lysosome. The lysosome uses its acid environment to break down the contents, with the help of proteases such as cathepsin D that function to degrade proteins and activate precursors of bioactive proteins in pre-lysosomal compartments.

2.3.1 Mitophagy Pathways

There are multiple autophagic proteins that are thought to be potential players in mitophagy (23, 29, 66, 80, 93, 122), the most characterized of which involves PINK-1 and Parkin. Once the mitochondrial membrane potential is reduced, the mitochondrial serine/threonine kinase,

Phosphatase and tensin homolog-induced putative kinase 1 (PINK-1), begins to assimilate on the outer mitochondrial membrane. The binding of PINK-1 recruits Parkin, a cytosolic E3 ubiquitin ligase that has been linked to Parkinson's disease (7, 23, 29, 55, 122). In healthy mitochondria with an optimal mitochondrial membrane potential, PINK1 is imported into the mitochondrial inner membrane, where it is cleaved by PARL and consequently degraded (93). The binding of Parkin to the mitochondrial membrane components like voltage-dependent anion channel (VDAC) results in the ubiquitination of mitochondrial components. PINK-1 will also phosphorylate the ubiquitin chain, recruiting cytosolic autophagic proteins such as the ULK and PI3K complex to the phagophore assembly site. The adaptor protein p62 also binds to the ubiquitin structure, and facilitates the binding to the LC3-2-phagosome structure around the mitochondrion, thereby forming the autophagosome.

Another pathway of mitophagy operates via BNIP-3 and NIP3-like protein X (NIX). BNIP3 and NIX are proteins related to the BH3-only family, which induce both cell death and hypoxia-mediated autophagy in cancer (26, 55, 92) and heart disease (92). The mechanism by which BNIP3/NIX begins is with the activation and insertion of BNIP3 and NIX and the opening of MPTP through an interaction with BAX or BAK, or a component of the mitochondrial permeability transition pore (MPTP). This leads to a loss of mitochondrial membrane potential, generation of reactive oxygen species, and eventual mitophagy. This system of mitophagy has garnered contrasting research, with some studies suggesting that this form of autophagy is necrotic in nature (92), while other studies show that in cases like cardiac hypoxia, this autophagic pathway can be protective (92). A second model of NIX-dependent mitophagy assumes that NIX possesses an ability to recruit autophagy components, independent of triggering mitochondrial depolarization (101, 149). NIX deficiency does not generally impair

autophagy in erythroid cells, but instead interferes with the targeting of mitochondria to autophagosomes. A study consistent with these findings found that NIX functions as an adaptor protein that recruits components of the autophagy machinery to mitochondria (101). A third model of NIX-dependent mitophagy is derived from a recently proposed model of crosstalk between autophagy and cell death pathways, where both BNIP3 and Beclin-1 were initially identified as BCL2 or BCL-XL-interacting proteins. The theory is that BNIP and NIX are able to competitively bind Beclin-1, and in this manner attenuate BCL-2 binding and inactivate Beclin-1 (149).

2.4 Protein Import Machinery

Mitochondria consist of two membranes, the outer membrane and the folded inner membrane, and two aqueous compartments, the intermembrane space and the matrix containing mitochondrial DNA (58, 139). Mitochondria play crucial roles in cellular energy production and in the metabolism of amino acids, iron, and lipids, as well as in apoptosis. Proteome analyses indicate that mitochondria contain approximately 1,500 different proteins in humans (137). Although mitochondria possess their own DNA, only about 1% of all mitochondrial proteins are encoded by the mitochondrial genome. The vast majority of mitochondrial proteins are synthesized as precursor proteins in the cytosol and are imported mainly by a post-translational mechanism. In order for these proteins to reach the inner mitochondrial membrane, they must be transported through the mitochondrial import machinery system. In the canonical pathway, the matrix-destined proteins are typically tagged with a N-terminal that function as targeting signals, and are imported through the translocase complex of the outer membrane (Tom), and the translocase complexes of the inner mitochondrial membrane (Tims) (58). The Tom complex is

responsible for proteins destined for the inner membrane space, matrix destined proteins, and the inner mitochondrial membrane destined proteins (11, 12, 34).

Once the target proteins enter the Tim complexes, they will localize to either the Tim23 or the Tim22 complex, depending on the destination. The proteins with a matrix-targeted signal will interact with the Tim23 complex, while those that lack this signal will interact with the Tim22 complex (11). The matrix-destined proteins enter the Tim23 complex, after which the precursor sequence of the proteins is clipped off, and they are pulled into the matrix via the chaperone protein mtHSP70 (104). This protein will then be exchanged with another chaperone, mtHSP60, which will deliver it the transcription factor to the nucleus and allow it to exert its genomic effects.

3.0 Retinoic Acid

Retinoic acid is a derivative of vitamin A, also known as retinol. Sources of Vitamin A include carrots as provitamin A (which can be converted into retinol) and liver tissue as retinyl esters. Upon ingestion of retinol, it is transported to the liver via cytosolic retinoid binding proteins (CRBP's) where it can undergo esterification to retinyl esters and eventual transport for utilization for vision in the retina, or transport to other cell types and consequent conversion into retinaldehyde. Retinaldehyde is then broken down by retinoic aldehyde dehydrogenase 1 (RALDH-1) into retinoic acid isomers (20). Retinoic acids are then bound to cytosolic retinoic acid binding proteins (CRABPS), and shuttled to neighboring cells, where they can diffuse through the lipid bilayer and interact with nuclear and mitochondrial receptors to exert their genomic effects. Retinoic acids control over 530 genes (9), which include genes responsible for metabolic and developmental processes. The utilization of retinoic acid in the organism is tightly

regulated, as effects vary on location, concentration and timing. The importance of these transporters will be further explored in chapters 3.1 and 3.2.

Two naturally occurring RA isomers, 9-cis retinoic acid (9-cisRA) and all-trans retinoic acid (ATRA), are of great interest due to their natural presence in the body, as well as due to their high affinity for retinoid receptors. Recent studies have investigated the effects of retinoic acid treatment in adipose, neurons and liver tissue (7, 96, 101, 129, 131, 144, 152, 154), and have shown significant elevations in mitochondrial biogenesis and oxygen consumption, which suggests they could affect muscle mitochondrial biogenesis. In these studies, both of the RA isomers facilitated an increase in PGC-1α mRNA levels, and ATP production levels, as well as SDHA-1, a marker of mitochondrial content (14, 43). In L6 muscle cells, retinoic acid treatment led to elevations in glucose transporters GLUT1 and GLUT 4 mRNA (125).

3.1 Retinoic Acid and Nuclear Gene Expression

Retinoic acid isomers 9cisRA and ATRA exert their genomic effects via the retinoic acid response elements (RARE), which involve the RAR and RXR receptors. The 9cisRA isomer is able to bind and activate both RAR and RXR, while ATRA only targets RAR. Each of these receptors can be further classified into 3 different subtypes, α, β, and γ, which have some overlapping functions. RAR are able to heterodimerize with other receptors such as PML (103), these receptors typically bind with RXR to produce RARE sites, while RXR receptors can also form heterodimers with members of the PPAR/thyroid/steroid/vitamin-D families of receptors (14, 43, 84, 108). As previously mentioned, RARE sites are prominent in many tissues and regulate the transcription of a wide array of genes, so the focus of this review will revolve around those relevant to muscle and muscle cell metabolism.

The effects RA exerts on the cells can depend on the presence of the two main RA transporters in the cell, CRABPs and fatty acid binding proteins (FABPs) (110, 121, 144). Tissues with higher levels of CRABPs will transport the RA to RAR/RXR RARE sites that promote cell cycle arrest and differentiation, while the RA bound to FABP-5 will be shuttled to PPAR/RXR RARE sites, and be involved in cell proliferation and energy homeostasis (110, 121, 144). This direct activation of the nuclear genome leads to the transcription of a wide array of genes associated with mitochondrial biogenesis, some of which focus on PPAR activation (Figure 1). The binding to FABP-5 will result in the RA being carried to PPAR receptors. Once FABP-5 delivers the RA to the receptor, RA will bind to PPAR and activate the transcription of proteins responsible for energy homeostasis and insulin responses (8, 17, 113, 115, 126). A similar form of binding occurs with 9-cisRA and RXR/PPAR receptors. The 9cis-RA isomer can bind both receptors, and once it binds to PPAR, it will initiate the transcription of proteins responsible for energy homeostasis and insulin responses as well. The potency of 9cisRA in terms of activating both RA receptors could explain why in research in diabetic rats, 9cis-RA proved more effective in restoring mitochondrial function than ATRA.

The indirect gene activation is accomplished via the binding of RA to RAR receptors found in the lipid rafts of the cell membrane, and eventual activation of kinases. Upon binding, a cascade of kinase activity is initiated, and these kinases include p38 MAPK or p42/44 MAPK, AMPK and CAMKII (9, 73, 146). The activation of kinases leads to PGC-1α transcription and phosphorylation, facilitating the activation the NRF/PPAR families of nuclear receptors, leading to transcription of mitochondrial proteins (120, 124). In addition to phosphorylating PGC-1α, RA's can also phosphorylate Mitogen and Stress-activated protein Kinase 1 (MSK-1), which will then phosphorylate a serine on the ligand binding domain (LBD) of RAR. This activation leads

to the recruitment of cyclin H/cdk 7 complex, which acts to phosphorylate RAR and allow it to be re-recruited to RAREs, where it will dimerize with RXR and initiate the transcription of target genes. In this configuration, RXR is dimerized in a non-permissive manner, meaning that only if RAR is bound will the RXR be able to be targeted by a ligand.

Overall, the signalling of retinoic acids is complex, and for the sake of simplifying pathways to those relevant to muscle cells and mitochondrial biogenesis, the focus of this review was to examine the activation of mitochondrial biogenesis via RARE and PPAR activation, or the indirect activation via the kinase activation pathway.

3.2 Retinoic Acid and Mitochondrial Gene Expression

Several mitochondral genes have been shown to be regulated by retinoic acid. These include NADH dehydrogenase subunit 5 (ND5; 5), cytochrome c oxidase subunit I mRNA, and 16srRNA, ATPase 6, ATPase 6, 8, and ND1, as well as protein levels of ATPase subunit a (6 gene) in a dose-dependent manner that peaked at 1nM (14, 43). When examining the possible mechanisms by which RA could be modulating the expression of these genes, there have been three potential mechanisms that have been identified: insulin-glucose mediated arch, the elevation of Tfam, and finally, the activation of RARE sites on the mtDNA. The optimal dose for mitochondrial functioning was found to vary across genotypes (43) . In a rat model mimicking human diabetes mellitus, is was observed that diabetic rats required more Vitamin A to attenuate the diabetic symptoms by restoring glucose-stimulated insulin secretion and reducing glucagon secretion (44) .

The second potential mechanism that has been identified came from the observation that increased dietary vitamin A can upregulate Tfam protein expression in adipocytes (14, 43, 44).

The mechanism by which this occurs is still unknown. It has been postulated that this could either be a direct effect on Tfam transcription, or via posttranscriptional regulation of Tfam by increased mtDNA levels. In addition to the activation of RARE sites in the nuclear genome, it has been shown that the mitochondria also possess RARE sites in their DNA, located in the heavy strand (43). This area of research is somewhat controversial. Receptors for peroxisome proliferators have been shown to localize to mitochondria, and retinoid receptors could potentially dimerize with these receptors and facilitate their activity. Recent research has shown the presence of CRABP I and II in mitochondria. Their function in mitochondria is currently under investigation.

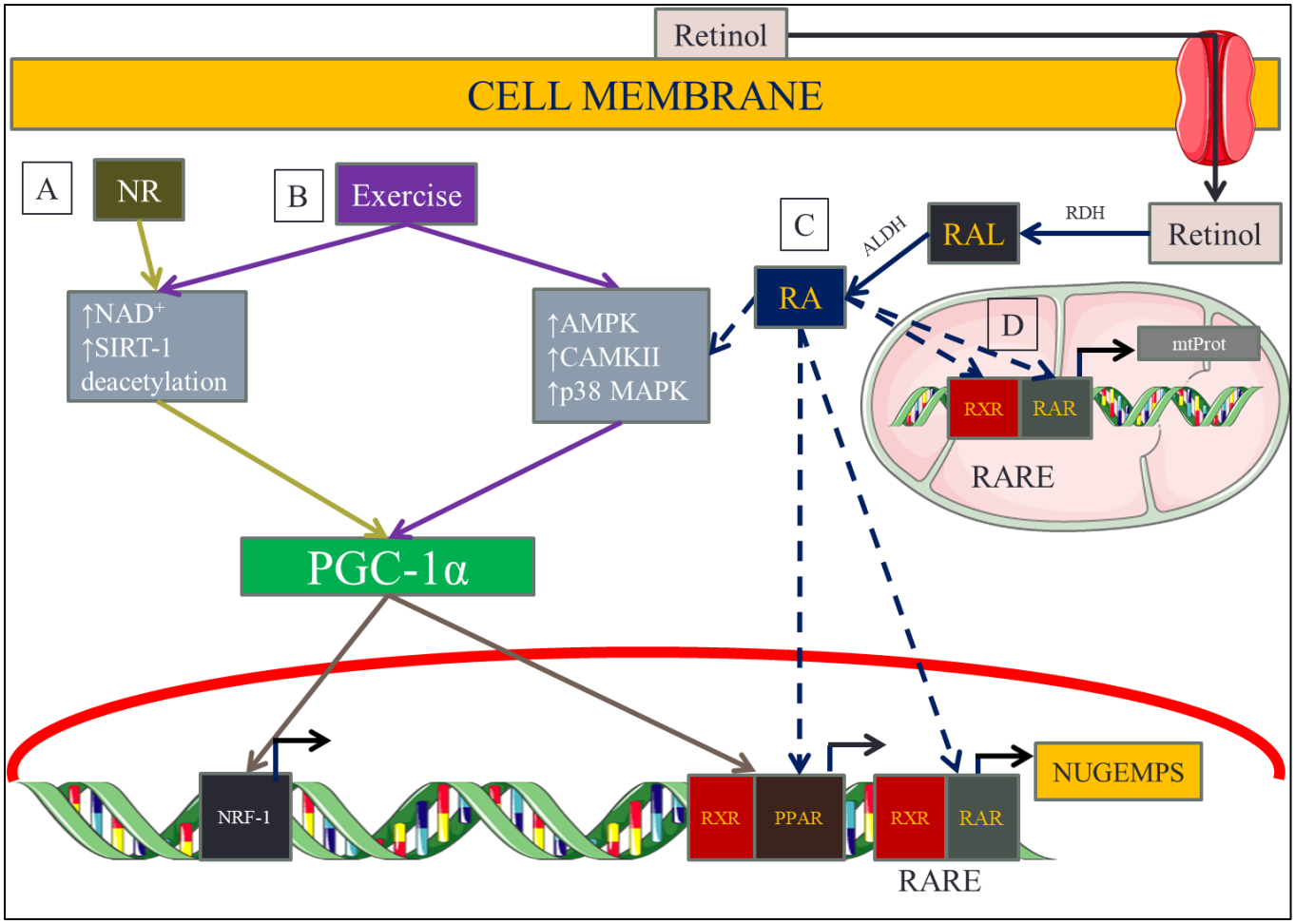

Figure 1. *Schematic of the mechanisms of RA isomer/CCA/NR pathways that facilitate mitochondrial biogenesis*. A) NR-mediated pathway facilitating mitochondrial biogenesis. B) Exercise-mediated pathways facilitating mitochondrial biogenesis. C) RA-isomer mediated pathways leading to mitochondrial biogenesis. D) RA-isomer mediated activation of RARE receptors in mtDNA, leading to eventual mt protein translation.

3.3 Retinoic Acid effect on Mitochondrial Biogenesis in Other Tissues

The activity of retinoic acid on mitochondrial biogenesis has been characterized in tissues other than muscle. When examining the effects of retinoic acid isomers on human liver tissue (HepG2 cells), treatment with 1μM of ATRA led to elevations in PGC-1α, β and NRF-1 mRNA levels (72, 131), all associated with mitochondrial biogenesis. There was also a significant elevation in ATP levels in cell culture with ATRA treatment. In studies that looked at murine WAT cell

tissue, treatment with ATRA lead to significant elevations in oxygen consumption, an increase in Mitotracker Green staining , TFAM, NRF-2, PGC-1β, PPARα mRNA and the mtDNA to nuclear DNA ratio (129). These effects also varied depending on the fat depot. Overall, the mitochondrial biogenesis augmentation in adipocytes appeared to be mediated via the PGC-1-NRF-1-TFAM axis. In SH-SY5Y neuroblastoma cells, those treated with RA for 7 days showed increased and long strip-shaped mitochondria with well-developed mitochondria cristae, compared to immature and spherical mitochondria observed with vehicle treatment. SH-SY5Y cells treated with RAs led to elevations in PGC-1α, COX5a, and NRF-1, all mRNAs associated with mitochondrial biogenesis (141).

4.0 Nicotinamide Riboside

Nicotinamide Riboside (NR) is a nucleoside, which incorporates nicotinamide and ribose. NR is a precursor of nicotinamide adenine dinucleotide (NAD). It is present in yeast, bacteria, and mammals, and is a source of Vitamin B3 (28, 77, 105). Yeast-containing food products and milk-derived products such as whey fractions have been reported to contain the nutrient, albeit in very small doses. The metabolic fate of NR in elevating NAD^+ levels in mammalian tissues was first investigated by Rowen and Kornberg in 1952 (28). This was further expanded on by the work of Charles Brenner (13, 130), who described the human nicotinamide riboside kinases (Nrk1 and Nrk2) as potential players in mediating NR metabolism. Further research showed that this pathway is independent of nicotinamide metabolism, and that NR is a potent stimulator of NAD^+ production in several cultured mammalian cell types, including mouse and human cells. Increases in NAD^+ were in some cases as high as 270% of controls (15). Together, this literature suggested that nicotinamide riboside has a unique metabolic pathway to synthesize NAD^+ independent of other studied Vitamin B3 compounds, and is very potent in enhancing NAD^+

levels. NAD^+ is a key metabolite, used in basic energy metabolism processes such as glycolysis, the citric acid cycle, and mitochondrial electron transport. Previous literature on NR function has demonstrated that NR increases insulin sensitivity and induces mitochondrial biogenesis (28), and it exhibits neuroprotective effects in a mouse model of Alzheimer's (28). In July 2013, nicotinamide riboside became available in supplement form with the brand name NIAGEN (Chromadex Incorporated, Irvine, California, USA).

4.1 Nicotinamide Riboside Pathway

NR has two potential pathways that it can participate in once it is taken up and metabolized by the cell. The first pathway is conversion into nicotinamide (NAM) via the action of purine nucleoside phosphorylase, followed by conversion of NAM into nicotinamide mononucleotide (NMN) by nicotinamide phosphoribosyl transferase (13, 90, 148). The second pathway involved the direct conversion of NR into NMN by the action of nicotinamide riboside kinases 1 and 2 (NRK1, 2). Both pathways lead to the synthesis of NMN, and from this point NMN is converted into NAD by NMN adenylyl transferase. Once NAD^+ is synthesized, it can then be utilized in NAD consumption processes by Sirtuins, CD38, and polyADPribosylpolymerases (PARPs) (15, 142), also named the NAD consumers. The PARP pathway is activated in response to DNA damage (e.g. DNA strand breaks) and genotoxic stress, and it utilizes NAD^+ to catalyze a reaction in which single strand breaks are repaired, while CD38 uses NAD^+ to generate cADP-ribose, a secondary messenger. Lastly, the sirtuin pathway is one of particular interest, with NAD-dependent deacetylase sirtuin-1 (SIRT-1) implicated in the deacetylation of PGC-1α, which would lead to an increase in PGC-1α activity (18, 45). However, members of PARP and the cADP-ribose synthase family have greater affinity for NAD^+ compared to sirtuins. These PARPS critically impact intracellular NAD^+ levels, and the remaking concentration of NAD^+

determines whether there is sirtuin activation. Multiple studies also suggested that PARP activity constitutes the main NAD^+ catabolic activity, which forces cells to synthesize NAD^+ from *de novo* or salvage pathways.

4.2 Nicotinamide Riboside and Mitochondrial Biogenesis in Muscle

The effects that NR exerts on elevating mitochondrial biogenesis have been characterized (77, 90, 130, 142, 148), and involve NR increasing the NAD^+ levels in mammalian and yeast cells (95, 142), and in turn activating sirtuin 1 (SIRT1) in order to deacetylate PGC-1α. Mammals contain seven sirtuins (SIRT1–7), located in different subcellular compartments (22, 95). The nucleus contains SIRT1, SIRT6 and SIRT7, the cytosol contains SIRT2, and mitochondria contain SIRT3, SIRT4 and SIRT5. The sirtuins are implicated in a wide variety of biological functions including control of cellular metabolism and energy homeostasis, aging and longevity, transcriptional silencing, cell survival, proliferation, differentiation, DNA damage response, stress resistance, and apoptosis. Sirtuins are normally activated during situations of energy deprivation, and act as metabolic sensors of the cells, since their activity is coupled to changes in the cellular NAD^+/NADH ratio (77). NR first came into play as a potential agonist of mitochondrial biogenesis in research done by Canto et al (7, 18, 142). The goal of this study was to examine the avenue of increasing the overall bioavailability of NAD^+ by supplementing with NR, rather than blocking NAD^+ consumption pathways PARP and CD38, in order to promote a shift towards Sirtuin-mediated NAD^+ usage. It was also found that NR supplementation dose-dependently increased intracellular NAD^+ levels in murine and human cell lines, with maximal effects at concentrations between 0.5 and 1 mM. In addition to increasing NAD^+ levels, increases in mitochondrial content and function were also found with NR treatment, in brown adipose tissue as well as in muscle (117). Additionally, NR has also been used to treat myopathy-

induced mitochondrial deficits, as well as age-related disorders (77, 91). Reduced NAD^+ levels have been reported in mitochondrial and age-related disorders, and NAD^+ levels also decline with age (148, 150).

5.0 Research Objectives

Based on the Review of Literature provided here, the purpose of this thesis was:

1) To examine the effects of retinoic acid isomers 9cisRA and ATRA on muscle cell mitochondrial biogenesis and autophagy-related proteins;
2) To investigate how Chronic Contractile Activity and Retinoic Acid promote mitochondrial biogenesis, and if the combination of the two treatments elevates biogenesis to levels higher than either condition alone;
3) To investigate how Retinoic acid interacts with a known agonist of mitochondrial biogenesis, Nicotinamide Riboside.

Chapter 2: Manuscript

THE EFFECTS OF RETINOIC ACID, NICOTINAMIDE RIBOSIDE AND CHRONIC CONTRACTILE ACTIVITY ON MITOCHONDRIAL BIOGENESIS IN SKELETAL MUSCLE CELLS

Nemanja Dovijarski and David A.Hood

Muscle Health Research Centre, School of Kinesiology and Health Science, York University, Toronto, Ontario, M3J 1P3, Canada

To whom correspondence should be addressed: Dr. David A. Hood, PhD

School of Kinesiology and Health Science

York University, Toronto, ON

M3J 1P3

Tel: (416) 736- 2100 ext. 66640

Email: dhood@yorku.ca

Abstract

Exercise is well known to be a potent inducer of mitochondrial biogenesis, showing elevations in mitochondrial content and function. Two nutritional compounds, the Retinoic Acid (RA) isomers and Nicotinamide Riboside (NR), have shown promise in terms of inducing mitochondrial biogenesis, and NR has been established as a supplement that can be taken to bolster mitochondrial content. Retinoic acid have facilitated biogenesis in other tissues, but to date have not examined skeletal muscle. We examined the effects of retinoic acid on biogenesis, by using it concurrently with NR, and with CCA, a cell culture model of exercise. After 4 days of treatment, our findings show elevations in the mitochondrial-encoded proteins with RA isomer treatment, while the nuclear encoded proteins were unaffected. NR elevated the nuclear encoded protein COX-IV, but had no effect on other nuclear proteins. In the RA isomer and CCA experiments, we observed elevations in COX I of ~3-fold with RA isomer treatment, while COX IV was augmented ~2-fold with CCA treatment. PGC-1α was also elevated with RA treatment by 2.2-fold. The combination of RA isomer and CCA treatments led to augmentation of PGC1-1α, which was further elevated by 2.5-fold. Interestingly Tfam was attenuated with RA treatment by 0.68-fold in the RA and NR series of experiments, while only 9cisRA suppressed the precursor form in the RA and CCA series of experiments. We speculate that RA exerts its effects mainly on the mitochondrial genome, and can function to supplement the dominantly nuclear DNA adaptations of CCA.

Introduction

Mitochondrial content in muscle tissue is regulated by a balance between breakdown (mitophagy) and synthesis (biogenesis). It is well established that exercise is a potent inducer of mitochondrial biogenesis in muscle, allowing for greater oxygen consumption and ATP generation (69, 76). Acute exercise creates an energy deficit and stimulates ATP turnover, leading to elevations in AMP, cytosolic Ca^{2+} flux, and ROS production (153). These processes lead to the activations of kinases such as AMPK, p38 MAPK, and CAMK, which are known to phosphorylate transcription factors, including a major regulator of mitochondrial biogenesis, PGC-1α (18, 35, 45, 63, 65, 67, 72, 87, 128, 134, 153). The recruitment of PGC-1α leads to the coactivation of PPAR and NRF families of transcription factors, which regulate the transcription of multiple proteins responsible for oxygen consumption and the biogenesis of the organelle (61, 67, 109, 125). Once new mitochondria have been generated, they fuse to form larger reticular mitochondrial structures which serve to minimize diffusion distances and maximize ATP production (7, 23).

While the effects of chronic exercise on mitochondrial content and function are well known (66), less information is available on the effects of possible nutrients that could facilitate, promote or synergize with exercise to produce a more pronounced effect on mitochondria. Such compounds could generate considerable scientific and commercial interest. The choice of nutrient to investigate may require a prior knowledge that it acts independently, or in cooperation with, the exercise signaling pathways. A derivative of Vitamin A called retinoic acid (RA) may facilitate mitochondrial biogenesis in a manner that appears partially distinct from that activated by exercise. RA isomers have been identified as potential agonists of mitochondrial biogenesis by studies that identified their ability to elevate mitochondrial content in adipocytes (129),

hepatocytes (96, 131) and neurons (144, 152). Retinoic acid is thought to target mitochondrial biogenesis through either ligand activation of the RXR-PPAR dimer, retinoic acid response element (RARE) sites found on nuclear and mtDNA, or indirect activation via kinase pathway phosphorylation of PGC-1α (153). The majority of the mechanisms that promote mitochondrial biogenesis are focused on PGC-1α activation, which increases the transcription of NUGEMPs and elevated fatty acid oxidation.

In addition to Vitamin A derivatives, we were intrigued by the potential activity of the derivative of Vitamin B3, nicotinamide riboside (NR), which operates via independent mechanisms. NR activates mitochondrial biogenesis through the NAD-Sirtuin pathway, which deacetylates and activates PGC-1α, launching a cascade of events that ends with the expression of nuclear genes encoding mitochondrial proteins (NUGEMPs) (94). It also provides higher levels of the electron acceptor molecule $NAD^{+,}$ which functions to promote ATP generation. Indeed, NR has in turn been commercialized as Niagen ®, a NR salt that can be consumed as a supplement. However in combination with exercise, it appeared to negatively affect the performance in rats performing a swimming test (79), possibly due to a reduction in fatty acid oxidation which is required to sustain the energy for prolonged exercise bouts. In contrast, retinoic acid has been found to elevate fatty acid oxidation in C2C12 muscle cells (3). We hypothesize that retinoic acid will have an adjunct effect on both CCA and NR, elevating biogenesis to a higher extent than either treatment alone through kinase-mediated PGC-1 activation and/or RARE site activation.

Thus, the primary objective of this study was to investigate the effects of RA isomers in myotubes, and the secondary objective was to examine how these RA isomers interact with NR

or chronic contractile activity (CCA), a cell culture model of exercise, to stimulate organelle biogenesis.

Methods

Cell culture. Passage 15 C_2C_{12} murine skeletal muscle cells were plated and proliferated on 6-well plates in growth media (GM), which is composed of Dulbecco's modified Eagle's Medium (DMEM) that was infused with 10% fetal bovine serum and 1% penicillin-streptomycin (P/S) antibiotic. Cells were incubated at 37^{o}C in 5% CO_2. Upon proliferation to 90-95% confluency, the growth medium was removed, and replaced with differentiation medium (DM (DMEM+ 1% p/s, 5% heat-inactivated horse serum)) in order to facilitate the differentiation of myoblasts into myotubes. The media was replaced daily. To investigate the effect of RA, DM containing 1μM of RA was added to 6-well plates containing myotubes for 4 days, with media replaced every 24h in drug experiments in Protocol 1, or pre and post CCA bout in Protocol 2. The appropriate dose was determined from previous research on mitochondrial biogenesis in other tissues, as well as dose-response studies. To investigate the effect of NR, DM containing 1mM of NR was added to 6-well plates. CCA plates were used in place of lids for the CCA-labelled cells, and cells were induced to contract over a 3h period. Cells were harvested 24h after the final CCA bout and/or nutrient delivery day.

CCA. Myotubes were stimulated on the 5th day of differentiation, as done in previous studies (31). Customized 6-well plate lids outfitted with two platinum wires per well were submerged into the media. The DM was replaced prior to stimulation and immediately after. For RA experiments, the DM was replaced with either DMSO-infused DM or RA-infused DM prior and

immediately after CCA. Electrical current was conducted for 3h a day (9V, 5Hz) with 21h recovery periods for a total of 4 days. Cells were collected 21h after the last CCA bout.

Protein Extraction. Cells were washed with ice-cold PBS and then removed from the plates via trypsinization 21h after the last day of CCA/24h after last NR and RA treatment. Protein extracts were prepared by suspending the cells in lysate buffer that was supplemented with phosphatase inhibitors and protease inhibitor cocktail. Cells were then frozen in liquid nitrogen and thawed in a 37^{o}C for 3 freeze-thaw cycles in order to lyse the cells. Samples were then centrifuged at 16,000g at 4^{o}C for 10 minutes, the pellets were discarded, and the supernatant fractions were collected and stored at -80^{o}C for subsequent immunoblotting analysis.

Immunoblotting. The protein concentration was quantified via Bradford Assay. Thirty μg of protein per sample was separated via electrophoresis on 10-15% SDS-polyacrylamide gels. The proteins were then transferred (Mini Trans-blot electrophoretic transfer cell, Bio-Rad, Mississauga, Canada) onto nitrocellulose membranes. After transfer, the membranes were blocked with 5% skim milk for 1h, and were then probed overnight at 4^{o}C with the appropriate primary antibodies. The full list of proteins and their respective antibodies are on Table 1. Blots were washed (3x5min) with wash buffer (Tris-buffered saline-Tween-20, 25mM Tris+HCl(pH 7.5), 1mM NaCl and 0.1% Tween-20), after which blots were incubated with the appropriate secondary antibody for 1h at room temperature. A second 3x5min wash was performed, and blots were visualized with chemiluminescence using Clarity Western ECL Substrate (Bio-Rad) and exposed in an imager. Signals were quantified with ImageJ Software (NIH, Bethesda, MD, USA) Values were normalized to the appropriate loading control.

Statistical Analysis. All data are represented as means ± SEM. Comparisons between groups in Protocol 1 (Figure 1) experiments and Protocol 2 experiments (Figure 2) were made with unpaired t-tests and two-way ANOVA tests in Protocols 1 and 2, with the two factors being either RA and NR, or RA and CCA. The kinase experiments comparisons between conditions were made with one-way ANOVA tests. Analyses were made with GraphPad Prism 7.0.Differences were considered significant if $p<0.05$

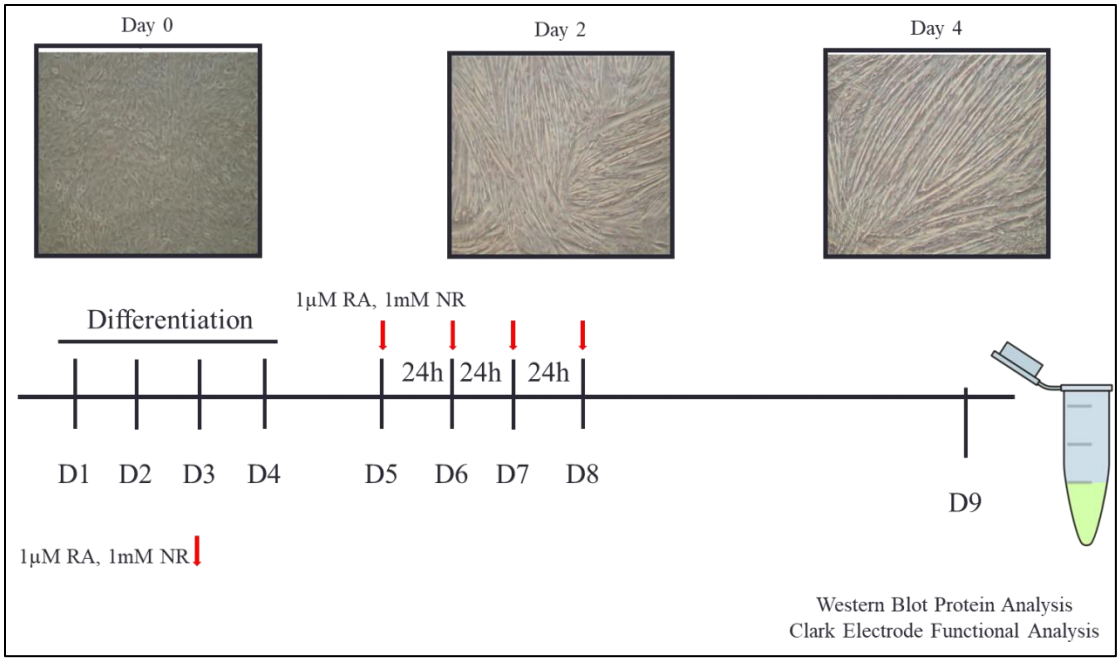

Figure 1**.** Protocol 1: the application of NR and RA isomers over 4 days post differentiation, in order to examine markers of mitochondrial biogenesis.

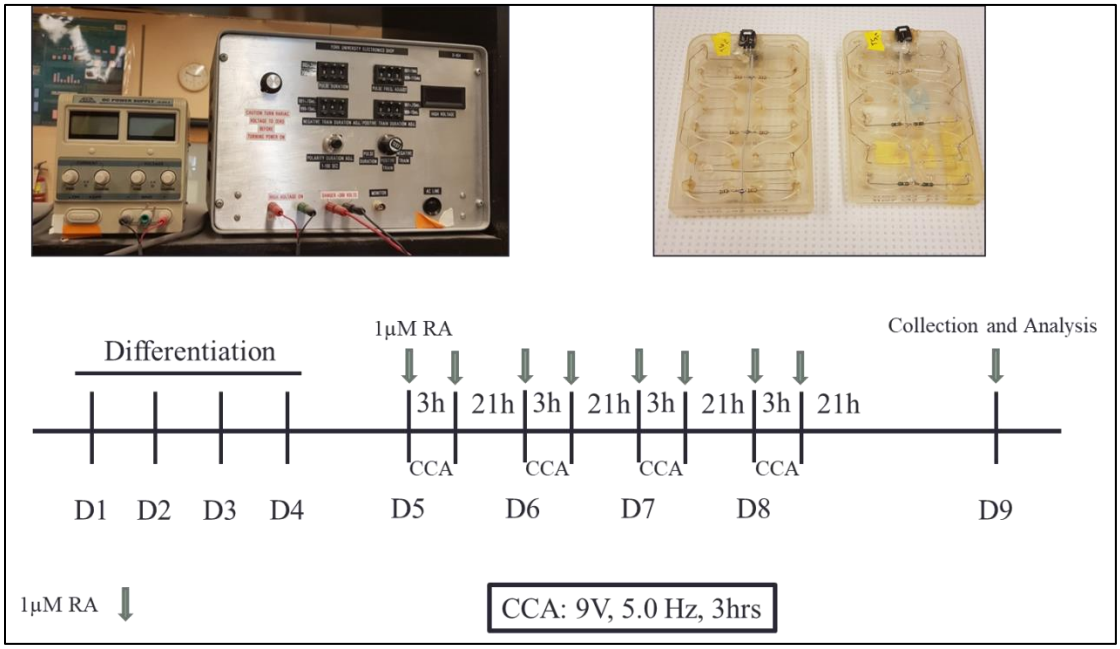

Figure 2**.** Protocol 2: the application of RA isomers as an adjunct to CCA over 4 days post differentiation, in order to examine mitochondrial turnover.

Table 1. Western Blot Proteins of Interest

Protein of Interest+ molecular weight	Company	Product No.	Primary Concentration	Secondary Concentration R=rabbit M=mouse
Kinases				
(p)-p38 (38kDa)	Cell Signalling	9211	1:1000	1:1000 R
(t)-p38 (38 kDa)	Cell Signaling	9212	1:1000	1:1000 R
(p)- CAMK II (50kDa)	Cell Signalling	3361	1:1000	1:1000 R
(t) - CAMK II (50kDa)	Cell Signalling	3362	1:1000	1:1000 R
(p)-AMPK (62kDa)	Cell Signaling	2532S	1:1000	1:1000 R
(t)-AMPK (62kDa)	Cell Signaling	2535S	1:1000	1:1000 R
Mitochondrial Biogenesis				
COX I (39kDa)	Abcam	Ab14705	1:500	4:2500 M
COX IV (20kDa)	Abcam	Ab14744	1:250	1:750 M
TFAM (24,28kDa)	in house	n/a	1:2500	1:3500 R
Citrate Synthase (38kDa)	Abcam	Ab96600	1:1000	1:1000 R
NRF-1	Rockland	200-401	1:1000	1:1000 R
PGC-1α	Millipore	AB3242	1:1000	1:3000 R
Loading Control				
Alpha-tubulin (50kDa)	Calbiochem	CP06	1:5000	1:1000 R
GAPDH (37kDa)	Abcam	Ab8245	1:100,000	1:5000 M
Autophagy				
LC3	Cell Signalling	2775	1:500	1:1000 R
P62	Sigma-Aldrich	P0067	1:6000	1:4000 M
Beclin	Cell Signalling	3738S	1:1000	1:1000 R
Protein Import Machinery + Chaperones				
Tim23	BD Biosciences	611222	1:1000	1:3000 R
Tom 40	Santa Cruz	sc-11414	1:1000	1:3000 R
mtHsp60	Enzo Life Sciences	ADI-SPA-806	1:1000	1:1000 M
mtHsp70	Enzo Life Sciences	ADI-SPA-825	1:1000	1:1000 M

Results

Retinoic Acid treatment elevated mt-DNA derived proteins, but not nuclear derived proteins that are associated with mitochondrial biogenesis. C2C12 myoblasts were treated with either vehicle, RA isomers, NR or the combination of RA isomers and NR. COX-I, a mitochondrially-encoded subunit of Complex IV increased 3.1-fold in 9cisRA-treated cells, 2.8- fold in ATRA-treated cells, and by 3.7-fold and 3.9-fold in NR+9cisRA/NR+ATRA respectively ($P<0.05$; Figure 3.C). The nuclear-encoded COX IV subunit was elevated only with NR treatment, while the addition of the RA isomers led to an interaction effect that negated the elevation seen with NR alone. The transcriptional co-regulator of mitochondrial biogenesis PGC-1α was unaltered by RA isomers and NR treatments. Lastly, citrate synthase, a key component of the Krebs cycle, was also unperturbed by treatments with RA isomers NR.

RA treatment lowers the expression of Tfam protein. Treatment with RA resulted in decreases in the precursor Tfam protein by 32%, and the mature Tfam protein expression levels by 27% ($P<0.05$; Figure 3G, H). The fraction of mature Tfam protein relative to the total Tfam remained unaltered.

RA elevated the protein levels of Tom40, but not Tim23, while NR led to elevations in mtHsp70. Tom40, an outer mitochondrial membrane transporter, was elevated by 70-72% with RA treatment ($P<0.05$; Figure 4C). NR treatment alone led to an elevation in protein levels of the chaperone mtHsp70 by 52% ($P<0.05$; Figure 4D), while the addition of RA isomers led to an interaction effect that nullified NR-mediated increase. Tim23 was unaltered by treatment with either nutrient.

RA elevated mtDNA-encoded mitochondrial proteins, but only some of the nuclear encoded proteins. C2C12 cells were treated with RA and 3h of CCA over 4 days post-differentiation. COX-I protein levels increased 2.0-2.4 fold with RA treatment alone, and ~3-fold elevations were seen in conjunction with CCA (Figure 5B; $P<0.05$). COX-IV protein levels were unaltered with RA treatment, but CCA treatment led to elevations between ~2-fold in all CCA conditions regardless of the RA isomers (Figure 5C; $P<0.05$). The master co-activator PGC-1α protein levels were elevated with RA treatment by 2.2-fold, while the combination of RA and CCA led to elevations between 2.4- 2.5 fold (Figure 5F; $P<0.05$).There were no significant alterations in protein levels of nuclear-encoded Citrate Synthase (Figure 5D) and the precursor Tfam protein form (Figure 5G) and mature Tfam form (Figure 5H).

RA and CCA elevated the protein levels of Tom40, but not Tim23 or the chaperones mtHsp60,70. RA and CCA treatment both had a main effect on Tom40 protein levels (2-fold and 1.5-fold respectively), while only RA treatment alone had a main effect leading to elevated Tim23 levels (post-hoc revealed ATRA was main reason for this effect,a 1.7-fold increase).

Retinoic acid treatment did not alter protein levels of autophagy-related proteins. The protein levels of p62, an adaptor protein, remained unaltered both with RA treatment alone, and in conjunction with CCA. The autophagosome protein LC3 I, which is lipidated to its mature form LC3 II, was also unaltered with RA and CCA treatments. The autophagy-related protein Beclin, was also unaltered with RA and CCA treatments.

Retinoic acid does not activate the kinase pathways in C2C12 myotubes. Treatment of C2C12 cells with 1μM RA for 30min did not result in increases of total nor phosphorylated AMPK, p38 MAPK or CAMK II kinases.

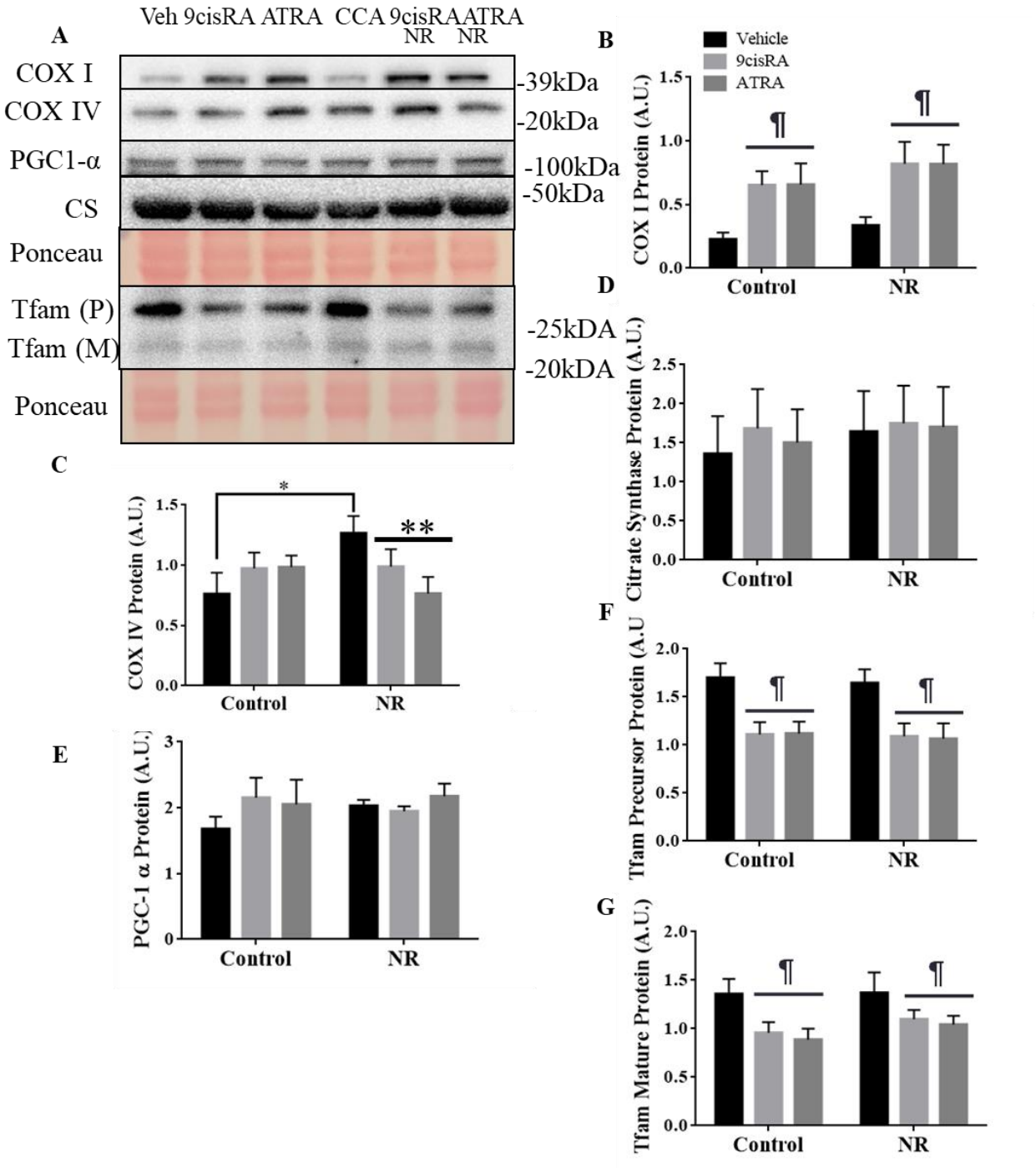
A
Veh 9cisRA ATRA CCA 9cisRA ATRA
NR NR
COX I
COX IV
PGC1-α
CS
Ponceau
Tfam (P)
Tfam (M)
Ponceau
-39kDa
-20kDa
-100kDa
-50kDa
-25kDA
-20kDA
B
Vehicle
9cisRA
ATRA
COX I Protein (A.U.)
Control
NR
C
COX IV Protein (A.U.)
Control
NR
D
Citrate Synthase Protein (A.U.)
Control
NR
E
PGC-1 α Protein (A.U.)
Control
NR
F
Tfam Precursor Protein (A.U
Control
NR
G
Tfam Mature Protein (A.U.)
Control
NR

Figure 3. *Treatment of C2C12 myotubes with retinoic acid and nicotinamide riboside results in increases in mt-DNA derived mitochondrial proteins.* (A). Representative Western Blots and graphical quantifications of : (B) COX-I, (C) COX-IV, (D) Citrate Synthase, (E) PGC-1α. (F) Representative Western Blots and graphical quantifications (G) Tfam precursor, (H) Tfam mature (I) Mature percentage of Total Tfam. Data are registered as mean ±SEM and are measured in arbitrary units/%. (¶: main effect of RA, *: Veh vs NR, **: interaction effect of NR +RA, $P<0.05$ vs vehicle; n=4-7).

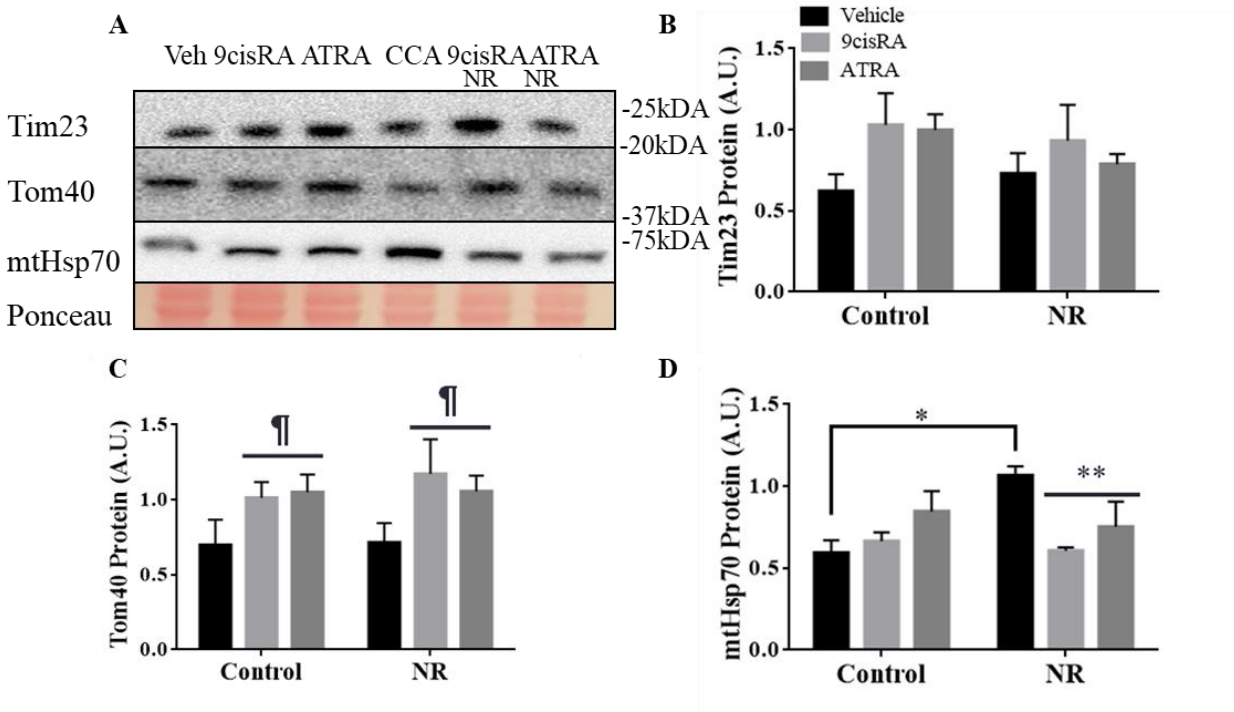

Figure 4. *Treatment of C2C12 myotubes with retinoic acid and nicotinamide riboside resulted in increases in import protein Tom40 expression, but only nicotinamide riboside led to chaperone elevation.* A).Representative Western Blots and graphical quantifications of; (B) Tim23, (C) Tom40, (D) mtHsp70. Data are registered as mean ±SEM and are measured in arbitrary units. (¶: main effect of RA, *: Vehicle vs NR, **: interaction effect of NR +RA, $P<0.05$ vs vehicle; n=4-5).

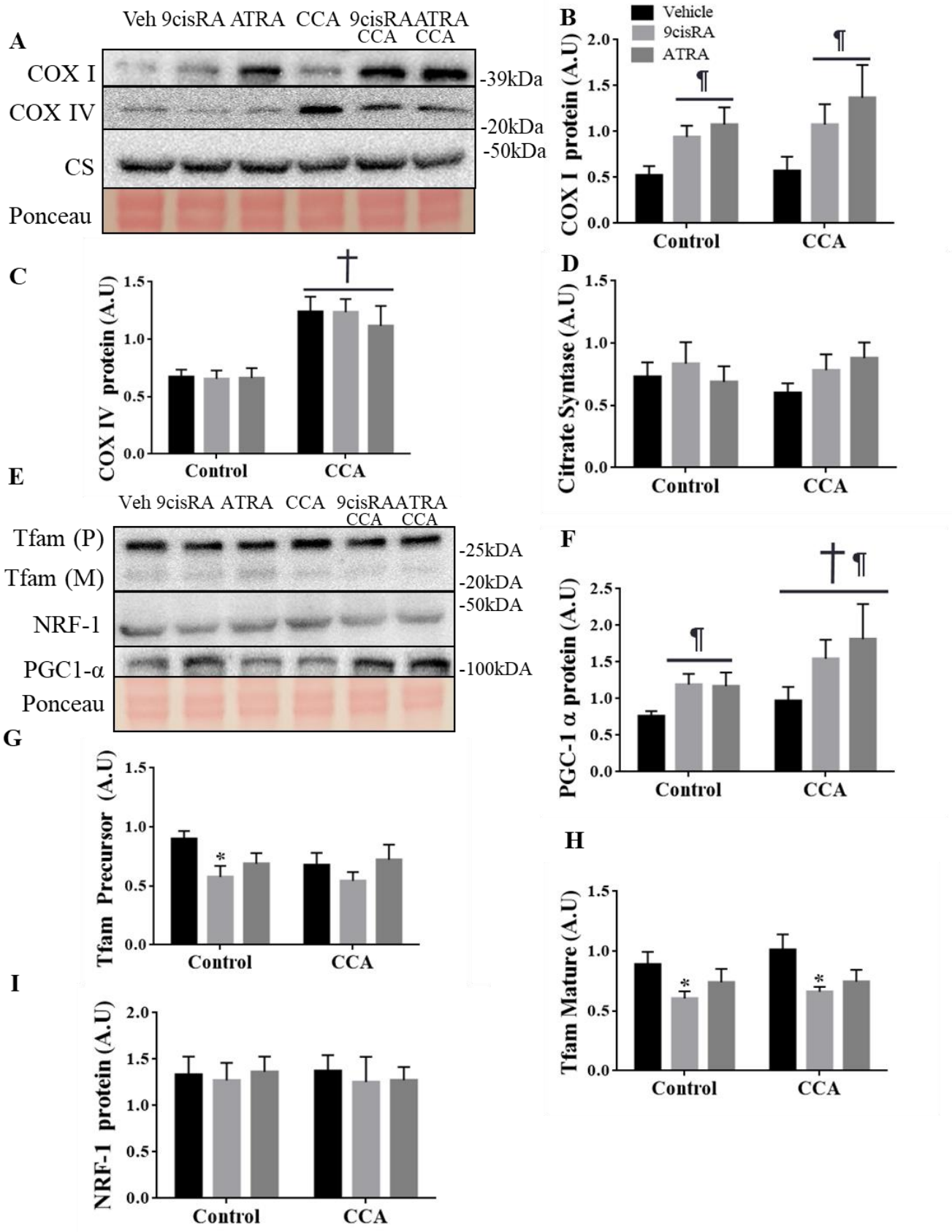
A
Veh 9cisRA ATRA CCA 9cisRA CCA ATRA CCA
COX I
COX IV
CS
Ponceau
-39kDa
-20kDa
-50kDa
B
Vehicle
9cisRA
ATRA
COX I protein (A.U)
Control
CCA
C
COX IV protein (A.U)
Control
CCA
D
Citrate Syntase (A.U)
Control
CCA
E
Veh 9cisRA ATRA CCA 9cisRA CCA ATRA CCA
Tfam (P)
Tfam (M)
NRF-1
PGC1-α
Ponceau
-25kDA
-20kDA
-50kDA
-100kDA
F
PGC-1 α protein (A.U)
Control
CCA
G
Tfam Precursor (A.U)
Control
CCA
H
Tfam Mature (A.U)
Control
CCA
I
NRF-1 protein (A.U)
Control
CCA

Figure 5. *Treatment of C2C12 myotubes with retinoic acid and CCA resulted in increases in mtDNA- derived mitochondrial proteins, but not nuclear-derived mitochondrial proteins*. A) Representative Western Blots and graphical quantifications of; (B) COX-I, (C) COX-IV, (D) Citrate Synthase. (E) Representative Western Blots and graphical quantifications of: (F) PGC-1α, (G) Tfam Precursor, (H) Tfam Mature. Data are registered as ±SEM and are measured in a rbitrary units. (¶: main effects of RA,†: main effect of CCA,* Veh vs CCA+ 9cisRA, $P<0.05$ vs vehicle; n=6-13).

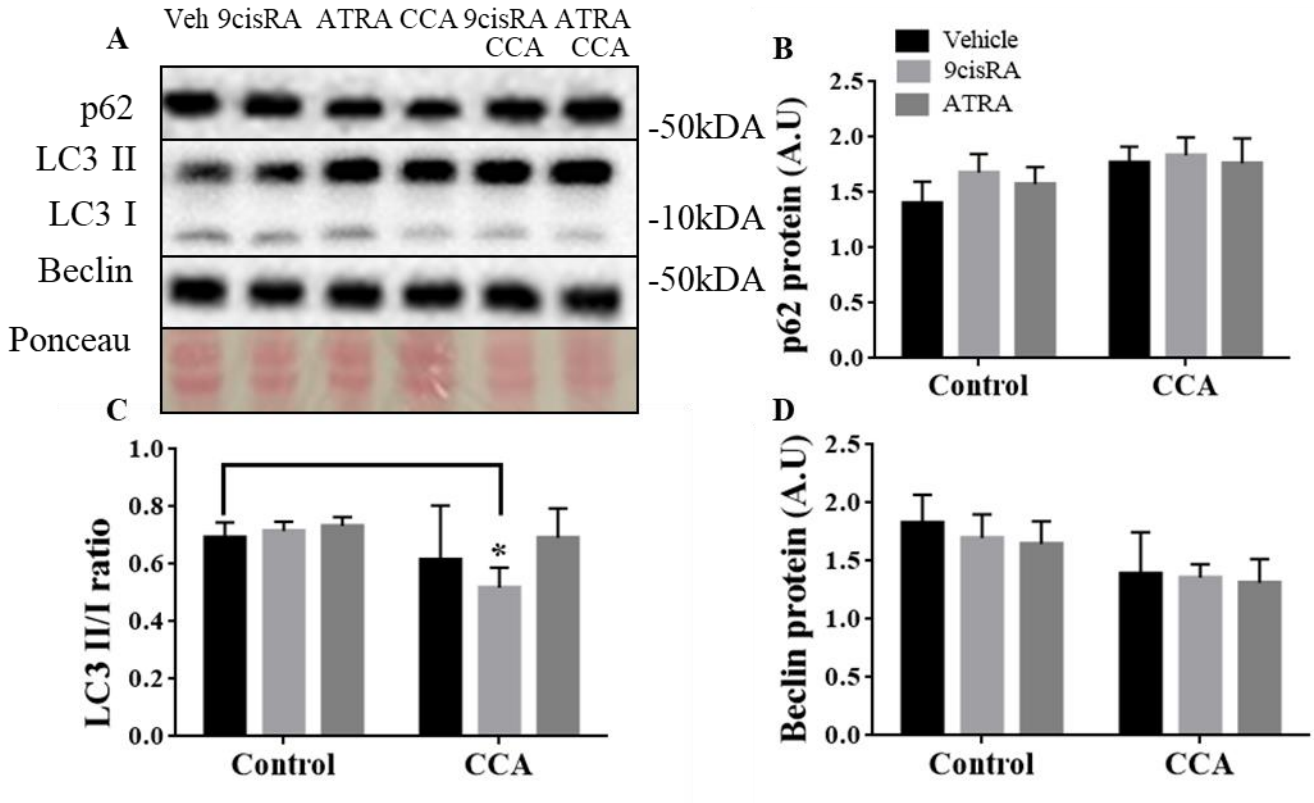

Figure 6. *Treatment of C2C12 myotubes with retinoic acid and CCA had no effect on autophagy in C2C12 cells.* (A) Representative Western Blots and graphical quantifications of: (B) p62, (C) LC3II/I ratio, (D) Beclin. Data are registered as mean±SEM (*,:veh vs 9cisRA+CCA) (n= 4-8).

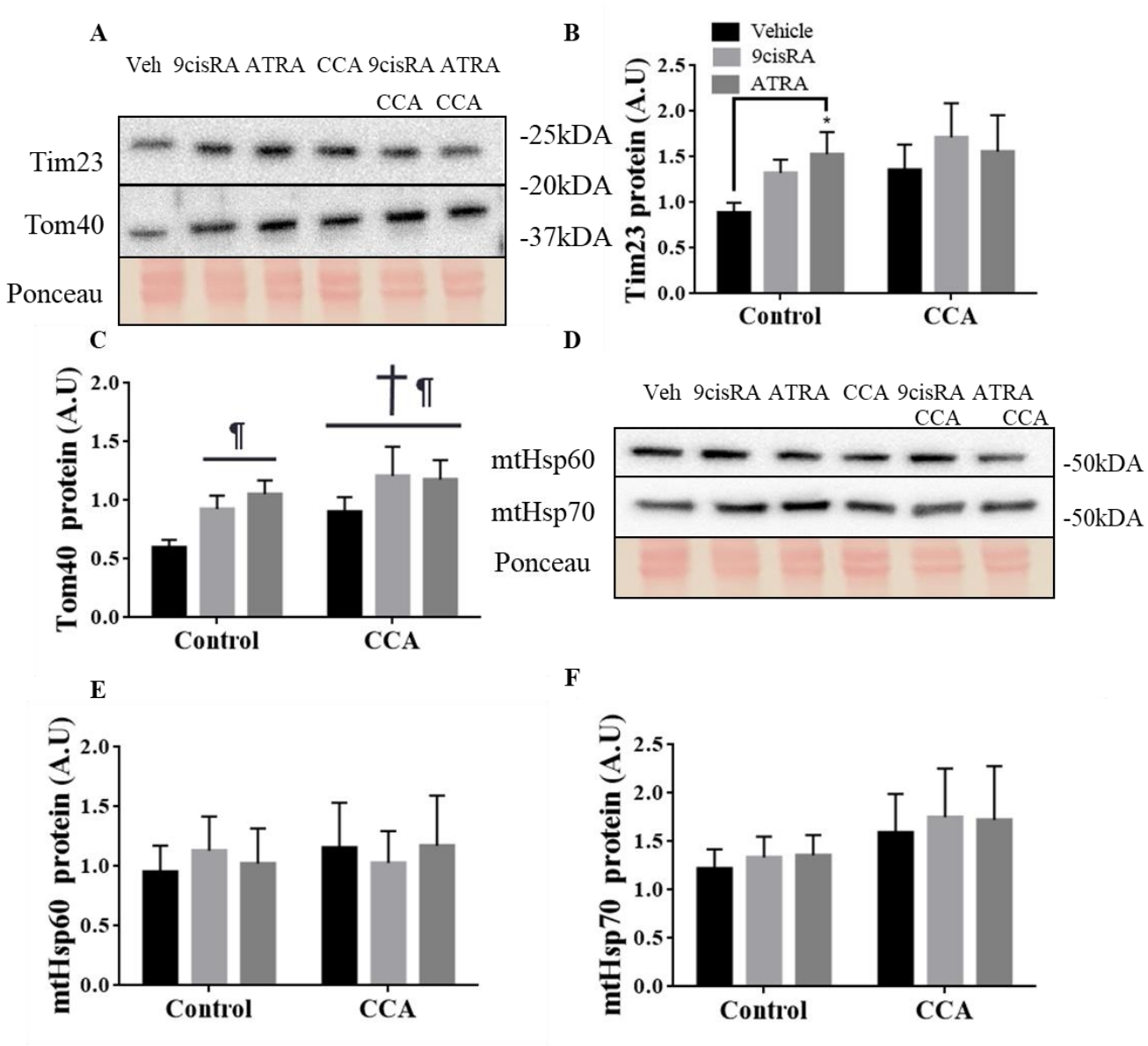

Figure 7. *Treatment of C2C12 myotubes with retinoic acid and CCA resulted in elevations in the import proteins Tim23 and Tom40, but did not alter mt-chaperone protein expression.* (A) Representative Western blots and graphical quantifications of: (B) Tim23, (C) Tom40. (D) Representative Western blots and graphical quantifications of: (E) mtHsp60, (F) mtHsp70. Data are registered as mean ±SEM and are measured in arbitrary units. (¶: main effect of RA, †,:main effect of CCA, *: Vehicle vs ATRA; n=4-11).

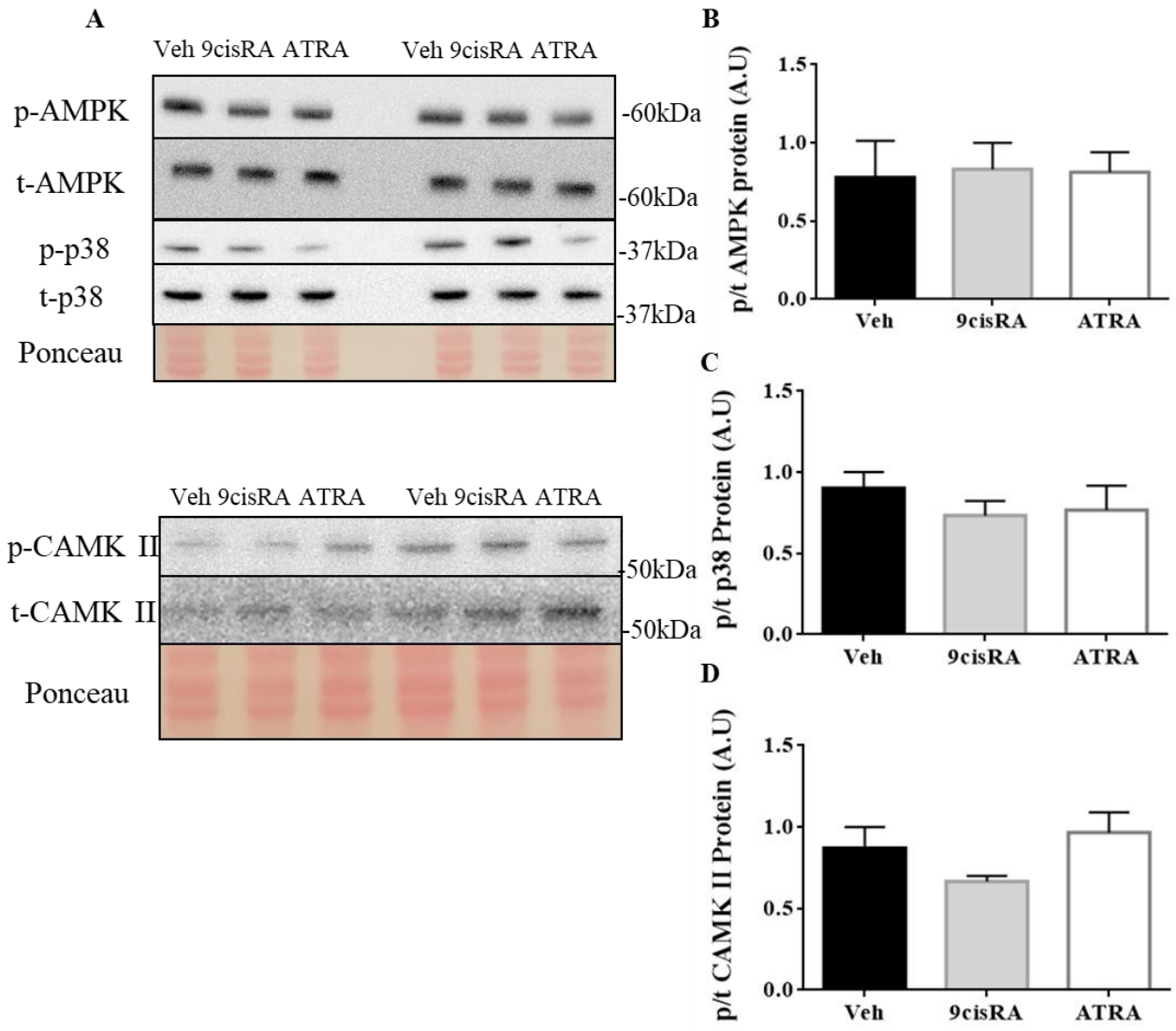

Figure 8. *Retinoic acid treatment for 30 minutes did not elevate kinase activity in C2C12 cells.* Treatment of C2C12 myotubes with 1μM RA did not result in elevations in kinase activity. (A) Representative Western Blots and graphical quantifications of (B) p-AMPK/t-AMPK ratio, (C) p-p38/t-p38 ratio (D)p-CAMKII/t-CAMKII. Data are registered as mean ±SEM and are measured as a ratio of p/t protein levels (n=4-6).

Discussion

Mitochondria are organelles responsible for providing energy for cellular functions in the form of ATP. Mitochondria are plastic in nature, and can be stimulated to divide and expand their networks in muscle tissue. Exercise has been well established as a potent inducer of mitochondrial biogenesis network expansion, while also leading to an increase in breakdown of dysfunctional mitochondria (55, 67). This process is mediated, in part, by exercise-induced increases in the activity of the master regulator PGC-1α (45). The activation of PGC-1α can be targeted in several ways, one of which is deacetylation, and the other being phosphorylation (153). In addition to exercise, several nutritional approaches that have the potential to have the same effects have emerged, which include resveratrol (94) and NR. Resveratol in particular has been shown to exhibit synergistic effects on mitochondrial biogenesis in C_2C_{12} myotubes when combined with CCA which is why we were interested to see if other compounds could also synergize with CCA. NR treatment resulted in elevations of mitochondrial biogenesis proteins in C_2C_{12} cells (89,91), but due to NR's overlap with CCA, and RA's numerous potential pathways that are separate from CCA, we felt that RA would be a better candidate for additivity and/or synergy studies.

Retinoic acid isomers have been shown to activate mitochondrial biogenesis, containing some mechanisms that are independent from the effects of NR and CCA, and this led to our interest in examining their potential for synergy. RA isomers operate by ligand activation of the RAR and RXR receptors, which represent the retinoic acid response elements (RARE), found in both the nuclear and mitochondrial genome. RA isomer treatment elevates mitochondrial biogenesis in tissue such as adipocytes (129), liver (97, 131) and neurons (144). However, the effects of RA isomers on myotube mitochondria are not fully understood. Thus, we treated C_2C_{12}

myotubes with a dose of 1μM, which is a supra-physiological dose compared to serum levels (3.8 to 5.pM) found in mice. The dose used in our studies has been used in previous literature in order to differentiate cells (24, 102), and was the maximal dose that did not elicit negative effects (86). RA did not lead to changes in PGC-1α in the RA and NR synergy experiments. In addition to this observation, RA treatment led to elevations in the mtDNA encoded COX-I subunit of Complex IV, which corroborates previous findings in rat testes (50). RA isomers did not impact the expression of the nuclear-derived subunit COX-IV, which suggested to us that the effects of RA on the ETC may be specific to mtDNA-encoded proteins.

With RA treatment, we observed decreases in Tfam protein levels, with decreases present in both the cytosolic precursor form and the matrix-destined mature form. This is contrary to previous findings (129), which found increases in Tfam in adipocytes. We examined other literature with regards to RA and/or Tfam regulation, and found that RA may potentially prevent Tfam from binding to mtDNA via the ERK-2 pathway activation (10). This could lead to Tfam being unable to bind to LSP and HSP on the mtDNA (Figure 1). Tfam's role in the mitochondria is potentially partially fulfilled by the binding of RA to the RARE site just downstream at the hormone response element site (HRE), activating HSP (heavy strand promoter) transcription, as COX-I was elevated despite Tfam being attenuated. Low levels of Tfam have been shown to be sufficient for LSP (light strand promoter) activation (51), suggesting that transcription could occur with low levels of the protein. We speculate that the block in Tfam activation and the RA activation of HSP transcription downstream of Tfam's binding site could lead to lower levels of Tfam in the cell via RARE site repression, as RARE sites without ligand activation serve as repressors (121)

Due to the changes we observed in Tfam, we investigated whether the protein import system that facilitates Tfam entry into the matrix was also affected by RA. Treatment with RA resulted in elevations of the Tom40 outer membrane channel, but did not affect Tim23 a component of the inner membrane. However, we saw no changes in the chaperone proteins mtHsp60 and 70 with RA treatment.

RA isomers are well known for their ability to facilitate autophagy in neurons, liver tissue, and cancer cells like leukemia (103). Treatment of leukemic NB4 neural cells with 1μM of ATRA resulted in an increase in LC3 II/I levels, and this was abolished upon the addition of chloroquine, an autophagy inhibitor. Surprisingly, we did not observe the elevations in autophagy that were seen in previous research. This may be due to the difference in tissue type, treatment time, or the lower doses of RA used in our experiments (1μM), while autophagy papers mostly had doses in the 5-10μM range, and examined different cell lines.

Nicotinamide Riboside (NR) treatment in myotubes demonstrated a marked increase in COX-IV protein levels, while the addition of RA led to an interaction effect that attenuated the increase. NR did not affect citrate synthase or Tfam protein levels, and had no impact on mitochondrial-encoded proteins such as COX-I. NR treatment had no effect on the protein import machinery, but did result in an elevation in the chaperone mtHsp70, while the addition of RA resulted in an interaction that inhibited the elevation in mtHsp70.

We have previously demonstrated that our cell culture model of exercise, CCA, resulted in significant elevations in mitochondrial biogenesis, indicated by elevations in PGC-1α, COX IV, and Tfam (133). Similarly, our results with CCA (alone) demonstrated elevations in COX-IV, but no significant impact on Tfam protein levels. We speculate that this may be due to higher

cell passages used in this experiment, as higher passages do not appear to be as responsive as younger passages used in our previous studies. This phenomenon is something we did not observe until now. The interaction of CCA and RA markedly elevated PGC-1α level, exhibiting main effects of CCA and of RA treatment. In this set of experiments, we saw RA treatment led to elevation of the protein levels of PGC-1α, something not seen Protocol 1, and something we believe to be a consequence of the longer exposure to retinoids in Protocol 2, in addition to Protocol 1 containing 4 treatments of retinoic acid compared to the 8 treatments in Protocol 2. When examining the protein levels of COX-I, there was a marked elevation with RA treatment, but no effect of CCA, which was similar to RA's effect in Protocol 1 experiments, while the CCA elevated COX-IV protein levels. In this case, CCA with RA supplementation had no bearing on COX-IV protein levels, which suggests the two pathways do not interfere with each other.

Although there was total Tfam level suppression in the NR and RA experiments, the combination of RA and CCA resulted in a significant reduction of Tfam in 9cisRA, but not ATRA treated cells. Due to the difference in protocol and exposure times to RA, it is possible that some of the RARE site repression may have been attenuated due to a longer exposure to RA, and a higher possibility of RA binding to RAR/RXR dimers that could be repressing Tfam transcription. We examined NRF-1, which is responsible for transcribing Tfam, and found that it was not altered with RA treatment, suggesting it is not the mechanism responsible for the attenuation in Tfam levels.

Due to the changes observed in Tfam, we also examined the import machinery and chaperone systems in the mitochondria. We observed elevations in Tim23, with ATRA treatment, but not with 9cisRA or CCA treatments, while Tom40, the outer membrane machinery

protein, was elevated with both isomers, as well as with the CCA treatment. There was no effect on the major chaperones that carry Tfam to the mtDNA, suggesting RA acts on the import channels alone.

Lastly, we examined whether RA activation of PGC-1α is mediated by the kinases typically activated during exercise, which include MAPK p38, AMPK, CAMK II (153). Contrary to our hypothesis, and to the elevations of CAMKII, p38 MAPK and AMPK seen in other literature (6, 18, 63, 73, 153), we did not observe any elevations in phosphorylated (activated) to total kinase ratio, which suggests that RA does not lead to kinase activation in skeletal muscle under the conditions in this study. We believe the reason we were unable to see activation may be due to the dose we have used of 1μM instead of the 10μM dose in another paper that examined RA.

In summary, it appears that our primary objective was partially met. RA isomers, given the conditions of this study, primarily influence the transcription of mtDNA proteins such as COX-I, while having no effect on nuclear encoded mitochondrial proteins. This suggests that RA isomers may indeed interact with mtDNA through RAR/RXR receptor activation. We found that RA attenuated total Tfam production, while having no effect on any other mitochondrial marker of biogenesis. Further investigation will be needed in the future studies in order to investigate the interaction between RA, and how activating retinoid receptors on Tfam promoters can attenuate its transcription and translation. We show here that the import pathways of the mitochondria were augmented, specifically in the case of the outer membrane, which suggests the decreases in Tfam were not post-translational. Contrary to our hypothesis, RA did not facilitate the activation of PGC-1α through increases in kinase activation, which include AMPK, p38 and CAMKII. RA may target PGC-1α activation and/or transcription through different pathways, having the

potential to facilitate PGC-1α transcription and eventual translation through PKA/cAMP/CREB pathway activation (88), and MEF2C activation (114), which have been shown in neural and cardiac tissue respectively. We believe that some limitations to our study are the lack of a functional assessment of mitochondria, such as measuring oxygen consumption with a Clark electrode. Another limitation was the lack of a secondary method to measure mitochondrial content such as confocal microscopy combined with a mitochondrial dye, which could serve to strengthen our finding of increased mitochondrial content. Overall, our study shows that while RA and CCA are not synergistic, they have complimentary effects, targeting different facets of mitochondrial biogenesis, and highlight the potential of adequate Vitamin A supplementation to assist in metabolic health.

References

1. **Adhihetty PJ**, **Ljubicic V**, **Hood DA**. Effect of chronic contractile activity on SS and IMF mitochondrial apoptotic susceptibility in skeletal muscle. *Am J Physiol Metab* 292: E748–E755, 2006.
2. **Adhihetty PJ**, **Uguccioni G**, **Leick L**, **Hidalgo J**, **Pilegaard H**, **Hood D a**. The role of PGC-1alpha on mitochondrial function and apoptotic susceptibility in muscle. *Am J Physiol Cell Physiol* 297: C217–C225, 2009.
3. **Amengual J**, **García-Carrizo FJ**, **Arreguín A**, **Mušinović H**, **Granados N**, **Palou A**, **Luisa Bonet M**, **Ribot J**, **Bonet ML**. Retinoic Acid Increases Fatty Acid Oxidation and Irisin Expression in Skeletal Muscle Cells and Impacts Irisin In Vivo. *Cell Physiol Biochem* 46: 187–202, 2018.
4. **Andersson SGE**, **Karlberg O**, **Canbäck B**, **Kurland CG**, **Whatley FR**, **Van Der Giezen M**, **Martin W**, **Tielens AGM**, **Allen JF**, **Raven JA**. On the origin of mitochondria: A genomics perspective. In: *Philosophical Transactions of the Royal Society B: Biological Sciences*, p. 165–179.
5. **Antico Arciuch VG**, **Elguero ME**, **Poderoso JJ**, **Carreras MC**. Mitochondrial Regulation of Cell Cycle and Proliferation. *Antioxid Redox Signal* 16: 1150–1180, 2011.
6. **Aronson D**, **Violan MA**, **Dufresne SD**, **Zangen D**, **Fielding RA**, **Goodyear LJ**. Exercise stimulates the mitogen-activated protein kinase pathway in human skeletal muscle. *J Clin Invest* 99: 1251–1257, 1997.

7. **Arribat Y**, **Broskey NT**, **Greggio C**, **Boutant M**, **Conde Alonso S**, **Kulkarni SS**, **Lagarrigue S**, **Carnero EA**, **Besson C**, **Cantó C**, **Amati F**. Distinct patterns of skeletal muscle mitochondria fusion, fission and mitophagy upon duration of exercise training. *Acta Physiol* 225: 13179, 2019.

8. **Aubry EM**, **Odermatt A**. Retinoic acid reduces glucocorticoid sensitivity in C2C12 myotubes by decreasing 11β-hydroxysteroid dehydrogenase type 1 and glucocorticoid receptor activities. *Endocrinology* 150: 2700–2708, 2009.

9. **Balmer JE**, **Blomhoff R**. Gene expression regulation by retinoic acid. *J Lipid Res* 43: 1773–1808, 2002.

10. **Battle TE**, **Levine RA**, **Yen A**. Retinoic acid-induced blr1 expression promotes ERK2 activation and cell differentiation in HL-60 cells. *Exp Cell Res* 254: 287–298, 2000.

11. **Bauer MF**, **Hofmann S**, **Neupert W**, **Brunner M**. Protein translocation into mitochondria: The role of TIM complexes. *Trends Cell Biol.* 10: 25–31, 2000.

12. **Becker T**, **Pfannschmidt S**, **Guiard B**, **Stojanovski D**, **Milenkovic D**, **Kutik S**, **Pfanner N**, **Meisinger C**, **Wiedemann N**. Biogenesis of the Mitochondrial TOM Complex. *Trends Biochem Sci* 283: 120–127, 2008.

13. **Belenky P**, **Christensen KC**, **Gazzaniga F**, **Pletnev AA**, **Brenner C**. Nicotinamide riboside and nicotinic acid riboside salvage in fungi and mammals quantitative basis for urh1 and purine nucleoside phosphorylase function in nad + metabolism. *J Biol Chem* 284: 158–164, 2009.

14. **Berdanier CD**, **Everts HB**, **Hermoyian C**, **Mathews CE**. Role of vitamin A in mitochondrial gene expression. In: *Diabetes Research and Clinical Practice*, p. 11–27.

15. **Bi Y**, **Gong M**, **Li T**, **Zhang Y**, **Shi Y**, **Guo M**, **Liu Y**, **Chen L**, **Jiang W**, **Qu P**, **Chen J**. Vitamin A bio-modulates apoptosis via the mitochondrial pathway after hypoxic-ischemic brain damage. *Mol Brain* 11, 2018.

16. **Blajszczak C**, **Bonini MG**. Mitochondria targeting by environmental stressors: Implications for redox cellular signaling. *Toxicology* 391: 84–89, 2017.

17. **Brun P-J**, **Wongsiriroj N**, **Blaner WS**. Retinoids in the pancreas. *Hepatobiliary Surg Nutr* 5: 1–14, 2016.

18. **Cantó C**, **Auwerx J**. PGC-1α, SIRT1 and AMPK, an energy sensing network that controls energy expenditure. *Curr. Opin. Lipidol.* 20: 98–105, 2009.

19. **Cantó C**, **Menzies KJ**, **Auwerx J**. NAD+Metabolism and the Control of Energy Homeostasis: A Balancing Act between Mitochondria and the Nucleus. *Cell Metab.* 22: 31–53, 2015.

20. **Carrera S**, **Cuadrado-Castano S**, **Samuel J**, **Jones GDD**, **Villar E**, **Lee SW**, **MacIp S**. Stra6, a retinoic acid-responsive gene, participates in p53-induced apoptosis after DNA damage. *Cell Death Differ* 20: 910–919, 2013.

21. **Carter HN**, **Chen CCW**, **Hood DA**. Mitochondria, Muscle Health, and Exercise with Advancing Age. *Physiology* 30: 208–223, 2015.

22. **Cerutti R**, **Pirinen E**, **Lamperti C**, **Marchet S**, **Sauve AA**, **Li W**, **Leoni V**, **Schon EA**, **Dantzer F**, **Auwerx J**, **Viscomi C**, **Zeviani M**. NAD+-dependent activation of Sirt1 corrects the phenotype in a mouse model of mitochondrial disease. *Cell Metab* 19: 1042–1049, 2014.

23. **Chen H**, **Chan DC**. Mitochondrial dynamics-fusion, fission, movement, and mitophagy-in neurodegenerative diseases. *Hum Mol Genet* 18, 2009.

24. **Chen J**, **Li Q**. Implication of retinoic acid receptor selective signaling in myogenic differentiation. *Sci Rep* 6: 1–8, 2016.

25. **Chen M**, **Baar K**, **Marison M**, **Kelly DP**, **Holloszy JO**, **Jones TE**, **Wende AR**, **Nolte LA**. Adaptations of skeletal muscle to exercise: rapid increase in the transcriptional coactivator PGC-1. *FASEB J* 16: 1879–1886, 2002.

26. **Chen Y**, **Lewis W**, **Diwan A**, **Cheng EH-Y**, **Matkovich SJ**, **Dorn GW**. Dual autonomous mitochondrial cell death pathways are activated by Nix/BNip3L and induce cardiomyopathy. *Proc Natl Acad Sci* 107: 9035–9042, 2010.

27. **Cherra SJ**, **Gusdon AM**, **Uechi G**, **Dagda RK**, **Wang KZQ**, **Zhu J**, **Chu CT**, **Balasubramani M**. ERK-mediated phosphorylation of TFAM downregulates mitochondrial transcription: Implications for Parkinson's disease. *Mitochondrion* 17: 132–140, 2014.

28. **Chi Y**, **Sauve AA**. Nicotinamide riboside, a trace nutrient in foods, is a Vitamin B3 with effects on energy metabolism and neuroprotection. *Curr. Opin. Clin. Nutr. Metab. Care* 16: 657–661, 2013.

29. **Chin C**, **Chen W**, **Erlich AT**, **Crilly MJ**, **Hood DA**. Parkin is required for exercise-induced mitophagy in muscle: impact of aging. *Am J Physiol Endocrinol Metab* 315: 404–415, 2018.

30. **Chipuk JE**, **Bouchier-Hayes L**, **Green DR**. Mitochondrial outer membrane permeabilization during apoptosis: the innocent bystander scenario Apoptosis and Caspase-Independent Cell Death: Where MOMP Happens. *Cell Death Differ* 13: 1396–1402, 2006.

31. **Connor MK**, **Irrcher I**, **Hood DA**. Contractile Activity-induced Transcriptional Activation of Cytochrome c Involves Sp1 and is Proportional to Mitochondrial ATP Synthesis in C2C12 Muscle Cells. *J Biol Chem* 276: 15898–15904, 2001.

32. **Davies KJA**, **Packer L**, **Brooks GA**. Biochemical Adaptation of Mitochondria , Respiration to Endurance Muscle , and Whole-Animal Training logical condition of chronic ethanol con- sumption , liver concentrations of certain clusters (N-2 , N-3 , N-4) are not constant but may decrease 20-30 *Arch Biochem Biophys* 299: 539–554, 1981.

33. **Dominy JE**, **Puigserver P**. Mitochondrial biogenesis through activation of nuclear signaling proteins. *Cold Spring Harb Perspect Biol* 5, 2013.

34. **Dudek J**, **Rehling P**, **van der Laan M**. Mitochondrial protein import: Common principles and physiological networks. *Biochim. Biophys. Acta - Mol. Cell Res.* 1833: 274–285, 2013.

35. **Duguez S**, **Féasson L**, **Denis C**, **Freyssenet D**. Mitochondrial biogenesis during skeletal muscle regeneration. *Am J Physiol Metab* 282: E802–E809, 2015.

36. **Duncan JG**. Peroxisome Proliferator Activated Receptor-Alpha (PPARα) and PPAR gamma coactivator-1alpha (PGC-1α) regulation of cardiac metabolism in diabetes. In: *Pediatric Cardiology*, p. 323–328.

37. **Duong V**, **Rochette-Egly C**. The molecular physiology of nuclear retinoic acid receptors. From health to disease. *Biochim Biophys Acta - Mol Basis Dis* 1812: 1023–1031, 2011.

38. **Egan B**, **Zierath JR**. Exercise Metabolism and the Molecular Regulation of Skeletal Muscle Adaptation. *Cell Metab* 17: 162–184, 2013.

39. **Eisner V**, **Lenaers G**, **Hajnóczky G**. Mitochondrial fusion is frequent in skeletal muscle and supports excitation-contraction coupling. *J. Cell Biol.* (2014).

40. **Emhoff C-AW**, **Brooks GA**, **Fattor JA**, **Carlson TJ**, **Messonnier LA**, **Horning MA**. Direct and indirect lactate oxidation in trained and untrained men. *J Appl Physiol* 115: 829–838, 2013.

41. **Eriksson A-S**, **Winkler HH**, **Näslund AK**, **Alsmark UCM**, **Kurland CG**, **Podowski RM**, **Andersson JO**, **Zomorodipour A**, **Andersson SGE**, **Sicheritz-Pontén T**. The genome sequence of Rickettsia prowazekii and the origin ofmitochondria. *Nature* 396: 133–140, 2002.

42. **Evans MJ**, **Scarpulla RC**. NRF-1: A trans-activator of nuclear-encoded respiratory genes in animal cells. *Genes Dev* 4: 1023–1034, 1990.

43. **Everts HB**, **Berdanier CD**. Regulation of Mitochondrial Gene Expression by Retinoids. IUBMB Life, 54: 45–49, 2002

44. **Everts HB**, **Claassen DO**, **Hermoyian CL**, **Berdanier CD**. Nutrient-gene interactions: Dietary vitamin A and mitochondrial gene expression. *IUBMB Life* 53: 295–301, 2002.

45. **Fernandez-Marcos P**, **Auwerx J**. Regulation of PGC-1a , a nodal regulator of mitochondrial biogenesis. *Am J Clin …* 93: 884–890, 2011.

46. **Fernández-Vizarra E**, **Enríquez JA**, **Pérez-Martos A**, **Montoya J**, **Fernández-Silva P**. Tissue-specific differences in mitochondrial activity and biogenesis. *Mitochondrion* 11: 207–213, 2011.

47. **Fitts R**, **Booth F**, **Winder W**, **Holloszy J**. Skeletal muscle respiratory capacity, endurance, and glycogen utilization. *Am J Physiol Content* 228: 1029–1033, 2017.

48. **Fong WM**, **Bewersdorf J**, **Nag S**, **Puente G**, **Nath S**, **Dancourt J**, **Yamamoto A**, **Melia TJ**, **Shteyn V**, **Antonny B**. Lipidation of the LC3/GABARAP family of autophagy proteins relies on a membrane-curvature-sensing domain in Atg3. *Nat Cell Biol* 16: 415–424, 2014.

49. **Fortini P**, **Ferretti C**, **Iorio E**, **Cagnin M**, **Garribba L**, **Pietraforte D**, **Falchi M**, **Pascucci B**, **Baccarini S**, **Morani F**, **Phadngam S**, **De Luca G**, **Isidoro C**, **Dogliotti E**. The fine tuning of metabolism, autophagy and differentiation during in vitro myogenesis. *Cell Death Dis* 7, 2016.

50. **Gaemers IC**, **Van Pelt AMM**, **Themmen APN**, **De Rooij DG**. Isolation and characterization of all-trans-retinoic acid-responsive genes in the rat testis. *Mol Reprod Dev* 50: 1–6, 1998.

51. **Garstka HL**, **Schmitt WE**, **Schultz J**, **Sogl B**, **Silakowski B**, **Pérez-Martos A**, **Montoya J**, **Wiesner RJ**. Import of mitochondrial transcription factor A (TFAM) into rat liver mitochondria stimulates transcription of mitochondrial DNA. *Nucleic Acids Res* 31: 5039–5047, 2003.

52. **Gifford JR**, **Richardson RS**, **Park SY**, **Ives SJ**, **Garten RS**, **Drakos S**, **Dela F**, **Larsen S**. Cardiac, Skeletal, And Smooth Muscle Mitochondrial Function; Are All Mitochondria Created Equal? *Med Sci Sport Exerc* 46: 96, 2017.

53. **Gordon JW**, **Rungi AA**, **Inagaki H**, **Hood DA**. Selected Contribution: Effects of contractile activity on mitochondrial transcription factor A expression in skeletal muscle. *J Appl Physiol* 90: 389–396, 2017.

54. **Graef M**, **Nunnari J**. Mitochondria regulate autophagy by conserved signalling pathways. *EMBO J* 30: 2101–2114, 2011.

55. **Hamacher-Brady A**, **Brady NR**. Mitophagy programs: Mechanisms and physiological implications of mitochondrial targeting by autophagy. *Cell. Mol. Life Sci.* 73: 775–795, 2016.

56. **Hamai N**, **Nakamura M**, **Asano A**. Inhibition of Mitochondrial Protein Synthesis Impaired C2C12 Myoblast Differentiation. *Cell Struct Funct* 22: 421–431, 1997.

57. **Handschin C**, **Spiegelman BM**. Peroxisome proliferator-activated receptor γ coactivator 1 coactivators, energy homeostasis, and metabolism. *Endocr Rev* 27: 728–735, 2006.

58. **Harbauer AB**, **Zahedi RP**, **Sickmann A**, **Pfanner N**, **Meisinger C**. The protein import machinery of mitochondria - A regulatory hub in metabolism, stress, and disease. *Cell Metab.* 19: 357–372, 2014.

59. **He L**, **Tian X**, **Yan C**, **Liu D**, **Wang S**, **Han Y**. Nicotine promotes the differentiation of C2C12 myoblasts and improves skeletal muscle regeneration in obese mice. *Biochem Biophys Res Commun* 511: 739–745, 2019.

60. **Herzberg NH**, **Zwart R**, **Wolterman RA**, **Ruiter JPN**, **Wanders RJA**, **Bolhuis PA**, **van den Bogert C**. Differentiation and proliferation of respiration-deficient human myoblasts. *BBA - Mol Basis Dis* 1181: 63–67, 1993.

61. **Higashida K**, **Holloszy JO**, **Koh J-H**, **Terada S**, **Han D-H**, **Hancock CR**. PPARβ Is Essential for Maintaining Normal Levels of PGC-1α and Mitochondria and for the Increase in Muscle Mitochondria Induced by Exercise. *Cell Metab* 25: 1176–1185.e5, 2017.

62. **Holloszy J**, **Coyle E**. Adaptations of skeletal muscle to endurance exercise and their metabolic consequences J. Appl.Physiol.:Respirat. Environ.ExercisePhysiol. 56(4): 831-838, 1984.

63. **Holloszy JO**. Regulation of mitochondrial biogenesis and GLUT4 expression by exercise. *Compr. Physiol.* 1: 921–940, 2011.

64. **Holloszy JO**, **Booth FW**. Biochemical Adaptations to Endurance Exercise in Muscle. *Annu Rev Physiol* 38: 273–291, 2003.

65. **Hood DA**. Coordination of metabolic plasticity in skeletal muscle. *J Exp Biol* 209: 2265–2275, 2006.

66. **Hood DA**, **Memme JM**, **Oliveira AN**, **Triolo M**. Maintenance of Skeletal Muscle Mitochondria in Health, Exercise, and Aging. *Annu Rev Physiol is online* 81: 19–41, 2019.

67. **Hood DA**, **Tryon LD**, **Carter HN**, **Kim Y**, **Chen CCW**. Unravelling the mechanisms regulating muscle mitochondrial biogenesis. *Biochem J* 473: 2295–2314, 2016.

68. **Hood DA**, **Uguccioni G**, **Vainshtein A**, **D'souza D**. Mechanisms of Exercise-Induced Mitochondrial Biogenesis in Skeletal Muscle: Implications for Health and Disease. *Compr Physiol* 1: 1119–1134, 2011.

69. **Hood DA**, **Uguccioni G**, **Vainshtein A**, **D'souza D**. Mechanisms of exercise-induced mitochondrial biogenesis in skeletal muscle: Implications for health and disease. *Compr Physiol* 1: 1119–1134, 2011.

70. **Hoppeler H**, **Lfithi P**, **Claassen H**, **Weibel ER**, **Howald H**. The ultrastructure of the normal human skeletal muscle. *Pflfigers Arch. 344, 217--232 (1973).*

71. **Howald H**, **Hoppeler H**, **Claassen H**, **Mathieu O**, **Straub R**. Influences of endurance training on the ultrastructural composition of the different muscle fiber types in humans. *Pflügers Arch Eur J Physiol* 403: 369–376, 1985.

72. **Irrcher I**, **Adhihetty PJ**, **Sheehan T**, **Joseph A-M**, **Hood DA**. PPARgamma coactivator-1alpha expression during thyroid hormone- and contractile activity-induced mitochondrial adaptations. *Am J Physiol Cell Physiol* 284: C1669–C1677, 2003.

73. **Ishijima N**, **Kanki K**, **Shimizu H**, **Shiota G**. Activation of AMP-activated protein kinase by retinoic acid sensitizes hepatocellular carcinoma cells to apoptosis induced by sorafenib. *Cancer Sci* 106: 567–575, 2015.

74. **Jacobs RA**, **Lundby C**. Mitochondria express enhanced quality as well as quantity in association with aerobic fitness across recreationally active individuals up to elite athletes. *J Appl Physiol* 114: 344–350, 2012.

75. **Jager S**, **Handschin C**, **St.-Pierre J**, **Spiegelman BM**. AMP-activated protein kinase (AMPK) action in skeletal muscle via direct phosphorylation of PGC-1. *Proc Natl Acad Sci* 104: 12017–12022, 2007.

76. **Joseph A-M**, **Pilegaard H**, **Litvintsev A**, **Leick L**, **Hood DA**. Control of gene expression and mitochondrial biogenesis in the muscular adaptation to endurance exercise. *Essays Biochem* 42: 13–29, 2006.

77. **Khan NA**, **Auranen M**, **Paetau I**, **Pirinen E**, **Euro L**, **Forsström S**, **Pasila L**, **Velagapudi V**, **Carroll CJ**, **Auwerx J**, **Suomalainen A**. Effective treatment of mitochondrial myopathy by nicotinamide riboside, a vitamin B3. doi: 10.1002/emmm.201403943.

78. **Khodabukus A**, **Baar K**, **Philp A**, **Donnelly K**, **Deldicque L**, **Dennis RG**. A Novel Bioreactor for Stimulating Skeletal Muscle In Vitro. *Tissue Eng Part C Methods* 16: 711–718, 2009.

79. **Kourtzidis IA**, **Stoupas AT**, **Gioris IS**, **Veskoukis AS**, **Margaritelis N V**, **Tsantarliotou M**, **Taitzoglou I**, **Vrabas IS**, **Paschalis V**, **Kyparos A**, **Nikolaidis MG**. The NAD+ precursor nicotinamide riboside decreases exercise performance in rats. *J Int Soc Sports Nutr* 13, 2016.

80. **Laker RC**, **Drake JC**, **Wilson RJ**, **Lira VA**, **Lewellen BM**, **Ryall KA**, **Fisher CC**, **Zhang M**, **Saucerman JJ**, **Goodyear LJ**, **Kundu M**, **Yan Z**. Ampk phosphorylation of Ulk1 is required for targeting of mitochondria to lysosomes in exercise-induced mitophagy. *Nat Commun* 8, 2017.

81. **Lau P**, **Nixon SJ**, **Parton RG**, **Muscat GEO**. ROR?? regulates the expression of genes involved in lipid homeostasis in skeletal muscle cells: Caveolin-3 and CPT-1 are direct targets of ROR. *J Biol Chem* 279: 36828–36840, 2004.

82. **Lee EJ**, **Kang YC**, **Park W-H**, **Jeong JH**, **Pak YK**. Negative transcriptional regulation of mitochondrial transcription factor A (TFAM) by nuclear TFAM. (2014). doi: 10.1016/j.bbrc.2014.05.082.

83. **Lefebvre P**, **Chinetti G**, **Fruchart JC**, **Staels B**. Sorting out the roles of PPARα in energy metabolism and vascular homeostasis. *J. Clin. Invest.* 116: 571–580, 2006.

84. **Lin YW**, **Lien LM**, **Yeh TS**, **Wu HM**, **Liu YL**, **Hsieh RH**. 9-cis retinoic acid induces retinoid X receptor localized to the mitochondria for mediation of mitochondrial transcription. *Biochem Biophys Res Commun* 377: 351–354, 2008.

85. **Lira VA**, **Benton CR**, **Yan Z**, **Bonen A**. PGC-1α regulation by exercise training and its influences on muscle function and insulin sensitivity. *Am J Physiol Metab* 299: E145–E161, 2010.

86. **Liu B**, **Li N**, **Jiang Y**, **Liu C**, **Ma L**, **Cong W**, **Xiao J**. Effects of Excessive Retinoic Acid on C2C12 Myogenesis. *J Hard Tissue Biol* 25: 97–103, 2016.

87. **Ljubicic V**, **Joseph AM**, **Saleem A**, **Uguccioni G**, **Collu-Marchese M**, **Lai RYJ**, **Nguyen LMD**, **Hood DA**. Transcriptional and post-transcriptional regulation of mitochondrial biogenesis in skeletal muscle: Effects of exercise and aging. *Biochim. Biophys. Acta - Gen. Subj.* 1800: 223–234, 2010.

88. **Lu T-C**, **Wang Z**, **Feng X**, **Chuang P**, **Fang W**, **Chen Y**, **Neves S**, **Maayan A**, **Xiong H**, **Liu Y**, **Iyengar R**, **Klotman PE**, **Cijiang He J**. Retinoic Acid Utilizes CREB and USF1 in a Transcriptional Feed-Forward Loop in Order To Stimulate MKP1 Expression in Human Immunodeficiency Virus-Infected Podocytes. *Mol Cell Biol* 28: 5785–5794, 2008.

89. **Lundby C**, **Jacobs RA**. Adaptations of skeletal muscle mitochondria to exercise training. *Exp Physiol Exp Physiol* 101: 17–22, 2016.

90. **Madsen S**, **Agerholm M**, **Jensen BAH**, **Dall M**, **Risis S**, **Larsen S**, **Goldenbaum J**, **Prats C**, **Vienberg SG**, **Graae A-S**, **Quistorff B**, **Basse AL**, **Treebak JT**. Perturbations of NAD + salvage systems impact mitochondrial function and energy homeostasis in mouse myoblasts and intact skeletal muscle. *Am J Physiol Metab* 314: E377–E395, 2017.

91. **Martens CR**, **Denman BA**, **Mazzo MR**, **Armstrong ML**, **Reisdorph N**, **McQueen MB**, **Chonchol M**, **Seals DR**. Chronic nicotinamide riboside supplementation is well-Tolerated and elevates NAD+ in healthy middle-Aged and older adults. *Nat Commun* 9, 2018.

92. **Mazure NM**, **Pouyssé J**, **Kroemer G**, **White E**. Hypoxia-induced autophagy: cell death or cell survival? This review comes from a themed issue on Cell regulation Edited by. *Curr Opin Cell Biol* 22: 177–180, 2010.

93. **Meissner C**, **Lorenz H**, **Hehn B**, **Lemberg MK**. Intramembrane protease PARL defines a negative regulator of PINK1-and PARK2/Parkin-dependent mitophagy. (2015).

94. **Menzies KJ**, **Singh K**, **Saleem A**, **Hood DA**. Sirtuin 1-mediated effects of exercise and resveratrol on mitochondrial biogenesis. *J Biol Chem* 288: 6968–6979, 2013.

95. **Michan S**, **Sinclair D**. Sirtuins in mammals: insights into their biological function. *Biochem J* 404: 1–13, 2007.

96. **Mitra R**, **Nogee DP**, **Zechner JF**, **Yea K**, **Gierasch CM**, **Kovacs A**, **Medeiros DM**, **Kelly DP**, **Duncan JG**. The transcriptional coactivators, PGC-1α and β, cooperate to maintain cardiac mitochondrial function during the early stages of insulin resistance. *J Mol Cell Cardiol* 52: 701–710, 2012.

97. **Nair SS**, **Prathibha P**, **Rejitha S**, **Indira M**. Ethanol induced hepatic mitochondrial dysfunction is attenuated by all trans retinoic acid supplementation. *Life Sci* 135: 101–109, 2015.

98. **Nakagawa Y**, **Kuwahara K**, **Takemura G**, **Akao M**, **Kato M**, **Arai Y**, **Takano M**, **Harada M**, **Murakami M**, **Nakanishi M**, **Usami S**, **Yasuno S**, **Kinoshita H**, **Fujiwara M**, **Ueshima K**, **Nakao K**. P300 plays a critical role in maintaining cardiac mitochondrial function and cell survival in postnatal hearts. *Circ Res* 105: 746–754, 2009.

99. **Noguchi M**, **Kasahara A**. Mitochondrial dynamics coordinate cell differentiation. *Biochem Biophys Res Commun* 500: 59–64, 2018.

100. **Novak I**, **Kirkin V**, **Mcewan DG**, **Zhang J**, **Wild P**, **Rozenknop A**, **Rogov V**, **Löhr F**, **Popovic D**, **Occhipinti A**, **Reichert AS**, **Terzic J**, **Dötsch V**, **Ney PA**, **Dikic I**. Nix is a selective autophagy receptor for mitochondrial clearance. *EMBO Rep* 11: 45–51, 2009.

101. **Obrochta KM**, **Kane MA**, **Napoli JL**. Effects of diet and strain on mouse serum and tissue retinoid concentrations. *PLoS One* 9: 99435, 2014.

102. **Obrochta KM**, **Kane MA**, **Napoli JL**. Effects of Diet and Strain on Mouse Serum and Tissue Retinoid Concentrations. *PLoS One* 9: 99435, 2014.

103. **Orfali N**, **McKenna SL**, **Cahill MR**, **Gudas LJ**, **Mongan NP**. Retinoid receptor signaling and autophagy in acute promyelocytic leukemia. *Exp. Cell Res.* 324: 1–12, 2014.

104. **Ornatsky OI**, **Connor MK**, **Hood DA**. Expression of stress proteins and mitochondrial chaperonins in chronically stimulated skeletal muscle. *Biochem J* 311 (Pt 1: 119–23, 1995.

105. **Parodi PW**. Cooperative action of bioactive components in milk fat with PPARs may explain its anti-diabetogenic properties. *Med Hypotheses* 89: 1–7, 2016.

106. **Pauly M**, **Collu-Marchese M**, **Hood D**, **Shuen M**, **Saleem A**. The regulation of mitochondrial transcription factor A (Tfam) expression during skeletal muscle cell differentiation. *Biosci. Rep.* (2015).

107. **Peralta S**, **Wang X**, **Moraes CT**. Mitochondrial transcription: Lessons from mouse models. *Biochim. Biophys. Acta - Gene Regul. Mech.* 1819: 961–969, 2012.

108. **Pérez E**, **Bourguet W**, **Gronemeyer H**, **De Lera AR**. Modulation of RXR function through ligand design. *Biochim Biophys Acta - Mol Cell Biol Lipids* 1821: 57–69, 2012.

109. **Pilegaard H**, **Saltin B**, **Neufer DP**. Exercise induces transient transcriptional activation of the PGC-1α gene in human skeletal muscle. *J. Physiol.* 546: 851–858, 2003.

110. **Poirier H**, **Braissant O**, **Niot I**, **Wahli W**, **Besnard P**. 9-c/s-Retinoic acid enhances fatty acid-induced expression of the liver fatty acid-binding protein gene. .

111. **Priesnitz C**, **Becker T**. Pathways to balance mitochondrial translation and protein import. (2018). doi: 10.1101/gad.316547.

112. **Puigserver P**, **Spiegelman BM**. Peroxisome proliferator-activated receptor-γ coactivator 1α (PGC-1α): Transcriptional coactivator and metabolic regulator. *Endocr. Rev.* 24: 78–90, 2003.

113. **Raichur S**, **Fitzsimmons RL**, **Myers SA**, **Pearen MA**, **Lau P**, **Eriksson N**, **Wang SM**, **Muscat GEO**. Identification and validation of the pathways and functions regulated by the orphan nuclear receptor, ROR alpha1, in skeletal muscle. *Nucleic Acids Res* 38: 4296–4312, 2010.

114. **Ren X**, **Li Y**, **Ma X**, **Zheng L**, **Xu Y**, **Wang J**. Activation of p38/MEF2C pathway by all-trans retinoic acid in cardiac myoblasts. *Life Sci* 81: 89–96, 2007.

115. **Rhee EJ**, **Plutzky J**. Retinoid metabolism and diabetes mellitus. *Diabetes Metab J* 36: 167–180, 2012.

116. **Rigobello MP**, **Scutari G**, **Friso A**, **Barzon E**, **Artusi S**, **Bindoli A**. Mitochondrial permeability transition and release of cytochrome c induced by retinoic acids. *Biochem Pharmacol* 58: 665–670, 1999.

117. **Rodrigues M**, **Kulkarni SS**, **Yanes O**, **Canela N**, **Migaud ME**, **Joffraud M**, **Auwerx J**, **Cantó C**, **Brenner C**, **Ratajczak J**, **Ras R**, **Redpath P**, **Trammell SAJ**, **Boutant M**. NRK1 controls nicotinamide mononucleotide and nicotinamide riboside metabolism in mammalian cells. *Nat Commun* 7, 2016.

118. **Rose AJ**, **Hargreaves M**. Exercise increases Ca2+-calmodulin-dependent protein kinase II activity in human skeletal muscle. *J Physiol* 553: 303–309, 2003.

119. **Scarpulla RC**. Nuclear control of respiratory gene expression in mammalian cells. *J Cell Biochem* 97: 673–683, 2006.

120. **Scarpulla RC**. Transcriptional Paradigms in Mammalian Mitochondrial Biogenesis and Function. *Physiol Rev* 88: 611–638, 2008.

121. **Schug TT**, **Berry DC**, **Shaw NS**, **Travis SN**, **Noy N**. Opposing Effects of Retinoic Acid on Cell Growth Result from Alternate Activation of Two Different Nuclear Receptors. *Cell* 129: 723–733, 2007.

122. **Sekine S**, **Youle RJ**. PINK1 import regulation; a fine system to convey mitochondrial stress to the cytosol. *BMC Biol.* 16: 2018.

123. **Shan P**, **Xu W**, **Huang Z**, **Pu J**, **Huang W**. Protective role of retinoid X receptor in H9c2 cardiomyocytes from hypoxia / reoxygenation injury in rats. *World J Emerg Med* 5: 122–127, 2014.

124. **Sheehan T**, **Hood DA**, **Irrcher I**, **Adhihetty PJ**, **Joseph A-M**. PPARγ coactivator-1α expression during thyroid hormone- and contractile activity-induced mitochondrial adaptations. *Am J Physiol Physiol* 284: C1669–C1677, 2013.

125. **Sin J**, **Andres AM**, **Taylor DJR**, **Weston T**, **Hiraumi Y**, **Stotland A**, **Kim BJ**, **Huang C**, **Doran KS**, **Gottlieb RA**. Mitophagy is required for mitochondrial biogenesis and myogenic differentiation of C2C12 myoblasts. (2016).

126. **Sleeman MW**, **Zhou H**, **Rogers S**, **Ng KW**, **Best JD**. Retinoic acid stimulates glucose transporter expression in L6 muscle cells. *Mol Cell Endocrinol* 108: 161–167, 1995.

127. **Snow RJ**, **Howlett KF**, **McGee SL**, **Garnham AP**, **Hargreaves M**, **Gibala MJ**. Brief intense interval exercise activates AMPK and p38 MAPK signaling and increases the expression of PGC-1α in human skeletal muscle. *J Appl Physiol* 106: 929–934, 2008.

128. **Terada S**, **Goto M**, **Kato M**, **Kawanaka K**, **Shimokawa T**, **Tabata I**. Effects of low-intensity prolonged exercise on PGC-1 mRNA expression in rat epitrochlearis muscle. *Biochem Biophys Res Commun* 296: 350–354, 2002.

129. **Tourniaire F**, **Musinovic H**, **Gouranton E**, **Astier J**, **Marcotorchino J**, **Arreguin A**, **Bernot D**, **Palou A**, **Bonet ML**, **Ribot J**, **Landrier J-F**. All- *trans* retinoic acid induces oxidative phosphorylation and mitochondria biogenesis in adipocytes. *J Lipid Res* 56: 1100–1109, 2015.

130. **Trammell SA**, **Schmidt MS**, **Weidemann BJ**, **Redpath P**, **Jaksch F**, **Dellinger RW**, **Li Z**, **Abel ED**, **Migaud ME**, **Brenner C**. Nicotinamide riboside is uniquely and orally bioavailable in mice and humans. *Nat Commun* 7, 2016.

131. **Tripathy S**, **Chapman JD**, **Han CY**, **Hogarth CA**, **Arnold SLM**, **Onken J**, **Kent T**, **Goodlett DR**, **Isoherranen N**. All-Trans-Retinoic Acid Enhances Mitochondrial Function in Models of Human Liver. *Mol Pharmacol* 89: 560–574, 2016.

132. **Tripathy S**, **Chapman JD**, **Han CY**, **Hogarth CA**, **Arnold SLM**, **Onken J**, **Kent T**, **Goodlett DR**, **Isoherranen N**. All-Trans-Retinoic Acid Enhances Mitochondrial Function in Models of Human Liver s. *Mol Pharmacol Mol Pharmacol* 89: 560–574, 2016.

133. **Uguccioni G**, **Hood DA**. The importance of PGC-1 in contractile activity-induced mitochondrial adaptations. *AJP Endocrinol Metab* 300: E361–E371, 2011.

134. **Vega RB**, **Huss JM**, **Kelly DP**. The Coactivator PGC-1 Cooperates with Peroxisome Proliferator-Activated Receptor alpha in Transcriptional Control of Nuclear Genes Encoding Mitochondrial Fatty Acid Oxidation Enzymes. *Mol Cell Biol* 20: 1868–1876, 2000.

135. **Ventura-Clapier R**, **Garnier A**, **Veksler V**. Transcriptional control of mitochondrial biogenesis: The central role of PGC-1α. *Cardiovasc. Res.* 79: 208–217, 2008.

136. **Viscomi C**, **Bottani E**, **Civiletto G**, **Cerutti R**, **Moggio M**, **Fagiolari G**, **Schon EA**, **Lamperti C**, **Zeviani M**. In vivo correction of COX deficiency by activation of the AMPK/PGC-1α axis. *Cell Metab* 14: 80–90, 2011.

137. **Vögtle FN**, **Meisinger C**. Sensing Mitochondrial Homeostasis: The Protein Import Machinery Takes Control. *Dev. Cell* 23: 234–236, 2012.

138. **Wagatsuma A**, **Sakuma K**. Mitochondria as a Potential Regulator of Myogenesis. *Sci World J* 2013: 1–9, 2013.

139. **Wiedemann N**, **Frazier AE**, **Pfanner N**. The Protein Import Machinery of Mitochondria. *J Biol Chem* 279: 14473–14476, 2004.

140. **Wu ZP**, **Andersson U**, **Zhang C**, **Adelmant G**, **Mootha V**, **Troy A**, **Cinti S**, **Lowell B**, **Scarpulla RC**, **Spiegelman BM**. Mechanisms controlling mitochondrial biogenesis and respiration through the thermogenic coactivator PGC-1.*Cell* 98: 115–124, 1999.

141. **Xun Z**, **Lee D-Y**, **Lim J**, **Canaria CA**, **Barnebey A**, **Yanonne SM**, **Mcmurray CT**. Retinoic acid-induced differentiation increases the rate of oxygen consumption and enhances the spare respiratory capacity of mitochondria in SH-SY5Y cells. *Mech Ageing Dev* 133: 176–185, 2012.

142. **Yamamoto H**, **Oosterveer MH**, **Fernandez-Marcos PJ**, **Youn DY**, **Cettour-Rose P**, **Gademann K**, **Cantó C**, **Rinsch C**, **Sauve AA**, **Cen Y**, **Schoonjans K**, **Andreux PA**, **Pirinen E**, **Auwerx J**, **Houtkooper RH**. The NAD+ Precursor Nicotinamide Riboside Enhances Oxidative Metabolism and Protects against High-Fat Diet-Induced Obesity. *Cell Metab* 15: 838–847, 2012.

143. **Yang Y**, **Karakhanova S**, **Hartwig W**, **D'Haese JG**, **Philippov PP**, **Werner J**, **Bazhin A V**. Mitochondria and Mitochondrial ROS in Cancer: Novel Targets for Anticancer Therapy. *J. Cell. Physiol.* 231: 2570–2581, 2016.

144. **Yu S**, **Levi L**, **Siegel R**, **Noy N**. Retinoic acid induces neurogenesis by activating both retinoic acid receptors (RARs) and peroxisome proliferator-activated receptor β/δ (PPARβ/δ). *J Biol Chem* 287: 42195–42205, 2012.

145. **Yun ML**, **Jung OL**, **Jung JH**, **Ji HK**, **Park SH**, **Ji MP**, **Kim EK**, **Suh PG**, **Hyeon SK**. Retinoic acid leads to cytoskeletal rearrangement through AMPK-Rac1 and stimulates glucose uptake through AMPK-p38 MAPK in skeletal muscle cells. *J Biol Chem* 283: 33969–33974, 2008.

146. **Yun ML**, **Jung OL**, **Jung JH**, **Ji HK**, **Park SH**, **Ji MP**, **Kim EK**, **Suh PG**, **Hyeon SK**. Retinoic acid leads to cytoskeletal rearrangement through AMPK-Rac1 and stimulates glucose uptake through AMPK-p38 MAPK in skeletal muscle cells. *J Biol Chem* 283: 33969–33974, 2008.

147. **Zhang F**, **Zhang L**, **Qi Y**, **Xu H**. Mitochondrial cAMP signaling. *Cell Mol Life Sci* 73: 4577–4590, 2016.

148. **Zhang H**, , **Ryu D**, **Wu Y**, **Gariani K**, **Wang X**, **Luan P**, **D'Amico D**, **Ropelle ER**, **Lutolf MP**, **Aebersold R**, **Schoonjans K**, **Menzies KJ**, **Auwerx J**. Nad(+) Repletion Improves Mitochondrial and Stem Cell Function and Enhances Life Span in Mice [Online]. *Science (80-)* 352: 1436–1443, 2016. http://science.sciencemag.org/ [25 Mar. 2019].

149. **Zhang J**, **Ney PA**. Role Of Bnip3 And Nix IN Cell Death, Autophagy, And Mitophagy. *Cell Death Differ* 16: 939–946, 2009.

150. **Zhang N**, **Sauve AA**. Regulatory Effects of NAD+ Metabolic Pathways on Sirtuin Activity. In: *Progress in Molecular Biology and Translational Science*. Academic Press, p. 71–104.

151. **Zhang R**, **Wang Y**, **Li R**, **Chen G**. Transcriptional Factors Mediating Retinoic Acid Signals in the Control of Energy Metabolism. *Int J Mol Sci* 16: 14210–14244, 2015.

152. **Zhang T**, **Zheng X**, **Yang L**, **Zhou R**, **Xie J**, **Li W-I**, **Chai Z**, **Yu B**, **He Q**. p38 Mitogen-activated protein kinase-dependent regulation of SRC-3 and involvement in retinoic acid receptor α signaling in embryonic cortical neurons. *IUBMB Life* 61: 670–678, 2009.

153. **Zhang Y**, **Uguccioni G**, **Ljubicic V**, **Irrcher I**, **Iqbal S**, **Singh K**, **Ding S**, **Hood DA**. Multiple signaling pathways regulate contractile activity-mediated PGC-1 gene expression and activity in skeletal muscle cells. *Physiol Rep* 2: e12008–e12008, 2014.

154. **Zhou Y**, **Zhang H**, **Zheng B**, **Ye L**, **Zhu S**, **Johnson NR**, **Wang Z**, **Wei X**, **Chen D**, **Cao G**, **Fu X**, **Li X**, **Xu H-Z**, **Xiao J**. Retinoic Acid Induced-Autophagic Flux Inhibits ER-Stress Dependent Apoptosis and Prevents Disruption of Blood-Spinal Cord Barrier after Spinal Cord Injury. *Int J Biol Sci* 12: 87–99, 2016.

155. **Zhu GH**, **Huang J**, **Bi Y**, **Su Y**, **Tang Y**, **He BC**, **He Y**, **Luo J**, **Wang Y**, **Chen L**, **Zuo GW**, **Jiang W**, **Luo Q**, **Shen J**, **Liu B**, **Zhang WL**, **Shi Q**, **Zhang BQ**, **Kang Q**, **Zhu J**, **Tian J**, **Luu HH**, **Haydon RC**, **Chen Y**, **He TC**. Activation of RXR and RAR signaling promotes myogenic differentiation of myoblastic C2C12 cells. *Differentiation* 78: 195–204, 2009.

156. **Zorzano A**. Regulation of mitofusin-2 expression in skeletal muscleThis paper is one of a selection of papers published in this Special Issue, entitled 14th International Biochemistry of Exercise Conference – Muscles as Molecular and Metabolic Machines, and has under. *Appl Physiol Nutr Metab* 34: 433–439, 2009.

Table 2: *A summary of the statistically significant effects of RA isomers and NR.on mitochondrial proteins with Protocol 1.*

Protocol 1	Vehicle	9cisRA	ATRA	NR	9cisRA+NR	ATRA+NR
Mt-DNA proteins	-	COX-I↑	COX-I↑	-	COX-I↑	COX-I↑
N-DNA proteins	-	Tfam↓	Tfam↓	COX-IV↑	Tfam↓	Tfam↓
PGC-1α	-	-	-	-	-	-
Import Proteins	-	Tom40↑	Tom40↑	-	Tom40↑	Tom40↑

Table 3. *A summary of the statistically significant effects of RA and CCA on mtDNA and nuclear encoded mitochondrial proteins with Protocol 2.*

Protocol 2	Vehicle	9cisRA	ATRA	CCA	9cisRA+ CCA	ATRA+ CCA
Mt-DNA Protein	-	COX-I↑	COX-I↑	-	COX-I↑	COX-I↑
N-DNA Protein	-	Tfam↓	-	COX-IV↑ Tom40↑	Mature Tfam↓ COX-IV↑	COX-IV↑
PGC-1α	-	↑	↑	↑	↑	↑
Import Proteins	-	Tom40↑	Tom40↑	-	Tom40↑	Tom40↑

Figure 9. *RA isomers can potentially exert partial mtDNA transcription.* Adapted from Berdanier et al (13), Everts et al (42). Retinoic Acid is able to bind to the HRE (Hormone Response Elements) of the mitochondrial DNA loop, and facilitate transcription of the heavy strand. RA isomers. This could potentially initiate mtDNA transcription by binding to the promoter region RXR and RARE sites. The arrows indicate transcription and replication start sites. Less is known about whether or not binding at the HRE-1 location can also facilitate transcription of the light strand.

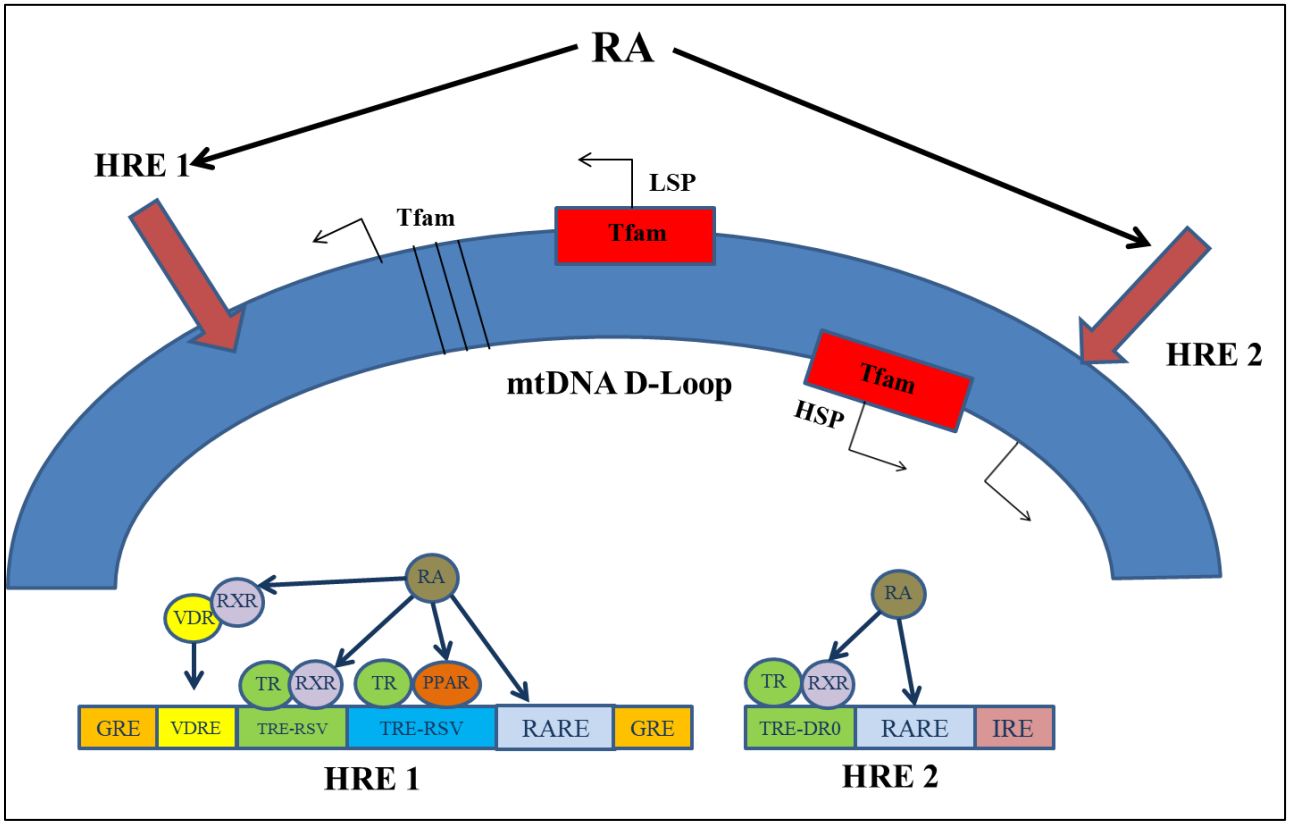

Future Work

1) Assessing the functionality of the mitochondria post CCA/RA/NR treatment would give a more complete picture of the mitochondrial quality and add depth to our work. Previous work from our lab has examined the oxygen consumption of cells treated with resveratrol (94), however my measurements of respiration with the Clark electrode were not successful. To this point, we have established that there is a higher level of selected mitochondrial proteins post- RA and CCA treatment, however measuring the oxygen consumption rate (OCR) and the Extracellular acidification rate (ECAR) with the new Seahorse© instrument could tell us the metabolic profile of the mitochondria and whether or not shifts towards fatty acid oxidation have occurred.
2) In order to examine how the functions of Tfam and RA may overlap in the mtDNA genome, a Tfam knockdown experiment with RA treatment may give insight into the interplay between RA and Tfam on mtDNA transcription. Knockout experiments are not viable (107), therefore a siRNA knockdown of Tfam, followed by RA treatment and measurement of mtDNA-encoded proteins will elucidate the interplay between the two.
3) To date, we have found that RA facilitates the translation of PGC-1alpha via kinase-independent activity, as none of the three major kinases have been elevated with RA treatment. The CREB and MEFC2 pathways are implicated in the transcription of PGC-1α (88, 114) but our study has not explored them as possible avenues of the facilitation of PGC-1α transcription and eventual translation. Repetition of these experiments, followed by nuclear/cytosolic separation and analysis of PGC-1α levels would give us insight on the activation status with RA treatment.

4) Lastly, it would be beneficial to examine RA treatment *in-vivo*, and whether or not the effects seen in muscle cell tissue carry over into live animals since RA is implicated in the function of other major tissues in the body. Examining RA treatment of diabetic mice in conjunction with exercise would allow us to further elucidate the fatty acid oxidation and glucose handling effects, the amelioration of diabetic symptoms seen in mice with RA treatment (14, 17, 151), and lastly, mitochondrial turnover. In conclusion, examining RA treatment in the whole system would deepen our understanding of RA and how it interacts with exercise in order to impact metabolism. A dose-response study would also allow us to see if higher RA concentrations would lead to augmented effects.

APPENDIX A- DATA AND STATISTICAL ANALYSIS

NR+ RA: **COX-I**

	Veh	9cisRA	ATRA	NR	9cisRA+NR	ATRA+NR
N1	0.15304	0.541094	0.504779	0.254833	0.57775001	0.7083537
N2	0.182104	0.506663	0.51283	0.294425	0.68687503	1.22475192
N3	0.126158	0.543935	0.258515	0.306003	0.53358235	0.54806303
N4	0.191065	0.648129	0.364542	0.126387	0.44693767	0.31939969
N5	0.231709	0.496398	0.99906	0.465955	1.12436456	0.8459956
N6	0.476569	1.18528	1.30329	0.573802	1.54441147	1.26199188
Two-way ANOVA	Ordinary					
Alpha	0.05					
Source of Variation	% of total	P value	P value su	Significant?		
Interaction	0.1166	0.9721	ns	No		
Nicotinamide Ribosi	3.928	0.1775	ns	No		
Retinoic Acid	34.17	0.0014	**	Yes		
ANOVA table	SS	DF	MS	F (DFn, D	P value	
Interaction	0.005656	2	0.002828	F (2, 30) =	P = 0.9721	
Nicotinamide Ribosi	0.1905	1	0.1905	F (1, 30) =	P = 0.1775	
Retinoic Acid	1.657	2	0.8285	F (2, 30) =	P = 0.0014	
Residual	2.996	30	0.09988			

NR+ RA: **COX-IV**

	Veh	9cisRA	ATRA	NR	9cisRA+NR	ATRA+NR
N1	0.457142	0.642972	0.951201	1.246299	0.81041089	0.71983949
N2	0.409607	0.832108	0.786634	1.545588	0.58313244	0.40666336
N3	0.569781	1.152477	0.761304	1.564983	1.00670309	1.01947244
N4	1.524163	1.438776	1.195963	1.377011	1.23826638	0.33102603
N5	0.586168	0.639863	0.87964	0.616566	0.7520418	0.99781544
N6	1.023322	1.142173	1.336457	1.25046	1.54244624	1.11874506
Two-way ANOVA	Ordinary					
Alpha	0.05					
Source of Variation	% of total	P value	P value su	Significant?		
Interaction	18.06	0.0427	*	Yes		
Nicotinamide Ribosi	1.975	0.3879	ns	No		
Retinoic Acid	2.786	0.5875	ns	No		
ANOVA table	SS	DF	MS	F (DFn, D	P value	
Interaction	0.8209	2	0.4105	F (2, 30) =	P = 0.0427	
Nicotinamide Ribosi	0.08977	1	0.08977	F (1, 30) =	P = 0.3879	
Retinoic Acid	0.1266	2	0.06331	F (2, 30) =	P = 0.5875	
Residual	3.508	30	0.1169			
T-Test						
Column B	NR					
vs.	vs.					
Column A	Veh					
Unpaired t test						
P value	0.0497					
P value summary	*					
Significantly differen	Yes					
One- or two-tailed P	Two-tailed					
t, df	t=2.232 df=10					

NR+ RA: **Tfam Precursor**

	Veh	9cisRA	ATRA	NR	9cisRA+NR	ATRA+NR
N1	2.005991	1.546914	1.477321	2.045553	1.32208547	1.40815239
N2	2.0322	1.012301	1.269745	1.862169	1.65299204	1.69414199
N3	0.880844	0.554427	0.506461	0.962822	0.62417582	0.70872326
N4	1.658563	1.439058	1.329961	1.709828	1.23435246	0.75968504
N5	1.647743	1.277239	1.145922	1.49582	0.73785713	0.53289672
N6	1.71516	0.992077	0.90351	1.471908	1.16783449	1.28601735
N7	1.962612	0.958215	1.207745	1.974368	0.89291242	1.07365801
Two-way ANOVA	Ordinary					
Alpha	0.05					
Source of Variation	% of total	P value	P value su	Significant?		
Interaction	0.03153	0.9908	ns	No		
Nicotinamide Ribosi	0.2425	0.708	ns	No		
Retinoic Acid	38.46	0.0002	***	Yes		
ANOVA table	SS	DF	MS	F (DFn, D	P value	
Interaction	0.002541	2	0.001271	F (2, 36) =	P = 0.9908	
Nicotinamide Ribosi	0.01955	1	0.01955	F (1, 36) =	P = 0.7080	
Retinoic Acid	3.1	2	1.55	F (2, 36) =	P = 0.0002	
Residual	4.938	36	0.1372			

NR+ RA: **Tfam Mature**

	Veh	9cisRA	ATRA	NR	9cisRA+NR	ATRA+NR
N1	1.198509	0.95097	0.7803	0.958235	1.21161235	0.83697589
N2	1.397873	0.66769	0.714747	1.052157	1.41134266	1.2130195
N3	0.835355	0.498836	0.507414	0.694169	0.63565718	0.64524955
N4	1.805714	1.217779	1.215895	2.006747	1.14927241	1.04371961
N5	1.925347	1.310866	1.223174	2.125797	0.94482003	1.0369291
N6	0.92774	1.033342	0.64574	1.108736	1.07263314	1.3221273
N7	1.415701	1.026604	1.133475	1.650449	1.25898101	1.20834736
Two-way ANOVA	Ordinary					
Alpha	0.05					
Source of Variation	% of total	P value	P value su	Significant?		
Interaction	0.7066	0.8468	ns	No		
Nicotinamide Ribosi	1.83	0.3585	ns	No		
Retinoic Acid	21.31	0.0118	*	Yes		
ANOVA table	SS	DF	MS	F (DFn, D	P value	
Interaction	0.04266	2	0.02133	F (2, 36) =	P = 0.8468	
Nicotinamide Ribosi	0.1105	1	0.1105	F (1, 36) =	P = 0.3585	
Retinoic Acid	1.287	2	0.6433	F (2, 36) =	P = 0.0118	
Residual	4.597	36	0.1277			

NR+ RA: **Citrate Synthase**

	Veh	9cisRA	ATRA	NR	9cisRA+NR	ATRA+NR
N1	0.319858	0.447458	0.368228	0.444736	0.62518472	0.43879668
N2	0.254284	0.421712	0.459736	0.45608	0.71202845	0.59223581
N3	0.910008	1.435779	1.367846	1.225986	1.06348964	1.07570279
N4	1.119856	1.577323	1.372748	1.329589	1.7367088	1.75505815
N5	2.338919	2.730033	2.53469	3.031815	3.20635817	2.81862661
N6	3.215384	3.501194	2.918528	3.381289	3.16252489	3.55166021
Two-way ANOVA	Ordinary					
Alpha	0.05					
Source of Variation	% of total	P value	P value su	Significant?		
Interaction	0.1694	0.9746	ns	No		
Nicotinamide Ribosi	0.7001	0.6476	ns	No		
Retinoic Acid	0.6429	0.907	ns	No		
ANOVA table	SS	DF	MS	F (DFn, D	P value	
Interaction	0.07382	2	0.03691	F (2, 30) =	P = 0.9746	
Nicotinamide Ribosi	0.3051	1	0.3051	F (1, 30) =	P = 0.6476	
Retinoic Acid	0.2802	2	0.1401	F (2, 30) =	P = 0.9070	
Residual	42.92	30	1.431			

NR+ RA: **PGC-1α**

	Veh	9cisRA	ATRA	NR	9cisRA+NR	ATRA+NR
N1	2.10118	2.664426	2.694689	1.874454	1.90043027	1.91843865
N2	1.733033	1.873163	1.77884	1.858456	2.170215	2.41581329
N3	1.186741	1.432181	1.117252	2.227577	1.81343415	1.79664782
N4	1.681099	2.644453	2.622733	2.149885	1.89705589	2.57604003
Two-way ANOVA	Ordinary					
Alpha	0.05					
Source of Variation	% of total	P value	P value su	Significant?		
Interaction	7.08	0.4873	ns	No		
Nicotinamide Ribosi	1.061	0.6415	ns	No		
Retinoic Acid	6.713	0.5051	ns	No		
ANOVA table	SS	DF	MS	F (DFn, D	P value	
Interaction	0.3175	2	0.1588	F (2, 18) =	P = 0.4873	
Nicotinamide Ribosi	0.04758	1	0.04758	F (1, 18) =	P = 0.6415	
Retinoic Acid	0.301	2	0.1505	F (2, 18) =	P = 0.5051	
Residual	3.819	18	0.2121			

NR+ RA: **Tim23**

	Veh	9cisRA	ATRA	NR	9cisRA+NR	ATRA+NR
N1	0.455771	1.615091	1.020756	0.343741	0.56744315	0.61256319
N2	0.359669	1.121597	1.179078	0.79646	0.38719307	0.7239974
N3	0.842077	1.00708	0.754723	0.626519	0.86112557	0.79627938
N4	0.560493	0.393416	0.79218	0.770954	1.26856704	0.82337038
N5	0.889755	1.01876	1.241682	1.115081	1.57939356	0.98620795
Two-way ANOVA	Ordinary					
Alpha	0.05					
Source of Variation	% of total	P value	P value su	Significant?		
Interaction	4.094	0.5467	ns	No		
Nicotinamide Ribosi	1.032	0.5815	ns	No		
Retinoic Acid	15.54	0.1168	ns	No		
ANOVA table	SS	DF	MS	F (DFn, D	P value	
Interaction	0.1305	2	0.06523	F (2, 24) =	P = 0.5467	
Nicotinamide Ribosi	0.03288	1	0.03288	F (1, 24) =	P = 0.5815	
Retinoic Acid	0.4953	2	0.2476	F (2, 24) =	P = 0.1168	
Residual	2.528	24	0.1053			

NR+ RA: **Tom40**

	Veh	9cisRA	ATRA	NR	9cisRA+NR	ATRA+NR
N1	0.411675	1.230645	0.755256	0.409733	0.78722211	0.7715069
N2	0.460717	0.86972	1.201367	0.597706	0.79719072	1.00960683
N3	0.777217	0.796156	0.967835	0.959866	1.73427318	1.24222167
N4	1.143015	1.153965	1.276153	0.894407	1.36742336	1.19698556
Two-way ANOVA	Ordinary					
Alpha	0.05					
Source of Variation	% of total	P value	P value su	Significant?		
Interaction	1.223	0.8515	ns	No		
Nicotinamide Ribosi	0.9131	0.6285	ns	No		
Retinoic Acid	30.02	0.037	*	Yes		
ANOVA table	SS	DF	MS	F (DFn, D	P value	
Interaction	0.02928	2	0.01464	F (2, 18) =	P = 0.8515	
Nicotinamide Ribosi	0.02187	1	0.02187	F (1, 18) =	P = 0.6285	
Retinoic Acid	0.7189	2	0.3595	F (2, 18) =	P = 0.0370	
Residual	1.625	18	0.09026			

NR+ RA: **mtHsp70**

	Veh	9cisRA	ATRA	NR	9cisRA+NR	ATRA+NR
N1	0.720919	0.76442	1.080749	0.952431	0.57468624	0.67108515
N2	0.59946	0.656441	0.670942	1.130639	0.59434768	0.53729659
N3	0.521339	0.637272	0.675036	0.9645	0.77722957	0.83952721
N4	0.838671	0.828196	0.69259	0.865215	0.97621958	1.16551318
Two-way ANOVA	Ordinary					
Alpha	0.05					
Source of Variation	% of total variation					
Interaction	14.26	P value	P value su	Significant?		
Nicotinamide Ribosi	9.699	0.1927	ns	No		
Retinoic Acid	5.002	0.1344	ns	No		
		0.5421	ns	No		
ANOVA table	SS					
Interaction	0.1138	DF	MS	F (DFn, D	P value	
Nicotinamide Ribosi	0.07737	2	0.05688	F (2, 18) =	P = 0.1927	
Retinoic Acid	0.0399	1	0.07737	F (1, 18) =	P = 0.1344	
Residual	0.5667	2	0.01995	F (2, 18) =	P = 0.5421	
T-Test						
Column B	NR					
vs.	vs.					
Column A	Veh					
Unpaired t test						
P value	0.0134					
P value summary	*					
Significantly differen	Yes					
One- or two-tailed P	Two-tailed					
t, df	t=3.463 df=6					

CCA+ RA: **COX-I**

	Veh	9cisRA	ATRA	CCA	9cisRA+CCA	ATRA+CCA
N1	0.252742	0.514703	0.607541	0.206468	0.5094314	0.5091134
N2	0.273371	0.609604	0.429473	0.357093	1.03406	1.232016
N3	0.456783	0.796754	0.917869	0.710399	1.183333	1.280402
N4	0.126412	0.328711	0.598258	0.310621	0.7023895	0.7685578
N5	0.342989	0.576279	0.700594	0.404698	0.6317692	0.5046039
N6	0.750224	1.464645	2.070752	0.78129	1.464752	2.768845
N7	1.67299	1.760236	2.98035	1.532209	2.405668	3.094999
N8	0.270368	0.479026	0.569366	0.263079	0.6699001	0.7915437
N9	0.271515	0.819358	0.867048	CCA DATA NOT COLLECTED		
N10	0.402684	1.261479	0.897823			
N11	0.280367	0.651189	0.589426			
N12	0.747248	1.617327	1.645698			
N13	1.010448	1.66364	1.805154			
N14	0.353691	0.685385	0.780494			
N15	0.616829	0.874567	0.688848			

Two-way ANOVA	Ordinary					
Alpha	0.05					
Source of Variation	% of total	P value	P value su	Significant?		
Interaction	0.538	0.8125	ns	No		
cca	1.334	0.3133	ns	No		
drug	16.88	0.0026	**	Yes		
ANOVA table	SS	DF	MS	F (DFn, D	P value	
Interaction	0.1589	2	0.07944	F (2, 63) =	P = 0.8125	
cca	0.394	1	0.394	F (1, 63) =	P = 0.3133	
drug	4.984	2	2.492	F (2, 63) =	P = 0.0026	
Residual	24.03	63	0.3814			

CCA+ RA: **COX-IV**

	Veh	9cisRA	ATRA	CCA	9cisRA+CCA	ATRA+CCA
N1	0.576586	0.351802	0.360395	0.669937	0.7450621	0.500551
N2	0.670905	0.393802	0.183566	1.187018	1.186149	0.7442985
N3	0.417745	0.390821	0.389675	0.934984	0.9978219	0.7608147
N4	0.385946	0.360393	0.569623	1.016755	1.267866	1.133084
N5	0.894968	0.848413	0.778549	1.54226	1.618556	1.159831
N6	0.432908	1.176445	1.357965	1.682505	1.341669	1.759642
N7	1.187054	0.806337	0.927649	1.708059	1.722744	1.909719
N8	0.506479	0.355647	0.341462	1.178301	1.001869	0.9542009
N9	0.761931	0.76462	0.746358	CCA DATA NOT COLLECTED		
N10	0.723015	0.8826	0.895053			
N11	0.902192	0.726687	0.593574			
N12	0.506048	0.708304	0.832317			
N13	0.762269	0.751864	0.623995			

Two-way ANOVA	Ordinary					
Alpha	0.05					
Source of Variation	% of total	P value	P value su	Significant?		
Interaction	0.538	0.8125	ns	No		
cca	1.334	0.3133	ns	No		
drug	16.88	0.0026	**	Yes		
ANOVA table	SS	DF	MS	F (DFn, D	P value	
Interaction	0.1589	2	0.07944	F (2, 63) =	P = 0.8125	
cca	0.394	1	0.394	F (1, 63) =	P = 0.3133	
drug	4.984	2	2.492	F (2, 63) =	P = 0.0026	
Residual	24.03	63	0.3814			

CCA+ RA: **Tfam Precursor**

	Veh	9cisRA	ATRA	CCA	9cisRA+CCA	ATRA+CCA
N1	0.717716	0.28666	0.372199	0.449609	0.450516113	0.482701329
N2	0.637772	0.447698	0.696437	0.624333	0.413127948	0.393573514
N3	0.782092	0.643529	0.766415	0.963671	0.798638492	0.745782072
N4	1.038424	0.879517	0.938006	1.008567	0.843441512	0.980792933
N5	1.019391	0.9191	0.965538	0.863256	0.48551608	1.093691828
N6	1.105406	0.468854	0.688911	0.278635	0.313127618	0.281241919
N7	0.987016	0.387483	0.402116	0.547151	0.487094208	1.079255557
Two-way ANOVA	Ordinary					
Alpha	0.05					
Source of Variation	% of total	P value	P value su	Significant?		
Interaction	4.292	0.3921	ns	No		
cca	2.062	0.343	ns	No		
drug	13.26	0.0641	ns	No		
ANOVA table	SS	DF	MS	F (DFn, D	P value	
Interaction	0.1216	2	0.0608	F (2, 36) =	P = 0.3921	
cca	0.05843	1	0.05843	F (1, 36) =	P = 0.3430	
drug	0.3756	2	0.1878	F (2, 36) =	P = 0.0641	
Residual	2.278	36	0.06327			
T-test						
Table Analyzed	TFAM Precursor Vehicle vs 9cisRA					
Column B	9cisRA					
vs.	vs.					
Column A	Vehicle					
Unpaired t test						
P value	0.0164					
P value summary	*					
Significantly differen	Yes					
One- or two-tailed P	Two-tailed					
t, df	t=2.788 df=12					

CCA+ RA: **Tfam Mature**

	Veh	9cisRA	ATRA	CCA	9cisRA+CCA	ATRA+CCA
N1	0.959341	0.46131	0.317739	1.111104	0.465016884	0.461252783
N2	0.709618	0.422844	0.570822	1.291391	0.752827692	0.583137915
N3	0.700575	0.719201	0.92461	0.588309	0.704367661	1.022193403
N4	0.964957	0.884821	1.156858	0.630865	0.635108801	0.602982154
N5	0.491197	0.625081	1.005203	1.526552	0.784529237	1.152074262
N6	1.33516	0.57428	0.640637	0.877593	0.583579659	0.537773232
N7	1.062356	0.539625	0.562929	1.059715	0.701270455	0.849769505
Two-way ANOVA	Ordinary					
Alpha	0.05					
Source of Variation	% of total	P value	P value su	Significant?		
Interaction	0.7924	0.8268	ns	No		
cca	1.269	0.4389	ns	No		
drug	23.36	0.0074	**	Yes		
ANOVA table	SS	DF	MS	F (DFn, D	P value	
Interaction	0.02482	2	0.01241	F (2, 36) =	P = 0.8268	
cca	0.03976	1	0.03976	F (1, 36) =	P = 0.4389	
drug	0.7317	2	0.3658	F (2, 36) =	P = 0.0074	
Residual	2.336	36	0.0649			
T-test						
Table Analyzed	TFAM Mature veh vs 9cisRA					
Column B	9cisRA					
vs.	vs.					
Column A	Vehicle					
Unpaired t test						
P value	0.0365					
P value summary	*					
Significantly differen	Yes					
One- or two-tailed P	Two-tailed					
t, df	t=2.354 df=12					

CCA+ RA: **Citrate Synthase**

	Veh	9cisRA	ATRA	CCA	9cisRA+CCA	ATRA+CCA
N1	1.218517	1.638595	1.24825	0.872496	1.28885969	1.348548924
N2	0.477796	0.418204	0.380803	0.360741	0.407432506	0.700702689
N3	0.438496	0.630846	0.437916	0.434156	0.570479114	0.495943666
N4	0.805329	0.743812	0.674896	0.578441	0.724846529	0.770442202
N5	0.671708	0.682338	0.665853	0.613962	0.706618033	0.852226655
N6	0.775183	0.90004	0.722866	0.741863	0.994289977	1.114188489
Two-way ANOVA	Ordinary					
Alpha	0.05					
Source of Variation	% of total	P value	P value su	Significant?		
Interaction	5.29	0.4259	ns	No		
cca	0.00173	0.981	ns	No		
drug	4.366	0.4926	ns	No		
ANOVA table	SS	DF	MS	F (DFn, D	P value	
Interaction	0.1704	2	0.08522	F (2, 30) =	P = 0.4259	
cca	5.57E-05	1	5.57E-05	F (1, 30) =	P = 0.9810	
drug	0.1407	2	0.07034	F (2, 30) =	P = 0.4926	
Residual	2.911	30	0.09702			

CCA+ RA: **PGC-1 alpha**

	Veh	9cisRA	ATRA	CCA	9cisRA+CCA	ATRA+CCA
N1	0.426403	1.075626	1.092075	0.741982	1.201746	1.304382
N2	0.334808	1.40211	1.339539	0.532943	1.63813	0.9441478
N3	0.654628	0.963233	0.717858	0.909767	0.9594332	1.220115
N4	0.7333	0.922234	0.582435	0.618605	0.9772882	1.350956
N5	0.984332	1.924525	2.582839	1.257874	1.915074	1.951808
N6	1.187963	2.625586	2.649163	1.761471	2.580405	4.110325
N7	0.713296	1.040137	0.921605	CCA DATA NOT COLLECTED		
N8	0.8991	0.801991	0.696777			
N9	0.645766	1.029698	0.773903			
N10	0.533626	0.687954	0.790714			
N11	1.105614	1.024698	0.839868			
N12	0.796258	0.801914	1.142197			
N13	0.873989	1.178082	1.072798			

Two-way ANOVA	Ordinary					
Alpha	0.05					
Source of Variation	% of total	P value	P value su	Significant?		
Interaction	1.585	0.596	ns	No		
cca	7.887	0.0268	*	Yes		
drug	14.24	0.0134	*	Yes		
ANOVA table	SS	DF	MS	F (DFn, D	P value	
Interaction	0.4018	2	0.2009	F (2, 51) =	P = 0.5960	
cca	1.999	1	1.999	F (1, 51) =	P = 0.0268	
drug	3.61	2	1.805	F (2, 51) =	P = 0.0134	
Residual	19.6	51	0.3843			

CCA+ RA: **NRF-1**

	Veh	9cisRA	ATRA	CCA	9cisRA+CCA	ATRA+CCA
N1	1.744831	1.754957	1.732793	1.674159	1.513267251	1.627157004
N2	1.577869	1.369597	1.518797	1.638734	1.88649025	0.954721074
N3	0.950118	1.081567	1.218517	0.976574	0.717634015	1.153138531
N4	1.063766	0.874403	0.988773	1.210048	0.900682157	1.35375297
Two-way ANOVA	Ordinary					
Alpha	0.05					
Source of Variation	% of total	P value	P value su	Significant?		
Interaction	0.6543	0.9419	ns	No		
cca	0.1107	0.8882	ns	No		
drug	1.262	0.8912	ns	No		
ANOVA table	SS	DF	MS	F (DFn, D	P value	
Interaction	0.0179	2	0.00895	F (2, 18) =	P = 0.9419	
cca	0.003029	1	0.003029	F (1, 18) =	P = 0.8882	
drug	0.03453	2	0.01727	F (2, 18) =	P = 0.8912	
Residual	2.68	18	0.1489			

CCA+ RA: **LC3 II/I**

	Veh	9cisRA	ATRA	CCA	9cisRA+CCA	ATRA+CCA
N1	1.374014	1.354117	1.290407	0.527991	0.4941397	0.8020372
N2	1.224006	1.348731	1.109691	1.158963	0.6078364	0.9118378
N3	0.850524	1.064299	0.987267	0.296409	0.3305946	0.4534357
N4	0.994319	1.03971	1.342847	0.479124	0.6401998	0.5984518
N5	0.559401	0.681252	0.681439	CCA DATA NOT COLLECTED		
N6	0.96133	0.817394	0.787624			
N7	0.652155	0.774135	0.719689			
N8	0.732835	0.595804	0.867135			
Two-way ANOVA	Ordinary					
Alpha	0.05					
Source of Variation	% of total	P value	P value su	Significant?		
Interaction	3.416	0.5538	ns	No		
cca	8.535	0.0929	ns	No		
drug	4.766	0.4412	ns	No		
ANOVA table	SS	DF	MS	F (DFn, D	P value	
Interaction	0.03539	2	0.01769	F (2, 30) =	P = 0.5538	
cca	0.08841	1	0.08841	F (1, 30) =	P = 0.0929	
drug	0.04937	2	0.02469	F (2, 30) =	P = 0.4412	
Residual	0.8807	30	0.02936			
T-test						
Column B	9cisRA+CCA					
vs.	vs.					
Column A	Control					
Unpaired t test						
P value	0.0148					
P value summary	*					
Significantly differen	Yes					
One- or two-tailed P	Two-tailed					
t, df	t=2.939 df=10					

CCA+ RA: **p62**

	Veh	9cisRA	ATRA	CCA	9cisRA+CCA	ATRA+CCA
N1	0.964251	1.345813	2.08312	1.862169	2.038981	1.993075
N2	1.090918	2.390689	1.760276	1.888766	1.395961	1.436267
N3	1.495361	1.933011	1.787895	1.80353	2.127916	2.647257
N4	2.738294	2.503004	1.835485	2.142894	2.326725	1.470028
N5	1.132009	1.916121	2.057727	1.82004	1.785906	1.953936
N6	1.261405	1.455852	1.334878	1.106211	1.32972	1.081594
N7	1.260569	1.039772	0.641423	CCA DATA NOT COLLECTED		
N8	0.762524	0.854552	0.907328			
N9	1.164486	1.738607	1.63267			
N10	2.190985	1.63286	1.72674			
Two-way ANOVA	Ordinary					
Alpha	0.05					
Source of Variation	% of total	P value	P value su	Significant?		
Interaction	0.815	0.8299	ns	No		
cca	5.232	0.1284	ns	No		
drug	1.812	0.662	ns	No		
ANOVA table	SS	DF	MS	F (DFn, D	P value	
Interaction	0.09668	2	0.04834	F (2, 42) =	P = 0.8299	
cca	0.6206	1	0.6206	F (1, 42) =	P = 0.1284	
drug	0.215	2	0.1075	F (2, 42) =	P = 0.6620	
Residual	10.84	42	0.258			

CCA+ RA: **Beclin**

	Veh	9cisRA	ATRA	CCA	9cisRA+CCA	ATRA+CCA
N1						
N2	1.917064	1.498013	1.938439	1.420024	1.553702934	1.775219518
N3	1.542369	2.599375	2.251252	3.134473	1.767070007	1.723545021
N4	1.858023	1.184313	0.980516	0.835418	1.095158663	0.686373182
N5	0.847596	1.391481	1.222222	1.029621	1.473350071	1.031386015
N6	2.534593	1.891389	1.549435	1.011436	1.108698328	1.773088509
N7	2.271364	1.612242	1.934172	0.916335	1.14066068	0.891810858
Two-way ANOVA	Ordinary					
Alpha	0.05					
Source of Variation	% of total	P value	P value su	Significant?		
Interaction	0.1867	0.9686	ns	No		
cca	11.17	0.0599	ns	No		
drug	0.9466	0.8513	ns	No		
ANOVA table	SS	DF	MS	F (DFn, D	P value	
Interaction	0.02057	2	0.01028	F (2, 30) =	P = 0.9686	
cca	1.231	1	1.231	F (1, 30) =	P = 0.0599	
drug	0.1043	2	0.05213	F (2, 30) =	P = 0.8513	
Residual	9.659	30	0.322			

CCA+ RA: **Tim23**

	Veh	9cisRA	ATRA	CCA	9cisRA+CCA	ATRA+CCA
N1	1.243396	2.486152	3.191163	1.709234	2.828723	2.581458
N2	0.873672	1.34927	1.203369	1.166294	1.060119	0.5242305
N3	1.792207	1.749553	1.729326	0.697743	1.384781	1.450562
N4	0.644062	1.040971	1.209887	0.975667	0.9375689	0.8791537
N5	0.900882	1.397515	1.895195	2.241009	2.360801	2.35036
N6	0.651785	1.210369	1.036504	CCA DATA NOT COLLECTED		
N7	0.691095	0.884985	1.007745			
N8	0.925122	1.644361	2.805973			
N9	0.602558	0.822988	0.851506			
N10	0.568686	0.939952	0.906231			
N11	0.890214	1.015765	0.991923			

Two-way ANOVA	Ordinary					
Alpha	0.05					
Source of Variation	% of total	P value	P value su	Significant?		
Interaction	1.801	0.6377	ns	No		
cca	4.257	0.1501	ns	No		
drug	7.176	0.1759	ns	No		
ANOVA table	SS	DF	MS	F (DFn, D	P value	
Interaction	0.3826	2	0.1913	F (2, 42) =	P = 0.6377	
cca	0.904	1	0.904	F (1, 42) =	P = 0.1501	
drug	1.524	2	0.762	F (2, 42) =	P = 0.1759	
Residual	17.67	42	0.4206			
T-test						
Table Analyzed	Tim23 Veh to ATRA					
Column B	ATRA					
vs.	vs.					
Column A	Vehicle					
Unpaired t test						
P value	0.0252					
P value summary	*					
Significantly differen	Yes					

CCA+ RA: **Tom40**

	Veh	9cisRA	ATRA	CCA	9cisRA+CCA	ATRA+CCA
N1	0.796204	1.867084	1.880158	1.009332	2.410642046	1.852778211
N2	0.142918	0.235456	0.478468	0.443115	0.81299217	0.739861155
N3	0.352892	0.7917	0.851708	0.894238	1.209869308	0.808411142
N4	0.880494	1.274893	1.479337	1.021877	1.125361063	1.271153715
N5	0.497801	0.808087	1.538402	1.338921	0.855726456	1.274848252
N6	0.607419	0.687	0.892972	0.720008	0.836872346	1.129833968
N7	0.57637	0.661053	1.328154	CCA DATA NOT COLLECTED		
N8	0.792832	0.907605	0.89625			
N9	0.868492	1.290346	1.282801			
N10	0.313478	0.667871	0.671202			
N11	0.543811	0.727438	0.52254			
N12	0.760941	0.793788	1.092412			
N13	0.664544	1.322355	0.777182			

Two-way ANOVA	Ordinary					
Alpha	0.05					
Source of Variation	% of total	P value	P value su	Significant?		
Interaction	0.7458	0.7807	ns	No		
cca	6.687	0.0396	*	Yes		
drug	12.29	0.0223	*	Yes		
ANOVA table	SS	DF	MS	F (DFn, D	P value	
Interaction	0.07776	2	0.03888	F (2, 51) =	P = 0.7807	
cca	0.6973	1	0.6973	F (1, 51) =	P = 0.0396	
drug	1.282	2	0.6409	F (2, 51) =	P = 0.0223	
Residual	7.971	51	0.1563			

CCA+ RA: **mtHsp60**

	Veh	9cisRA	ATRA	CCA	9cisRA+CCA	ATRA+CCA
N1	1.425384	1.574645	1.723214	1.530523	1.239547495	1.629245833
N2	0.673344	0.757804	0.685609	0.62859	0.647041334	0.613678254
N3	0.501352	0.524985	0.421478	0.434953	0.544432541	0.328989707
N4	1.218604	1.665865	1.269404	2.028819	1.684826149	2.11764157
Two-way ANOVA	Ordinary					
Alpha	0.05					
Source of Variation	% of total	P value	P value su	Significant?		
Interaction	1.408	0.8795	ns	No		
cca	0.5462	0.755	ns	No		
drug	0.1024	0.9906	ns	No		
ANOVA table	SS	DF	MS	F (DFn, D	P value	
Interaction	0.1045	2	0.05226	F (2, 18) =	P = 0.8795	
cca	0.04056	1	0.04056	F (1, 18) =	P = 0.7550	
drug	0.007603	2	0.003801	F (2, 18) =	P = 0.9906	
Residual	7.273	18	0.4041			

CCA+ RA: **mtHsp70**

	Veh	9cisRA	ATRA	CCA	9cisRA+CCA	ATRA+CCA
N1	1.805861	1.495881	1.43061	1.539157	1.600956923	1.543890545
N2	0.615733	0.669282	0.672455	0.445395	0.560272143	0.316462208
N3	0.573586	0.178991	0.435642	0.517167	0.261483583	0.361693936
N4	3.148214	3.153754	2.497906	2.872071	3.069393655	3.075177099
N5	2.09942	2.613112	2.630495	2.401572	3.222521524	3.600406041
N6	1.194223	1.447779	1.419924	1.783551	1.794438417	1.450527448
N7	1.13107	1.216373	0.968662	CCA DATA NOT COLLECTED		
N8	0.819392	1.156899	0.953944			
N9	0.939154	1.451114	2.68602			
N10	0.830507	0.853733	0.859824			
N11	0.802285	1.027037	1.1338			
N12	0.952386	1.065727	0.974268			
N13	0.933032	1.006466	0.985177			
Two-way ANOVA	Ordinary					
Alpha	0.05					
Source of Variation	% of total	P value	P value su	Significant?		
Interaction	0.01403	0.9963	ns	No		
cca	4.151	0.1423	ns	No		
drug	0.4559	0.8854	ns	No		
ANOVA table	SS	DF	MS	F (DFn, D	P value	
Interaction	0.006218	2	0.003109	F (2, 51) =	P = 0.9963	
cca	1.839	1	1.839	F (1, 51) =	P = 0.1423	
drug	0.202	2	0.101	F (2, 51) =	P = 0.8854	
Residual	42.24	51	0.8283			

RA: Kinase Activity: **phosphorylated/total ratio of AMPK**

	Veh	9cisRA	ATRA		
N1	0.176462509	0.472397669	0.365738989		
N2	0.421778008	0.310882277	0.675900491		
N3	0.384068166	0.708759018	0.643799205		
N4	0.750008445	0.896652621	1.077093233		
N5	1.596853176	1.324893361	1.210249766		
N6	1.348778124	1.274451892	0.901556004		
Table Analyzed	p/t AMPK 30min				
ANOVA summary					
F	0.02063				
P value	0.9796				
P value summary	ns				
ANOVA table	SS	DF	MS	F (DFn, D	P value
Treatment (between	0.008203	2	0.004101	F (2, 15) =	P = 0.9796
Residual (within colu	2.983	15	0.1989		
Total	2.991	17			

RA: Kinase Activity: **phosphorylated/total ratio of p38/MAPK**

	Veh	9cisRA	ATRA		
N1	0.922871396	0.72288687	0.920516551		
N2	1.213092944	0.712817239	0.636755186		
N3	0.620556995	0.584798374	1.126938926		
N4	0.726986314	0.64897811	1.181976903		
N5	0.769110677	0.562716186	0.292087081		
N6	1.165390636	1.169154636	0.448560188		
Table Analyzed	p/t-p38 30 min				
ANOVA summary					
F	0.596				
P value	0.5635				
P value summary	ns				
ANOVA table	SS	DF	MS	F (DFn, DFd)	
Treatment (between	0.09632	2	0.04816	F (2, 15) = 0.5960	
Residual (within colu	1.212	15	0.08081		
Total	1.308	17			

RA: Kinase Activity: **phosphorylated/total ratio of CAMK II**

	Veh	9cisRA	ATRA	
N1	0.922871396	0.72288687	0.920516551	
N2	1.213092944	0.712817239	0.636755186	
N3	0.620556995	0.584798374	1.126938926	
N4	0.726986314	0.64897811	1.181976903	
Table Analyzed	p/t-CAMK 30 min			
ANOVA summary				
F	2.109			
P value	0.1774			
P value summary	ns			
ANOVA table	SS	DF	MS	
Treatment (between	0.1868	2	0.09338	
Residual (within colu	0.3985	9	0.04428	F (DFn, DFd)
Total	0.5853	11		F (2, 9) = 2.109

APPENDIX B- ADDITIONAL DATA

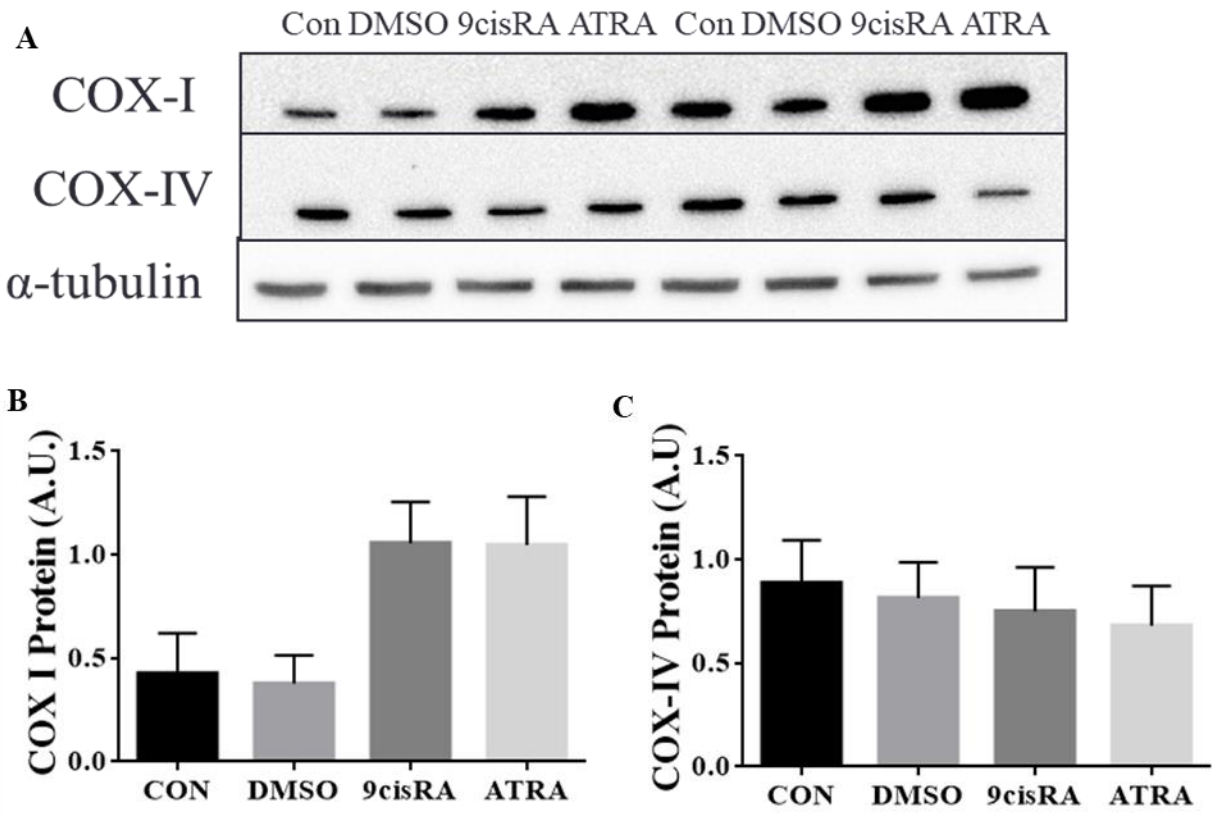

Figure S1. *RA isomer-supplemented differentiation leads to elevations in mitochondrial, but not nuclear encoded mitochondrial proteins.* Myoblast differentiation was supplemented with: control (DM), DMSO (Vehicle) and the RA isomers over the course of 4 days with 1μM of RA. (A). Representative Western Blots and graphical quantifications of: (B) COX-I, (C) COX-IV. Data are registered as mean ±SEM and are measured in arbitrary units. (¶, main effect of RA, $P<0.05$ vs vehicle; n=4).

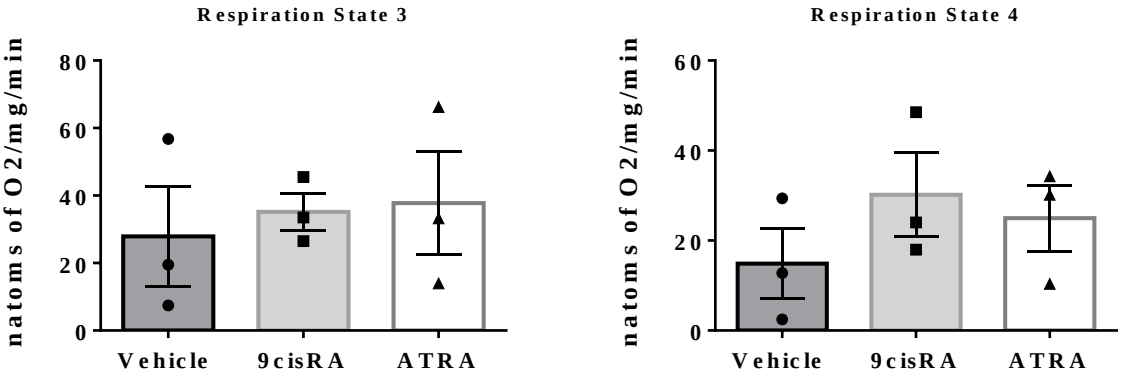

Figure S2. *Respiration in RA isomer-treated myotubes.* Myotubes were treated with 1µM of RA isomers 9cisRA and ATRA . (A). Stage 3 respiration with RA isomer treatment (B) Stage 4 Respiration with RA isomer treatment.

APPENDIX C- LABORATORY METHODS AND PROTOCOLS

CELL CULTURE

Cells

1. C2C12 murine skeletal muscle cells (ATCC, CRL-1772)

Materials

1. Dulbecco's Modified Eagle's Medium (DMEM; Sigma D-5796/500ml)
2. Fetal Bovine Serum (FBS; Fisher Scientifitc SH3039603C/500ml)
    a. Aliquoted into 50ml sterile conical tubes and stored at -20°C
3. Penicillin/Streptomycin (P/S; Invitrogen 15140-122/100ml)
    a. Sterile aliquots of 6mls and stored at -20°C)
4. Horse Serum (HS; Invitrogen 16050-114/1000ml)
    a. Aliquoted into 50ml sterile conical tubes and stored at -20°C
    b. Heat-inactivated for 30 minutes at 56.0°C
5. 0.25% Trypsin-EDTA (1x), phenol red (Invitrogen 25200-072/500ml)
    a. Sterile aliquots of 30mls stored at -20°C
6. Dulbecco's Phosphate Buffered Saline (PBS; Sigma D-8537/500ml)
7. 15ml conical tubes, sterile (BD Falcon 352097)
8. 50ml conical tubes, sterile (BD Falcon 352098)
9. 175cm^2 canted/vented tissue cultured flasks (BD Falcon 353112)
10. 6-well sterile tissue culture dish (Sarstedt 83.1839.300)
11. Gelatin (Sigma G1890)
    a. 0.1% solution autoclaved for sterilization

Procedure

1. Allow myoblasts to proliferate in 175cm2 flask with growth medium (GM; DMEM supplemented with 10% FBS and 1% P/S) until 70% confluent.
2. Prepare six 6-well dishes for plating by coating the bottom surface with 0.1% gelatin and allow to fully dry in laminar flow hood.
3. Pre-heat GM, trypsin and PBS in 37°C water bath for 30 minutes prior to use.
4. Discard old GM from tissue culture flask and wash with 10mls of PBS to rinse off remaining GM.
5. Apply 5mls of trypsin in the flask and place in the incubator at 37°C for 3 minutes.
6. Remove flask from incubator and gently knock sides of the flask to ensure cells are lifted from flask bottom. Remove trypsin with cells and place into a sterile 15ml conical tube.
7. Rinse flask with 5mls GM and add to sterile 15ml conical tube containing the cells.
8. Spin tube for 3 minutes at 1400rpm at room temperature.
9. Discard the supernatant and add 1ml of GM for resuspension with 1ml pipette.
10. Add 3mls of GM to resuspended cell mixture for a total volume of 4mls.
11. Fill each well of tissue culture dishes with 2mls of GM and add 100µl of cell mixture to each well.
12. Rotate plate in a circular motion for 30secs and subsequently place into 37°C incubator overnight.
13. The following day remove GM from cells and replace with differentiation medium (DM; DMEM supplemented with 5% heat-inactivated HS and 1% P/S) once myoblasts are 90-95% confluent.
14. Refresh DM every other day. Mature myotubes will form after five days and be ready for contractile activity.

TREATMENT OF C2C12 MYOTUBES WITH RETINOIC ACID

Cells

2. C2C12 murine skeletal muscle cells (ATCC, CRL-1772)

Materials

1. Dulbecco's Modified Eagle's Medium (DMEM; Sigma D-5796/500ml)
2. Fetal Bovine Serum (FBS; Fisher Scientifitc SH3039603C/500ml)
    a. Aliquoted into 50ml sterile conical tubes and stored at -20°C
3. Penicillin/Streptomycin (P/S; Invitrogen 15140-122/100ml)
    a. Sterile aliquots of 6mls and stored at -20°C)
4. Horse Serum (HS; Invitrogen 16050-114/1000ml)
    a. Aliquoted into 50ml sterile conical tubes and stored at -20°C
    b. Heat-inactivated for 30 minutes at 56.0°C
5. 0.25% Trypsin-EDTA (1x), phenol red (Invitrogen 25200-072/500ml)
    a. Sterile aliquots of 30mls stored at -20°C
6. Dulbecco's Phosphate Buffered Saline (PBS; Sigma D-8537/500ml)
7. 15ml conical tubes, sterile (BD Falcon 352097)
8. Dimethyl Sulfoxide (DMSO, Sigma D-8418/100ml)
9. 50ml conical tubes, sterile (BD Falcon 352098)
10. 6-well sterile tissue culture dish (Sarstedt 83.1839.300)
11. All-trans Retinoic Acid,*CAS* (Cayman Chem, *№ 302-79-4*)(2mM stock)
12. 9-cis Retinoic acid (Sigma-Aldrich, R4643-1MG) (2mM stock)
13. 6x 6-well dishes containing differentiated myotubes (Day 4)
    *note that CCA labelled plates require ~4mL of media in order to contact electrode lids

Procedure

1. Warm DM (contains DMEM, 5% heat inactivated horse serum, 1% Penicillin/Streptomycin) in 37^{o}C water bath.
2. Label 3x15ml, and 3x50mL tubes, and their corresponding 6 well dishes as Vehicle (DMSO) /9cisRA/ATRA, and CCA/9cisRA+CCA/ATRA+CCA
3. Pipette 11.974mL of DM into 3x15ml tubes, and double the amount in the 50mL tube. Add 6µl of 2mM 9cisRA/ATRA, and the equivalent volume of vehicle to the appropriate tubes and vortex.
4. Aspirate old DM present in the 6-6 well plates, wash with PBS, and aspirate PBS.
5. Aliquot the DM containing vehicle/9cisRA/ATRA into the appropriate 6-well dishes
6. Store dishes into the incubator for 24h (21 if done in combination with CCA)
7. Repeat 1-6 over a total of 4 days
8. Collect and analyze cells.

TREATMENT OF C2C12 MYOTUBES WITH NICOTINAMIDE RIBOSIDE

Cells

3. C2C12 murine skeletal muscle cells (ATCC, CRL-1772)

Materials

1. Dulbecco's Modified Eagle's Medium (DMEM; Sigma D-5796/500ml)
2. Fetal Bovine Serum (FBS; Fisher Scientifitc SH3039603C/500ml)
    a. Aliquoted into 50ml sterile conical tubes and stored at -20°C
3. Penicillin/Streptomycin (P/S; Invitrogen 15140-122/100ml)
    a. Sterile aliquots of 6mls and stored at -20°C)
4. Horse Serum (HS; Invitrogen 16050-114/1000ml)
    a. Aliquoted into 50ml sterile conical tubes and stored at -20°C
    b. Heat-inactivated for 30 minutes at 56.0°C
5. 0.25% Trypsin-EDTA (1x), phenol red (Invitrogen 25200-072/500ml)
    a. Sterile aliquots of 30mls stored at -20°C
6. Dulbecco's Phosphate Buffered Saline (PBS; Sigma D-8537/500ml)
7. 15ml conical tubes, sterile (BD Falcon 352097)
8. 50ml conical tubes, sterile (BD Falcon 352098)
9. 6-well sterile tissue culture dish (Sarstedt 83.1839.300)
10. Nicotinamide Riboside Chloride (CAS#: 23111-00-4) |(100mM stock)
11. 6 6-well dishes containing differentiated myotubes (Day 4)

*note that CCA labelled plates require ~4mL of media in order to contact electrode lids

Procedure

1. Warm DM (contains DMEM, 5% heat inactivated horse serum, 1% Penicillin/Streptomycin) in 37^{o}C water bath.
2. Pipette 11.800mL of DM into a 15ml conical tube. Add 200µl of 100mM NR to form a final concetration of 1 mM.
3. Aspirate old DM present in the 6-6 well plates, wash with PBS, and aspirate PBS.
4. Aliquot the DM containing NR into the appropriate 6-well dishes
5. Store dishes into the incubator for 24h
6. Repeat 1-6 over a total of 4 days
7. Collect and analyze cells

PREPARATION OF PROTEIN EXTRACTS FROM CELL CULTURE

Reagents

1. 5X Passive Lysis Buffer diluted in ddH20 to 1X (Promega E194A)
2. Phosphate Buffered Saline (PBS; Sigma D-8537)
3. Protease Inhibtors
    a. Leupeptin (10mg/ml stock)
    b. Aprotinin (10mg/ml stock)
    c. Pepstatin (10mg/ml stock)
    d. PMSF (500mM stock)
    e. DTT (1M stock)
4. Phosphatase Inhibitors
    a. Sodium Orthovanadate (250mM stock)
    b. PhosSTOP tablets (10X concentrated stock)

Procedure

1. Prepare fresh lysis buffer with protease and phosphatase inhibitors.
2. Remove media and wash cells 3X with 2mls of ice-cold PBS. Aspirate last wash.
3. Add 150µl of freshly prepared lysis buffer containing protease and phosphatase inhibitors into wells. Scrape the wells with a rubber cell scraper and place cell lysate into an eppendorf. Place eppendorf on ice. If required, combine multiple wells with a total of 150µl to increase final protein concentration.
4. Vortex sample briefly and place in liquid nitrogen. Thaw sample in water bath set to 37°C for 2 minutes. Repeat step four 2X for a total of 3 freeze-thaw cycles.
5. Spin the samples at 4°C for 5 minutes at 16.1rcf.
6. Collect the supernatant and place into a newly labeled eppendorf tube.
7. Measure the total protein concentration using the Bradford Assay.
8. Store samples at -20°C.

MITOCHONDRIAL ISOLATION FROM C2C12 MYOTUBES

Adapated from: Frezza C, Cipolat S, Scorrano L. Nature Protocols 2007;2(2):287-95.

Materials

1. Cold PBS (Sigma D-8537)
2. Cell Scraper
3. Mitochondrial Isolation tubes
4. Teflon Pestle
5. Glass Potter

Mitchondrial Isolation Buffer (MIB)

1. 10ml of 0.1M Tris-MOPS
    a. Dissolve 6.05g of Tris in 250ml of ddH_20 pH to 7.4 using MOPS powder.
    b. Volume up to 500ml.
    c. Store at 4ºC.
2. 1ml of 0.1M EGTA/Tris
    a. Dissolve 19.05g of EGTA in 250ml of ddH_20 pH to 7.4 using Tris powder/HCl.
    b. Volume up to 500ml.
    c. Store at 4ºC.
3. 20ml of 1M sucrose
    a. Dissolve 171.65g of sucrose in 500ml of ddH_20. Stir until fully dissolved.
    b. Aliquot into 20ml volumes in sterile conical tubes.
    c. Store at -20ºC.
4. Volume up to 100ml with ddH_20.
5. pH to 7.4.
6. Store at 4ºC.

Method

1. Pre-heat GM, trypsin in 37°C water bath for 30 minutes prior to use.
2. Discard old DM from tissue culture flask and wash with 10mls of PBS to rinse off remaining GM.
3. Apply 5mls of trypsin in the flask and place in the incubator at 37°C for 3 minutes.
4. Remove flask from incubator and gently knock sides of the flask to ensure cells are lifted from flask bottom. Remove trypsin with cells and place into a sterile 15ml conical tube.
5. Rinse flask with 5mls GM and add to sterile 15ml conical tube containing the cells.
6. Spin tube for 3 minutes at 1400rpm at room temperature.
7. Discard the supernatant and add 10mL of PBS for resuspension.
8. Spin tube for 3 mins at 1400rpm at room temperature
9. Wash cells with cold PBS and resuspend.
10. Centrifuge the cells at 600g for 10 minutes at 4ºC.
11. Pre-cool Teflon pestle and glass potter on ice.
12. Discard the supernate and resuspend the cells in 3mls of ice-cold MIB.

13. Transfer cell solution to glass potter.
14. Homogenize the cells using Teflon pestle at 1600rpm for 30 strokes in the glass potter. DO NOT USE A GLASS PESTLE, IT WILL DESTROY THE MITOCHONDRIA!
15. Transfer the homogenate from the glass potter to mitochondrial isolation tube.
16. Centrifuge at 600g for 10 minutes at 4ºC.
17. Collect the supernate (contains mitochondria and cytosol) and place into a second clean pre-chilled mitochondrial isolation tube.
18. Centrifuge the supernate at 7000g for 10 minutes at 4ºC.
19. Discard the supernate and the resultant pellet is the mitochondria.
20. Gently wash and resuspend the pellet with 200µl of MIB.
21. Transfer mitochondrial solution to a 1.5ml eppendorf.
22. Spin in a microcentrifuge at 7000g for 10 minutes at 4ºC.
23. Discard the supernate and resuspend the mitochondrial pellet with 50-100µl of MIB depending on mitochondrial yield.
24. Use fresh mitochondria immediately for respiration analysis.

RESPIRATION OF ISOLATED MITOCHONDRIA FROM CELLS

Materials

1. Hamilton syringe
2. Oxygen electrode

Reagents

1. VO_2 buffer
    a. Combine the following in a clean beaker
        i. 250mM sucrose 5.13g
        ii. 50mM KCl 0.222g
        iii. 25mM Tris base 0.18g
        iv. 10mM K_2HPO_4 0.104g
    b. Add 30mls of ddH20 to the beaker and stir until everything is dissolved.
    c. pH to 7.4
    d. Volume up to 60µl in a graduated cylinder.
    e. Place solution into clean bottle, label and store at 4ºC.
    f. Solution is good for one week only.
2. Glutamate
    a. Make 2X concentrated solution of 123.34mg/ml in ddH_20
3. ADP
    a. Make a 2X concentrated solution of 11.27mg.ml in ddH_20
4. NADH
    a. Make a 2X concentrated solution of 119.18mg.ml in ddH_20

Method

1. Turn on water bath to 30ºC to warm the electrode unit. Ensure electrode is clean of all debris and membrane is intact. Rinse with ddH_20 if necessary.
2. Turn on oxygen meter and open 782 oxygen system software on the connected computer.
3. Make glutamate, ADP and NADH solutions fresh in eppendorfs. Place on ice.
4. Once electrode has reached 30ºC add 250µl of VO_2 buffer and 50µl of mitochondria. (Minimum volume for the oxygen chamber is 300µl)
5. Place miniature stir bar in oxygen chamber and stir to mix VO_2 buffer and mitochondria. Place cork on top of chamber and ensure no air is in the chamber with the mitochondria and VO_2 buffer.
6. Let the solution stabilize and then using the software program calibrate the solution in the oxygen chamber to “high”.
7. After calibration is complete let the software record the basal drift for 2 minutes.
8. Warm glutamate in the 30ºC water bath.
9. Add 5µl of glutamate (State IV) using the Hamilton syringe and record changes in oxygen consumption for at least 2 minutes.
10. Warm ADP in the 30ºC water bath.
11. Add 5µl of ADP (State III) with the Hamilton syringe and record changes in oxygen consumption for at least 2 minutes.

12. Add 5µl of NADH with the Hamilton syringe and record any changes in oxygen consumption. This is to test for any damaged mitochondria as NADH would need a cellular transporter to get inside intact mitochondria.
13. Determine protein concentration of isolated mitochondria immediately using the Bradford assay.
14. Analyze rates of oxygen consumption using the software provided. Values are in %O2/ hour needs to be converted to %O2/min.
15. Correct oxygen consumption for protein concentration.

Equation:

$$\textbf{natoms } O_2\textbf{/mg/min} = \frac{\textbf{\%O2/min}}{\textbf{total µg of protein}} \times \frac{(1000 \times 111.25)}{100}$$

%O2/min – oxygen consumption (State IV or III) corrected for basal drift
Total µg of protein – volume of mitochondria x µg/µl of mitochondria
1000 – to convert from µg to mg
111.25 – amount of O_2 in 250µl of VO_2 buffer (0.25mls buffer = 111.25 natoms O_2)
100 – to get percentage

Example Calculation:

Basal drift = 20.00/hr
State III $\%O_2$/hr = 160.00/hr
Volume of VO_2 buffer = 250µl
Volume of mitochondria = 50µl
Protein concentration of mitochondria = 4µg/µl

State III %O2/min = (160-20)/60 = 2.3
Total µg of protein = 50µl x 4µg/µl = 200µg

$$\frac{2.3}{200} \times \frac{(1000 \times 111.25)}{100} = 12.79 \text{natoms } O_2\text{/mg/min}$$

WESTERN BLOTTING AND IMMUNODETECTION

Reagents

1. Transfer Buffer
    a. 0.025M Tris-HCl pH 8.3 12.14g
    b. 0.15M Glycine 45.05g
    c. 20% Methanol 800ml
    d. make up to 4L with ddH_20
    e. store at 4°C
2. Ponceau S stain
    a. 0.1% (w/v) Ponceau S
    b. 0.5% (v/v) Acetic Acid
    c. Store at room temperature
3. Wash Buffer
    a. Tris-HCl pH 7.5 12g
    b. NaCl 58.5g
    c. 0.1% Tween 10ml
    d. Store at room temperature
4. Blocking Solution
    a. 5% (w/v) skim milk power in wash buffer OR
    b. 5% (w/v) BSA in wash buffer
5. Enhanced Chemiluminescence Fluid (ECL; Santa Cruz sc-2048)
6. Film/Developer/Fixer

Procedure

1. Transfer Procedure

a. Remove electrophoresis plates from chamber and separate the plates.
b. Cut away unnecessary parts of the gel using a spatula and measure remaining gel size.
c. Using a paper cutter cut 6 pieces of Whatman paper per gel to the same size as the gel. Wearing gloves cut nitrocellulose membrane (GE Healthcare RPN303D) to the dimensions of the gel.
d. Assemble Whatman paper, nitrocellulose memebrane and gel as shown below:

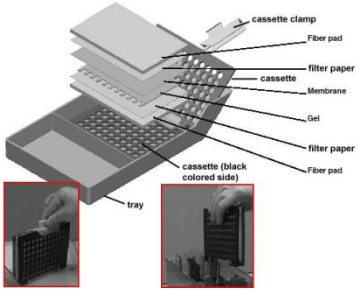

e. Close the cassette and place in the transfer chamber with the black side of the cassette facing the back side of the chamber.
f. Place ice pack in the chamber.
g. Place lid on the chamber and connect the leads to the power supply.

h. Turn on the power supply and run at 120V for 2 hours. This can vary depending on the size of the protein of interest.

2. Removal of transfer membrane:

a. Turn off the power supply and disconnect leads from the power supply then remove the lid from the chamber.
b. Remove the cassette from the chamber.
c. With gloves on, remove the Whatman paper and gel and place the nitrocellulose membrane in a plastic dish.
d. Add Ponceau S stain on the membrane and gently swirl.
e. Drain off the remaining Ponceau S and save for reuse.
f. Rinse the membrane with ddH_20 to reduce the red background. Wrap membrane in saran wrap and scan image.
g. Cut the membrane while protein bands are still visible at the desired molecular weight.
h. Rotate membrane at room temperature in wash buffer until remaining Ponceau S has been removed.
i. Incubate membrane for 1 hour with rotation in blocking solution.
j. Incubate membrane with desired antibody diluted in blocking solution overnight at 4ºC. Membrane is placed face down into the solution on a glass plate covered in parafilm. To maintain a moist environment overnight, wet a small kimwipe and form it into a ball and place in each corner of the dish. Cover the dish with saran wrap.

3. Immunodetection

a. Wash the blots in wash buffer with gentle rotation for 5 minutes 3X.
b. Incubate the blots for 1-2 hours with the appropriate secondary antibody diluted in blocking solution.
c. Membrane is placed face down in solution on a glass plate covered with parafilm. Place moist kimwipes in each corner of the dish and cover the dish with saran wrap.
d. Following the incubation, wash the membrane 3X for 5 minutes with wash buffer.

4. Enhanced Chemiluminescence Detection

a. Mix ECl fluids “A” and “B” in a 1:1 ratio in a disposable Rohr tube.
b. Place blots on saran wrap face up and apply ECL solution for 2 minutes.
c. Dab off excess ECL on a kimwipe and place blots face down on a fresh piece of saran wrap and wrap tightly.
d. Expose blot to film (time will vary depending on protein and antibody).
e. Place film into developer (time will vary).
f. Once image appears place film into fixer for 2 minutes. Wash with fresh water when complete.

SDS POLYACRYLAMIDE GEL ELECTROPHORESIS (SDS-PAGE)
PROTEAN BIO-RAD SYSTEM

Reagents

1. Acrylamide/Bis-Acrylamide, 30% Solution 37.5:1 (BioShop 10.502)
    a. Store at 4°C
2. Under Tris Buffer
    a. 1M Tris-HCl, pH 8.8 (60.5g/500ml)
    b. Store at 4°C
3. Over Tris Buffer
    a. 1M Tris-HCl, pH 6.8 (12.1g/100ml)
    b. Bromophenol Blue (for colour)
    c. Store at 4°C
4. Ammonium Persulfate (APS)
    a. 10% (w/v) APS in ddH_20 (1g/10ml)
    b. Stored at 4°C
5. Sodium Dodecyl Sulfate (SDS)
    a. 10% (w/v) in ddH_20 (1g/10ml)
    b. Store at room temperature
6. TEMED (Sigma T-9281)
7. Electrophoresis Buffer, pH 8.3 (10L)
    a. 25mM Tris 30.34g, 192mM Glycine 144g, 0.1% SDS 10g
    b. Volume to 10L with ddH_20
    c. Store at room temperature
8. 6X SDS
    a. Warm 100% glycerol in water bath at 65°C for 30 minutes
    b. Combine 1.2g SDS, 0.06g Bromophenol Blue, 3mls of 1M Tris, pH 6.8 and 1ml of ddH_20 and stir at 4°C for 5 minutes
    c. Add 3mls of 100% glycerol, stir and aliquot mixture.
    d. Store at -20°C
    e. Add 5% (v/v) ß-mercaptoethanol (Sigma M6250) to 6X SDS <u>just prior</u> to use
9. *tert*-Amyl alcohol ReagentPLus, 99% (Sigma 152463)

Procedure

1. **Prepare electrophoresis rack:**
    a. Clean glass plates thoroughly with soap followed by 95% ethanol then ddH_20.
    b. Dry carefully with a kimwipe.
    c. Assemble glass plates as shown below:

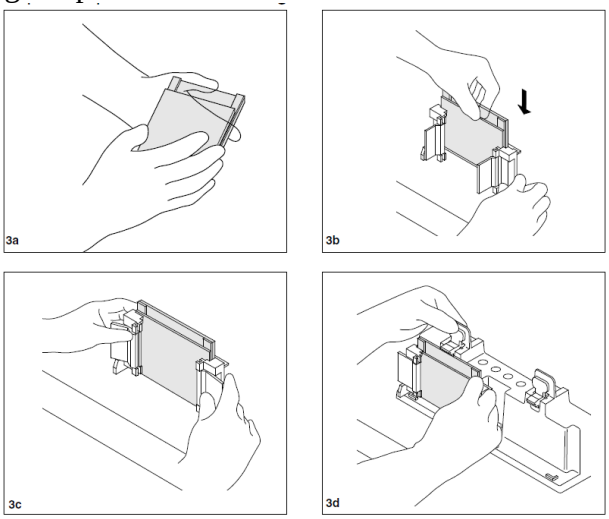

    d. Check the seal y adding a small volume of ddH_20 then pour off and let dry.
2. **Prepare separating gels:**
    a. Mini Protean 3 Bio-Rad System volumes:

	8%	**10%**	**12%**	**15%**	**18%**
Acrylamide	2.7 ml	3.3 ml	4.0 ml	5.0 ml	6.0 ml
ddH_20	4.1 ml	3.5 ml	2.8 ml	1.8 ml	0.8 ml
Under Tris	3.0 ml	3.0 ml	3.0 ml	3.0 ml	3.0 ml
SDS	100µl	100µl	100µl	100µl	100µl
APS	100µl	100µl	100µl	100µl	100µl
TEMED	10µl	10µl	10µl	10µl	10µl

    b. Mix the contents of the separating gel without adding APS or TEMED. Stir.
    c. Add APS and TEMED. Stir.
    d. Slowly pour the entire volume of the solution into the space between the two plates while keeping plates tilted to prevent bubble formation.
    e. Add *tert*-Amyl alcohol to coat top surface of gel solution.
    f. Allow 30 minutes for gel polymerization.
    g. Remove *tert*-Amyl alcohol by pouring it off and remove any remainder with a kimwipe. Rinse with ddH_20.

3. **Prepare stacking gel:**
    a. For a single mini gel use the following volumes:

Acrylamide	500 µl
Over Tris	625 µl
ddH_20	3.75 ml
SDS	50 µl
APS	50 µl
TEMED	7.5 µl

    b. Mix the contents of the stacking gel without adding APS or TEMED. Stir.
    c. Add APS and TEMED. Stir.
    d. Using a Pasteur pipette slowly add the entire volume from the beaker in between the plates.
    e. Add comb for desired number of wells.
    f. Allow 30 minutes for gel polymerization.

4. **Prepare samples:**
    a. Turn of the block heater to 95ºC.
    b. Pipette required volume of sample into new eppendorf with 6X SDS (1 volume of sample to 1/6 sample volume of 6X SDS). Keep samples on ice until all samples are prepared.
    c. Briefly spin each sample to bring volume to the bottom of the eppendorf.
    d. Incubate each sample at 95 ºC for 5 minutes in the heating block to denature the proteins.
    e. Briefly spin again to return volume to the bottom of the eppendorf.

5. **Assemble Mini-PROTEAN gel caster system:**
    a. See images below:

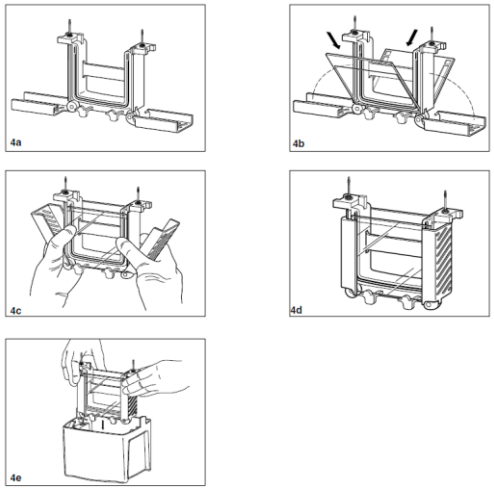

    b. If you are only running one gel a plastic rectangular pseudo plate must be clamped on the other side of the caster.

c. Fill with electrophoresis buffer between the plates and outside of the plates in the chamber.
d. Slowly remove the comb using both hands (one on each side) by pulling the comb straight upwards.
e. Fix any wells that are deformed using a small spatula.
f. Clean out the wells using a syringe filled with electrophoresis buffer.
g. Withdraw the entire volume of the sample using a Hamilton syringe. Inject volume slowly into the bottom of the well.

6. Gel electrophoresis

a. Immediately after all samples are loaded place the lid on the gel chamber.
b. Place positive and negative plugs into the power supply and turn on power supply.
c. Set power supply to 120V. Gel will run for ~2 hours depending on percent gel made.
d. When the bromophenol blue has run off the bottom of the gel turn off the power supply. Remove plugs from power supply and remove lid.
e. Prepare for electrotransfer of proteins from the gel to nitrocellulose membrane.

ELECTRICAL STIMULATION OF MYOTUBES IN CULTURE

Cells

1. C2C12 murine skeletal muscle cells, differentiated into mature myotubes

Materials

1. Electrical Stimulator
   Gange bipolar output (+/- amplitude adjustable using one knob)
   Output voltage range = 0 to +/- 30V
   Maximum output current = 1A
   Adjustable output pulse duration from 0.001 to 0.1secs (10-1kHz)
   Adjustable output pulse repetition from 0.0005 to 0.01secs (100-2kHz)
   Adjustable polarity duration range from 1 to 100secs (0.01 to 1Hz)
   Polarity duration range = time duration for the output "pulse burst" to be positive before switching to a similar negative (amplitude) pulse burst. Positive and negative duration are of equal value except for the amplitude.

2. 6-well sterile plastic culture dishes (Sarstedt 83.1839.300) with lids modified for implantation of platinum electrode wires (see image below). Bottom of plates should be coated with sterile 0.1% gelatin.

Procedure

1. Before each bout of stimulation, electrodes are cleaned with 70% ethanol and placed in the laminar flow hood for 30mins under UV light for sterilization.
2. DM is refreshed 30mins prior to stimulation protocol.
3. Differentiated myotubes are stimulated in a parallel circuit (four 6-well dishes at once) at 5Hz, 9V for 3 hours in 2mls of DM.
4. Once the 3 hours is complete, DM should be refreshed once again.
5. The cells are allowed to rest for 21 hours until the next bout of stimulation. The total protocol lasts for 4 days and 21 hours and cells are harvested following the last 21 hour rest period.

A) Electrical Stimulator

B) Modified six-well plate lid

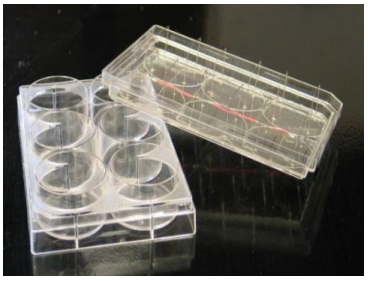

APPENDIX D- OTHER CONTRIBUTIONS TO LITERATURE

Oral Presentations

1. Dovijarski N and Hood DA. The effect of Retinoic acid isomers on mitochondrial biogenesis in muscle cells. KAHS Graduate Seminar, York University, Toronto, ON. Jan 19th, 2018
2. Dovijarski N and Hood DA. The effect of Retinoic acid on mitochondrial turnover in C2C12 cells. Ontario Exercise Physiology Conference, Barrie, Jan 27th, 2018.
3. Dovijarski N and Hood DA. The concurrent application of Chronic Contractile Activity and Retinoic Acid on C2C12 muscle cell Mitochondrial Biogenesis. Canadian Society of Exercise Physiology Conference 2018. Sheraton Niagara Falls, Nov 1st, 2018